2014-06-11

Hölder Extensions for Non-Standard Fractal Koch Curves

Joshua Taylor Fetbrandt
Brigham Young University - Provo

Hölder Extensions for Non-Standard Fractal Koch Curves

Joshua T. Fetbrandt

A thesis submitted to the faculty of
Brigham Young University
in partial fulfillment of the requirements for the degree of

Master of Science

Rodney Forcade, Chair
David Cardon
David Wright

Department of Mathematics

Brigham Young University

June 2014

ABSTRACT

Hölder Extensions for Non-Standard Fractal Koch Curves

Joshua T. Fetbrandt
Department of Mathematics, BYU
Master of Science

Let K be a non-standard fractal Koch curve with contraction factor α. Assume α is of the form $\alpha = 2 + 1/m$ for some $m \in \mathbb{N}$ and that K is embedded in a larger domain Ω. Further suppose that u is any Hölder continuous function on K. Then for each such $m \in \mathbb{N}$ and iteration $n \geq 0$, we construct a bounded linear operator Π_n which extends u from the prefractal Koch curve K^n into the whole of Ω. Unfortunately, our sequence of extension functions $\Pi_n u$ are not bounded in norm in the limit because the upper bound is a strictly increasing function of n; this prevents us from demonstrating uniform convergence in the limit.

Keywords: fractal, koch curve, extension

Acknowledgments

It is hard to appropriately capture just how how much work went into this document with a few hundred words. Between the late nights of debugging code, weeks of trying to grasp the original problem, and months of writing/revising/reworking the text as a whole, I can confidently say this is the most complicated document I have ever produced. With that said, I am also confident that this project would not have been realized without an exceptional support system.

At the top of the list is my committee (Rodney Forcade, David Cardon, David Wright), the Brigham Young University Department of Mathematics, my wife, and my family. I could not have completed this work without their continued support and dedication to my education. In particular, the flexible framework set forth by my committee chair, Rodney Forcade, has been invaluable in my progression. In addition, David Cardon and David Wright meticulously proofread the document and provided numerous suggestions.

Emily Evans also deserves a tremendous thank you. On top of being an incredible instructor, mentor, and friend, she never lost faith in me or my abilities and reinvigorated my research when times got tough. She was always by my side when I needed it, and I will always be grateful for that.

Michael Andersen and Nickolas Callor also contributed countless hours of proofreading. I would still be lost on the sea of big words, short sentences, and poor word choice without their tireless contribution.

Finally, I am indebted to the students I had the opportunity to work with along the way. They were always a beacon of creativity and hope, and continually reminded me that I can do anything I set my mind to.

Contents

List of Tables

List of Figures

Chapter 1. Introduction

Jonsson and Wallin were pioneers in the field of extension functions over fractal sets. Among other things, they demonstrated that certain classes of continuous functions (defined on fractal sets) are extendable. In particular, the extension into larger domains happens via bounded linear extension operators. Their result, unfortunately, does not guarantee uniqueness or provide a construction of such an operator for any pair of fractal set and continuous function. As such, early attempts to build such an operator were fruitless.

The problem remained open until 2012 when Evans succeeded in constructing the first such operator for the standard fractal Koch curve. Her method depended on a regular discretization of the domain and a Hölder continuous[1] function defined on the fractal. In addition, she provided a scaffolding for future work, namely a regular discretization for non-standard fractal Koch curves. Our goal is to use this generalized discretization to extend her results to a class of non-standard fractal Koch curves. To achieve this, we begin with a discussion on the overarching questions, previous attempts, and various techniques surrounding the current body of research in this area.

Extension functions have been a cornerstone of research for almost a century. As such, three questions have set themselves above the rest with the breadth of research surrounding them. If we let $f\colon E \to \mathbb{R}$ be a function defined on a (potentially non-structured) subset E of $\mathbb{R}^n$, we can consider the following questions (each of which could provide a lifetime of viable work).[2]

(i) Does f extend to a function $F \in C(\mathbb{R}^n)$ so that $F|_E = f$?

(ii) If f extends to a function F as above, what are the characteristics of F (i.e., is F continuous, differentiable)?

[1] A function f is $\beta-$Hölder continuous on A if there is a $C \in \mathbb{R}$ so that

$$|f(X) - f(Y)| \leq C|X - Y|^\beta$$

for all $X, Y \in A$ and some $\beta \in (0, 1]$. The C is the Hölder seminorm.

[2] A complete list of notation can be found in the Nomenclature section.

(iii) If f extends to a function F as above, is the norm[3] of F bounded?

Because these questions are incredibly broad, the breadth of research surrounding these questions is substantial. In a nutshell, we know a considerable amount under certain hypotheses (i.e., when we have differentiability or regular continuity). These contrived situations, however, are not the primary focus of our discussion. Our discussion will be focused on the approach taken to solve variations on these situations.

At the forefront of the research is the seminal work of Whitney in [1, 2, 3]. While he was not the first to consider extension functions, he was the first person to consider separating domains to build extension functions. In [1], Whitney proved

Theorem 1. *Let A be a closed subset of E and $f(x) = f_0(x)$ be of class C^m (m infinite or finite) in A in terms of the*

$$f_k(x) = R_k(x, a) + \Sigma_{\sigma_l \leq m - \sigma_k} \frac{f_{k+l}(a)}{l!}(x - a)^l$$

where $\sigma_k \leq m$ denotes the k^{th} multi-index. Then there is a function $F(x)$ of class C^m in E in the ordinary sense, such that (1) $F\Big|_A = f$, (2) $D_k F\Big|_A = f_k$ ($\sigma_k \leq m$), and (3) $F(x)$ is analytic in $E - A$.

Whitney proved this result by subdividing the domain into cubes, and—after extending the function on each cube—he merely assembles the extension function by reassembling the cubes. This methodology was monumental in our development, and fundamentally retooled modern thought in mathematics. Because this was such a fundamental shift in thought, several mathematicians have used variations on Whitney's methods to tackle far more difficult problems.

Glaeser became the first mathematician in over twenty years to have any success at generalizing Whitney's methods in [4]. His research on paratangent bundles (a topological relative of Taylor polynomials) allowed him to partially tackle a generalization of Whitney's

[3]The choice of norm depends on the situation.

theorem in higher dimensions. After this advance, however, it took yet another half century for more progress to be made. In 2002, Bierstone et al. proved an analogue of Whitney's Theorem for higher dimensional spaces in [5] using iterated paratangent bundles, an analogue of Glaeser's paratangent bundles.

On a (slightly) different (but closely related) front, the work of Brudnyi and Shvartsman in [6, 7] and Fefferman in [8, 9] has been of particular interest. Brudnyi and Shvartsman's reformulation of Whitney's Theorem relies on the existence of a continuous linear extension operator which is determined by local approximations of the original continuous function. Fefferman, on the other hand, abandons generalizations of Whitney's Theorem to study extension and interpolation operators of finite sets in $\mathbb{R}^n$, and concerns himself with the following three questions.

(i) How can we decide whether there is a function $F \in C^m(\mathbb{R}^n)$ so that $F|_E = f$?

(ii) How do we compute $\|f\|_{C^m(E)} := \inf\{\|F\|_{C^m(\mathbb{R}^n)} \colon F \in C^m(\mathbb{R}^n), F|_E = f\}$?

(iii) Is there a bounded linear map $T \colon C^m(E) \to C^m(\mathbb{R}^n)$ so that $Tf|_E = f$ for all $f \in C^m(E)$?

It is readily apparent from this overview that the technique for reasonably-structured sets of $\mathbb{R}^n$ has roughly remained unaltered since the time of Whitney, but this leaves a hole in our knowledge. In particular, these results do not address extension functions for d-sets[4] (i.e., none of the researchers asked questions with regard to fractal sets). Another shortcoming of this work is that none of these researchers (including Whitney) give sufficient detail on constructing an extension function because they considered the problem only in terms of existence and uniqueness.

The first of these shortcomings was addressed by Jonsson and Wallin in [11, 12]. They proved

[4]Let F be a closed subset of $\mathbb{R}^n$ and $0 < d \leq n$. Define $B(x, r)$ to be the closed ball with center x and radius r. A positive Borel measure μ with support F is called a d-measure on F if—for some constants $c_1, c_2 > 0$—$c_1 r^d \leq \mu(B(x, r)) \leq c_2 r^d$, for $x \in F$ and $0 < r \leq 1$. The set F is call a d-set if there is a d-measure on F. See [10].

Theorem 2. *Let $\alpha > 0$, $0 < d \leq n$, $1 \leq p \leq \infty$, $1 \leq q \leq \infty$, $\beta = \alpha - (n-d)/p$, and the nonnegative integer k satisfy $k < \beta \leq k+1$. Let $B_\beta^{p,q}(F)$ denote the Besov*[5][6] *space defined on the d-set F and $\Lambda_\alpha^{p,q}(\mathbb{R}^n)$ denote the Besov space on $\mathbb{R}^n$. There is an operator $\mathcal{E}\colon B_\beta^{p,q}(F) \to \Lambda_\alpha^{p,q}(\mathbb{R}^n)$ so that if $f = \{f^{(j)}\}_{|j|\leq k} \in D_\beta^{p,q}(F)$, then $\mathcal{E}f \in C^\infty(\overline{F})$ and*

(i) $\|\mathcal{E}f\|_{\Lambda_\alpha^{p,q}(\mathbb{R}^n)} \leq c\|f\|_{B_\beta^{p,q}(F)}$, where c does not depend on f[7]*, and*

(ii) $D^j(\mathcal{E}f)|_F = f^{(j)}$ $d-$a.e., $|j| \leq k$.

The operator $\mathcal{E}$ is linear if β is not an integer. It depends on β, but it is constant in the interval $k < \beta < k+1$.

This theorem essentially states that we can extend functions defined on fractal sets to larger domains via bounded linear operators. The proof of the theorem, however, still lacks sufficient guidance on constructing such an operator, leaving the second observation completely unattended. After a number of years and failed attempts to construct such an operator, Evans partially rectified this problem for the standard Koch curve in [13].

Evans constructed the operator using a discretization technique she developed in [14]. This technique is highly unusual, however, in the sense that it is, in part, generated around a continuous function, and not the other way around. In essence, this key detail minimizes the types of elements in the discretization by maximizing self-similarity. This simplifies the explicit calculation of the extension function. It is this regular discretization technique and approach which brings us to our main result.

For any $m \in \mathbb{N}$, we extend her construction of an extension operator to a larger class of non-standard fractal Koch curves with contraction factor $\alpha = 2 + 1/m$ using the generalized

[5]For $\alpha > 0$, $1 \leq p \leq \infty$, and $1 \leq q \leq \infty$, we say a function f is in the Besov space $B_\alpha^{p,q}(F)$ if $f \in L^p(\mu)$ and there is a sequence $B = \{B_j\}_{j=0}^\infty$ so that for every net $\mathcal{N}$ with mesh 2^{-j} there is a function $s(\mathcal{N}) \in \mathcal{P}_{[\alpha]}(\mathcal{N})$ satisfying $\|f - s(\mathcal{N})\|_p \leq 2^{-j\alpha}B_j$ where $\mathcal{P}_{[\alpha]}(\mathcal{N})$ is the set of functions which on each cube Q in the net $\mathcal{N}$ coincide with a polynomial of degree at most the integer part of α. See [10].

[6]A net $\mathcal{N}$ with mesh r is a division of $\mathbb{R}^n$ into equally big cubes Q with edges of length r, obtained by intersecting $\mathbb{R}^n$ with hyperplanes orthogonal to the axes. See [10].

[7]The $B_\alpha^{p,q}(F)$-norm of f is $\|f\|_p + \inf\|B\|_q$ where the infimum is taken over all such sequences B in the definition of $B_\alpha^{p,q}$. See [10].

discretization laid out in [14][8]. That is, we extend a Hölder continuous function, u, defined on a fractal Koch curve, K, satisfying the Hölder estimate to a larger domain $\Omega \subset \mathbb{R}^2$ containing an embedding of K. In other words, the method presented henceforth will prove

Theorem 3 (Main Theorem)**.** *Let $m \in \mathbb{N}$ define a contraction factor $\alpha = 2 + 1/m$, and assume that K is the Koch curve corresponding to α with vertex set V. Assume further that Ω is a domain containing K and u is any Hölder continuous function on K. We define a continuous linear operator Π_n such that*

(i) $\Pi_n : C^\beta(K) \mapsto C^\beta(\Omega)$,

(ii) $\|\Pi_n u\|_{\Omega,\beta} \leq C_1 \|u\|_{K,\beta}$,

(iii) and $\sup_{X \in \Omega} |\Pi_n u(X) - \Pi_{n+p} u(X)| \leq C_2 \|u\|_{S,\beta}$

where C_1 and C_2 are numerical constants independent of u but dependent on α and n.

[8]While this restriction on $\alpha \in (2, 4]$ is semi-arbitrary, additional technique will need to be developed to handle situations for irrational α and α of the form $\alpha = 2 + p/q$, $p, q \in \mathbb{N}$, $gcd(p, q) = 1$. See Section 4.2 to get a feel for the additional technique which will need to be developed.

Chapter 2. Construction of the Koch Curve and the Mesh

The Koch curve is the well-recognized upper portion of the Koch snowflake. Evans, in [13], and Lancia and Vivaldi, in [10], give a complete exposition and motivation for the definition of the Koch curve. Evans goes further to develop our meshing technique in [14]. We will present the highlights of their work and refer the reader to [10, 13, 14] for a complete discussion on these topics.

2.1 Intuition of the Koch Curve

We begin our discussion of the Koch curve with an intuitive construction. Assume we have a line segment S^0 with end points $(0,0)$ and $(l,0)$ and that $\alpha \in (2,4]$. Moreover, define the set of vertices $\{(0,0),(l,0)\}$ to be V^0. We proceed by dividing S_0 into three pieces so that the two outer segments have length l/α; this forces the center segment to be of length $l(\alpha-2)/\alpha$. Now we "attach" an isosceles triangle with sides of length l/α, l/α, and $l(\alpha-2)/\alpha$ over the central segment and "erase" the base segment of length $l(\alpha-2)/\alpha$. The resulting set of five vertices will be V^1 and the set of line segments will be S^1. See Figure 2.1(a).

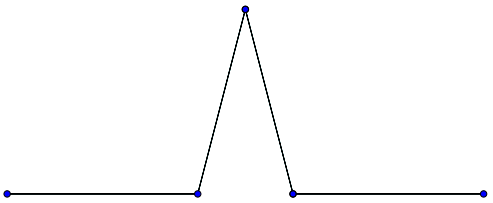

(a) V^1 is the set of blue points; S^1 is the set of segments

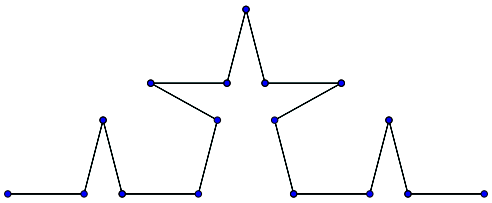

(b) V^2 is the set of blue points; S^2 is the set of segments

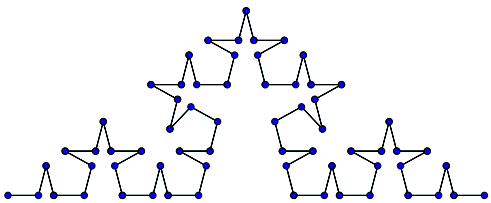

(c) V^3 is the set of blue points; S^3 is the set of segments

Figure 2.1: A Visualization of the Vertex and Segment Sets

From here, the process is straightforward. For all $n \geq 1$, we apply the previous process to each segment of S^n and define S^{n+1} to be the set of segments. The set S^n is considered to be the prefractal curve. In a similar manner, define V^{n+1} to be the collection of vertices of the segments of S^{n+1}. Figure 2.1(b) shows S^2 and V^2, while Figure 2.1(c) shows S^3 and V^3.

Remark 1. *The base angle θ of the isosceles triangle placed over the center of any segment is independent of the iteration and the orientation of the triangle. Thus, we may determine the value of θ as a function of α by considering the isosceles triangle in the first iteration. Since the base length is $l(\alpha-2)/\alpha$ and side length l/α, we find $\cos(\theta) = (\alpha-2)/2$. Moreover, the restriction on α (i.e., $\alpha \in (2,4]$) implies $\theta \in (0, \pi/2]$. Because this restriction on θ gives a unique inverse of cosine, we have*

$$\theta = \cos^{-1}\left(\frac{\alpha-2}{2}\right) = \cos^{-1}\left(\frac{\alpha}{2} - 1\right).$$

Remark 2. *As the number of iterations increases, the number of segments and vertices increases. However, only the sequence of sets of vertices are nested. It is for this reason that we will think of the Koch curve as a collection of vertices.*

It is visually apparent that this process creates a self-similar shape. More importantly, however, is the extent to which this shape is self-similar. This iterative process essentially creates four scaled copies of the vertex and segment sets, rotates them to the proper angle, and then translates copies into the correct position (see the contractive similitudes in Section 2.2 for a rigorous definition). It is in this light which we give the definition of the Koch curve.

2.2 Rigorous Definition of the Koch Curve

Let $\alpha \in (2,4]$ and define $\theta = \cos^{-1}\left(\frac{\alpha}{2} - 1\right)$. Define $\{\psi_1, \psi_2, \psi_3, \psi_4\}$ to be the following contractive similitudes:

$$\psi_1(z) = \tfrac{z}{\alpha}, \qquad \psi_2(z) = \tfrac{z}{\alpha}e^{i\theta} + \tfrac{1}{\alpha},$$
$$\psi_3(z) = \tfrac{z}{\alpha}e^{-i\theta} + \tfrac{1}{2} + \tfrac{i}{\alpha}\sin\theta, \quad \psi_4(z) = \tfrac{z+\alpha-1}{\alpha},$$

for $z \in \mathbb{C}$. See Figure 2.2 for a visualization of the contractive similitudes applied to a segment with varied α values.

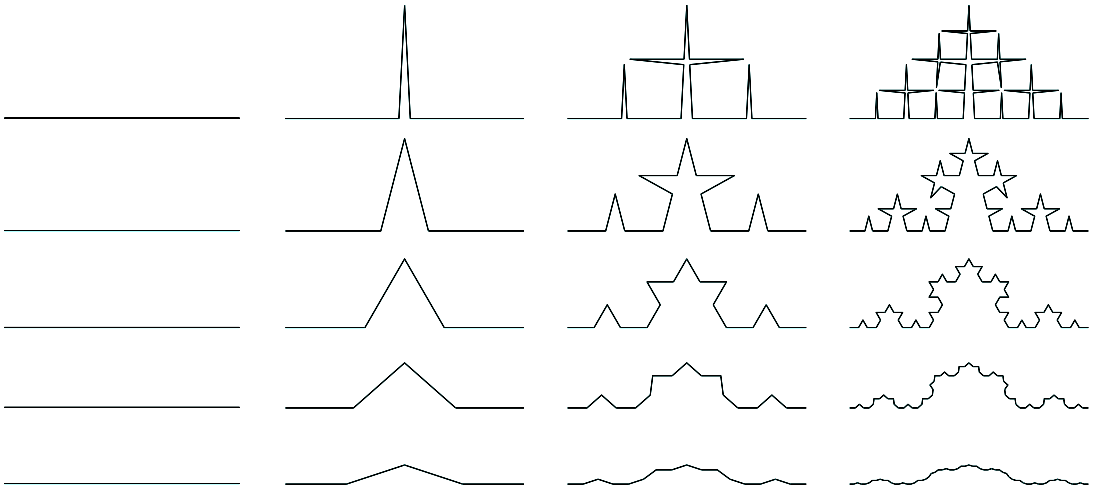

Figure 2.2: A visualization of the contractive similitudes for various α. Lines 1 – 5 have α values 2.1, 2.5, 3, 3.5, and 3.9, respectively. Columns 1 – 4 are iterations $n = 0$, $n = 1$, $n = 2$, and $n = 3$, respectively. Notice that the prefractal gets sharper as α approaches two and smoother as α approaches four.

For each positive integer n, consider arbitrary n-tuples of indices

$$i|n = (i_1, i_2, i_3, \ldots, i_n)$$

where each $i_m \in \{1, 2, 3, 4\}$. Define $\psi_{i|n}(z) = (\psi_{i_1} \circ \psi_{i_2} \circ \cdots \circ \psi_{i_n})(z)$ and, for any set $G \subset \mathbb{R}$, let $G_{i|n} = \psi_{i|n}(G)$.

Remark 3. *We can think of this process as creating an "address" for each vertex along the fractal.*

Now we generalize to an arbitrary line segment of $\mathbb{R}^2$. Let P_1 and P_2 be the endpoints of

our line segment in $\mathbb{R}^2$ and define $V_0 = \{P_1, P_2\}$. For each integer positive integer n, let

$$V^n = \bigcup_{i|n} V^0_{i|n}.$$

Set

$$V^\infty = \bigcup_{n=0}^{\infty} V^n$$

and define K to be the closure of V^∞ in $\mathbb{R}^2$. The set K is the Koch curve.

Although we will consider the Koch curve as the collection of vertices, we will need the notion of each prefractal step K^n (i.e., the collection the vertices V^i and segments S^i) being a polygonal curve defined by the vertices V^n and segments S^n in the previous section.

2.3 Building the Mesh

The key to our construction involves triangulating the domain. We say this is the key to our construction because we will extend the function piecewise over our triangulation.

As we triangulate the domain, we will seek a triangulation which minimizes the types of elements (e.g., to just triangles or quadrilaterals) and to minimize the classes of elements within these types (e.g., similar isosceles triangles). In particular, we restrict our mesh to only triangles. Achieving both these conditions will allow us to classify portions of the grid. Moreover, this triangulation will serve as a scaffolding for our extension. In addition to these properties, we will require a scaffolding that is self-similar.

2.3.1 Polygonal Domain Mesh Generation in the Context of Our Problem. Creating a discretization of an arbitrary domain is an art with many sophisticated techniques. One of the primary techniques is the use of polygons to construct conforming and nonconforming grids. Conforming triangulations are ones in which no vertex is attached to the middle of an edge, while nonconforming triangulations are ones in which a vertex is attached to the middle of an edge of one of the elements of the mesh. We illustrate this idea with

Figure 2.3. Notice that the left triangulation is conforming while the right triangulation is a nonconforming.

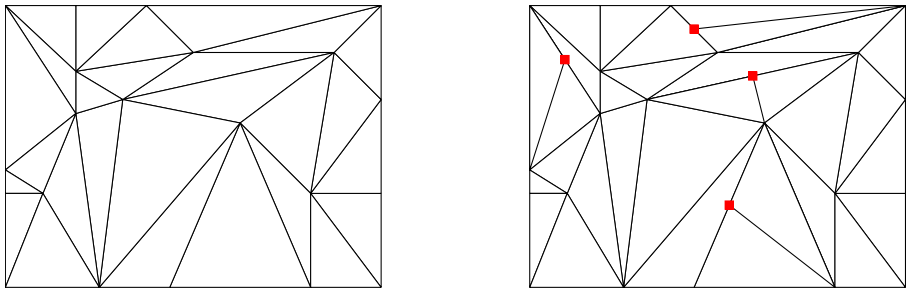

(a) conforming triangulation (b) nonconforming triangulation

Figure 2.3: An Example of Conforming and Nonconforming Triangulations

One factor which will influence our choice of the triangulation is the aspect ratio. The aspect ratio of a mesh element is the ratio of the longest side to the shortest side. When applied to triangles, the aspect ratio is essentially a measure of the set of resulting angles in our mesh. In practice, this means the aspect ratio is close to one if all of the angles are relatively close in value, and that one angle is substantially smaller than the others when the aspect ratio is relatively large. Our goal is to avoid triangles with large aspect ratios because these triangles provide poor seminorm estimates.

As noted multiple times, the key property we need is self-similarity because each prefractal is self-similar. Maximizing self-similarity minimizes the number of spacial relationships and enables us to tile regions of the plane without running an excessive number of refinement algorithms. Together, these properties maximize computational efficiency.

One way to approach these goals is with a Delaunay triangulation. This classic triangulation, designed by Boris Delaunay in 1934 for crystallography, addresses each of these concerns in a certain respect and remains one of the standard methods for triangulating domains. His method is built around the principle that the interior of the circumcircle of any triangle contains no other vertex used in the triangulation. This condition is a great tool because it maximizes the minimum angle across all elements used in the triangulation, meaning we avoid poor aspect ratios. In addition, this method also ensures a coarse structure

on the triangulation if we start with the right number of well-placed points. Moreover, the coarse structure keeps the number of relations between the elements relatively small. While we won't use a Delaunay triangulation for our mesh, we will apply this method to sets of points on our fractal to gain insight into a triangulation we should use.

Figure 2.4 captures a number of insights. First and foremost, given any polygonal domain $\Omega \subset \mathbb{R}^2$, we will associate with it a polygonal mesh, $\mathcal{T}$, so that (i) the closure of Ω is the union of these polygons, (ii) the interiors of the polygons are nonempty, and (iii) the interiors of the polygons are disjoint. If we were to restrict ourselves to only these conditions, we would likely get column one of Figure 2.4 because general triangulations use randomly selected points to triangulate with. This sequence of grids, however, is clearly no good for our current situation because we have assumed each is embedded in the domain, meaning we should expect self-similarity.

Now we consider columns two and three of Figure 2.4. Given only these two choices, the sequence of grids in column three appears to be a better triangulation for multiple reasons. All of the triangulations in columns two and three use points of the prefractal to determine the triangulation, but the triangulations are drastically different. At first glance, you notice that the aspect ratio of the triangles in column two is horrendous; in addition, there is little uniformity among the elements. In contrast, the triangulation of column three uses the largest number of points along the prefractal to determine the triangulation; this allows the triangulation to minimize the number of distinct elements while striving for self-similarity.

As it turns out, neither triangulation is well-suited for our work because tiling regions with either of these patterns will require additional refinement along the boundaries. Moreover, neither the number of triangle types nor the aspect ratio of either triangulation is bounded. Even though neither triangulation is optimal for our situation, the key lies in the commonality of these grids.

The first observation we make is that the more "equally spaced" (or, "predictably placed") points we have, the better the aspect ratio of our elements becomes. The second observation

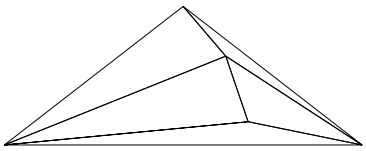

(a) $n = 1$ Delaunay triangulation with 5 random points

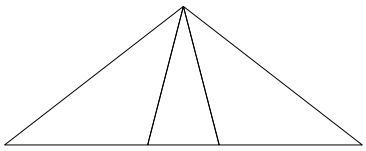

(b) $n = 1$ Delaunay triangulation with 5 Koch curve boundary points

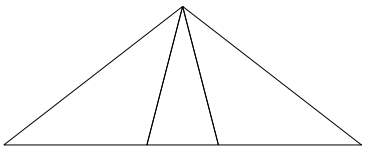

(c) $n = 1$ Delaunay triangulation with 5 Koch curve vertices

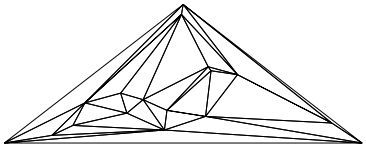

(d) $n = 2$ Delaunay triangulation with 17 random points

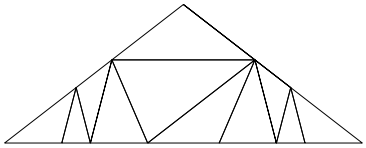

(e) $n = 2$ Delaunay triangulation with 13 Koch curve boundary points

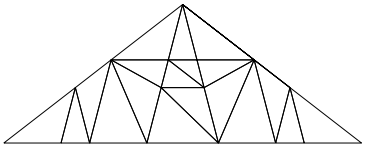

(f) $n = 2$ Delaunay triangulation with 17 Koch curve vertices

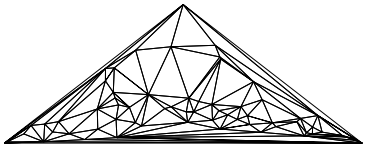

(g) $n = 3$ Delaunay triangulation with 65 random points

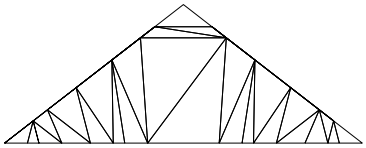

(h) $n = 3$ Delaunay triangulation with 29 Koch curve boundary points

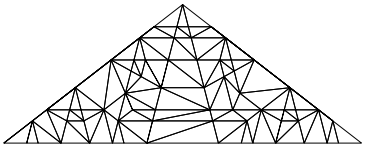

(i) $n = 3$ Delaunay triangulation with 65 Koch curve vertices

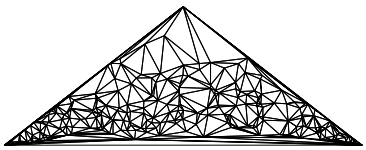

(j) $n = 4$ Delaunay triangulation with 257 random points

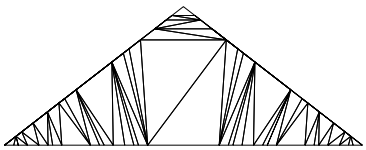

(k) $n = 4$ Delaunay triangulation with 61 Koch curve boundary points

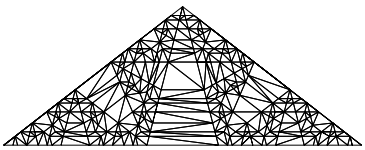

(l) $n = 4$ Delaunay triangulation with 257 Koch curve vertices

Figure 2.4: Automatic Triangulations of the Prefractal

is the self-similarity apparent in the triangulations. First, notice that the $n = 1$ triangulations are identical; this, by itself, is not notable, but the lower left corners of both grid schemes for $n = 2$, $n = 3$, and $n = 4$ are similar to the $n = 1$ grids. Finally, we must observe that the more points we have implies the grid will tend towards being similar; the triangulation in Figure 2.4(i) is clearly trying to consist of two types of triangles, namely the two triangles which occur in the $n = 1$ grids, but fails to achieve such a goal because of lack of points to triangulate with. We overcome these difficulties in the next section.

2.3.2 Triangulating the Triangle. In Section 2.3.1, we introduced a triangular region upon which the Koch curve was to be discretized. In this section, we formally define this region, which we will term the intermediate domain, and follow it with a rigorous description of the triangulation. This section follows that given by Evans in [14].

We define the intermediate domain, i.e., the triangular domain, to have coordinates $(0, 0)$, $(1, 0)$, and $(1/2, \sin(\theta)/\alpha)$, where $\theta = \cos^{-1}(\alpha/2 - 1)$. These vertices correspond to three of the five vertices along the first prefractal of the Koch curve (see Figure 2.5 for a visualization). The center triangle defined by the prefractal Koch curve from Figure 2.5(b) will be referred to as the main triangle. Based on the orientation specified in this figure, we will refer to the horizontal segment as the "base" and the remaining edges as the "sides".

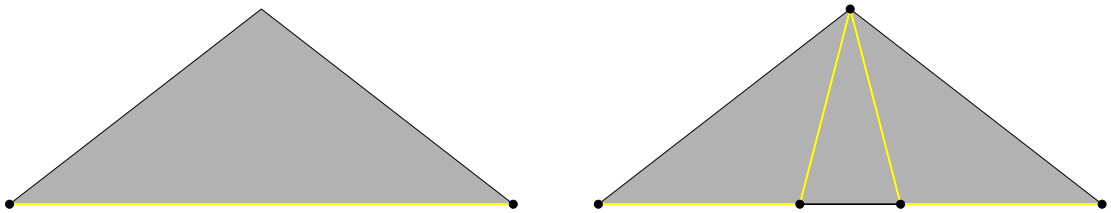

(a) $n = 0$ Koch curve in the intermediate domain.

(b) $n = 1$ Koch curve in the intermediate domain.

Figure 2.5: This figure represents the intermediate domain. As noted previously, the vertex set V^n is contained within V^{n+1}, so $(0, 0)$ and $(1, 0)$ are the two points shown on Figure 2.5(a). The third point defining the domain, namely $(1/2, \sin(\theta)/\alpha)$, is the highest point on Figure 2.5(b).

Now we address the question of triangulating this domain for any iteration. Given an iteration n, our previous description of the Koch curve gives a unique prefractal which lies within this. Because we have restricted our choice of α to values of the form $2 + 1/m$ for $m \in \mathbb{Z}$, we define $T := 2m + 1$ and declare T to be the number of similar triangles we place along the base of the main triangle, where the outermost vertices of these T triangles coincide with the vertices of the base segment. This construction then allows us to place $T^2 - T$ additional similar triangles within the main triangle; this gives a total of T^2 triangles filling the main triangle. See Figure 2.6 for a visualization as the iteration and complexity of the prefractal increase.

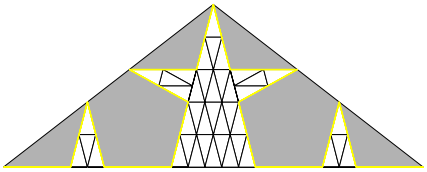

Figure 2.6: This figure illustrates the first step in filling the area of the intermediate domain. In this case, $T = 5$ and $m = 2$.

The second step in filling the areas uses the diagonal segments in the intermediate domain. We place a prefractal Koch curve which is one step behind the current iteration and its associated mesh along each of the diagonals. This has the effect of taking a scaled version of the left third of the horizontal and placing it along the diagonal as can be seen in Figure 2.7.

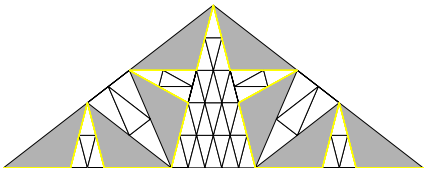

Figure 2.7: This figure illustrates the second step in filling the area of the intermediate domain. In this case, $T = 5$ and $m = 2$.

The third and final step in the subdivision fills the remaining gray area. For $n \geq 2$, the remaining gray regions get subdivided into 4^{n-1} triangles similar to the current gray region we are filling. See Figure 2.8 for an illustration of this process.

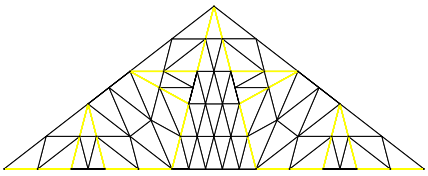

Figure 2.8: This figure illustrates the final step in filling the area of the intermediate domain. In this case, $T = 5$ and $m = 2$.

2.3.3 Triangulating the Diamond Domain ω. The diamond domain is the diamond consisting of eighteen copies of the intermediate domain arranged as in Figure 2.9.

We triangulate this domain using the triangulation provided by Section 2.3.2 on each of the eighteen triangles. After triangulating ω in this fashion, we subdivide each element

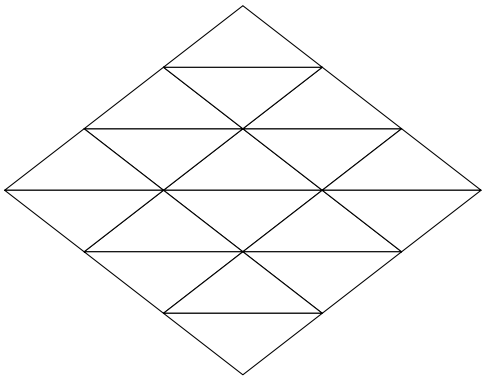

Figure 2.9: The diamond domain, ω, is eighteen copies of ω_Δ in this arrangement.

of the mesh into four similar triangles. We do this to preserve continuity throughout the extension function, as will be demonstrated in the next chapter.

Chapter 3. Defining the Extension Function

The definition of our extension function is critical to the argument following this chapter. Thus we give an extensive treatment of this topic.

It is natural to ask whether Hölder continuous functions[1] over fractal sets even exist. In particular, we are curious to know if Hölder continuous functions exist over an arbitrary Koch curve with contraction factor α. As it turns out, Lancia and Vivaldi show that such functions exist in [10]. Thus, we take the existence of our function to extend as given in the following discussion.

First and foremost, we will require that the extension function is linearly affine along the line segments connecting the vertices of the Koch curve. After this requirement has been met, we will require that the extension function is linearly affine across each of the faces in the triangulation. Individually, neither of these conditions guarantee continuity of the extension from the prefractal into the region over our given mesh defined in Section 2.3.3. Together, however, the conditions applied in this order guarantee continuity of the extension function. As we will see, these conditions will be sufficient to preserve β-Hölder continuity throughout the region if we assume existence of a Hölder continuous function on the fractal.

Along with these assumptions, we will also require an inheritance property over portions of the domain. This property will help us bound the seminorm[2] estimates.

All figures in this chapter are given without the subdivision step described in Section 2.3.3.

[1] A function f is $\beta-$Hölder continuous on A if there is a $C \in \mathbb{R}$ so that

$$|f(X) - f(Y)| \leq C|X - Y|^{\beta}$$

for all $X, Y \in A$ and some $\beta \in (0, 1]$. The C is the Hölder seminorm.

[2] The Hölder seminorm is $|u|_{A,\beta} = \sup_{\substack{X_1, X_2 \in A \\ X_1 \neq X_2}} \frac{|u(X_1) - u(X_2)|}{|X_1 - X_2|^{\beta}}$.

3.1 The First and Second Colorings of the Mesh

We begin the discussion of the extension function with two separate colorings of the mesh for any given $n \geq 0$. The first coloring scheme will be used for theoretical purposes only, while the second scheme gives insight into how we would go about constructing the extension function computationally. Both color schemes have there merits, and we will switch between them as needed.

3.1.1 The First Coloring. The first coloring of the mesh separates the mesh into three categories with three colors. The first category, namely red triangles, are triangles adjacent to the prefractal; we will call a triangle in this set a primary sidecar triangle and denote the set of all primary sidecar triangles by ω_{SC}. A triangle in this set must have at least one vertex of the mesh along the prefractal. The second set of triangles, namely the white triangles, is the set of triangles adjacent to the set of primary sidecar triangles; we will call a triangle in this set a transition triangle and will denote the set of all transition triangles as ω_{TR}. Finally, the third set of triangles, namely the blue triangles, are all of the triangles not contained in the previous sets; we will call a triangle in this set an exterior triangle and will denote the set of all exterior triangles by ω_{EX}. See Figure 3.1(a) for a visualization of this separation.

One aspect of this coloring you will notice from Figure 3.1(a) is that select triangles of ω_{TR} have three vertices in common with triangles of ω_{SC} (these triangles are denoted by the green triangles in Figure 3.1(b)). As noted in the opening statements of this chapter, our extension function will be linear affine across the faces, so triangles which have all three vertices determined by an earlier average should be included within that set. Thus the green triangles should be regrouped with the primary sidecar triangles of ω_{SC} as in Figure 3.1(c). It is from this standpoint that we separate the mesh henceforth.

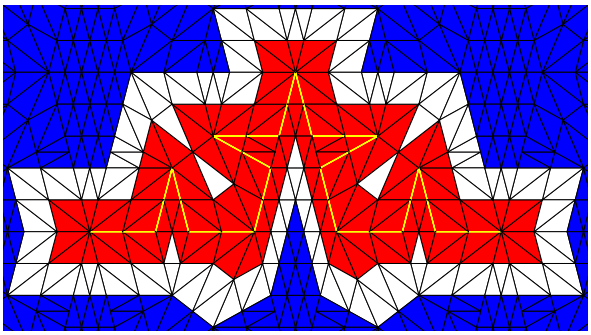

(a) This figure represents the set of primary sidecar triangles in red; the transition triangles in white; and the exterior triangles in blue. In this case, $\alpha = 2.5$ and $n = 2$.

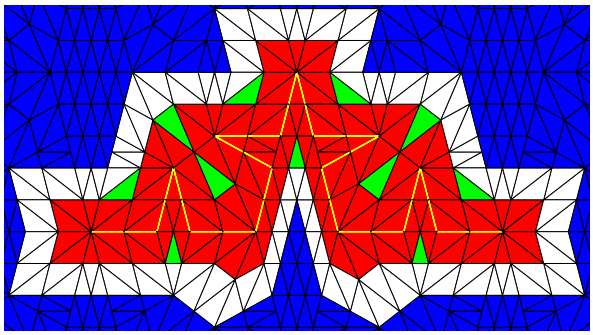

(b) This figure represents the splitting of ω_{TR} into two sets. The green set of triangles share all three vertices with triangles of ω_{SC} while the white triangles have at most two vertices in common with the triangles of ω_{SC}. In this case, $\alpha = 2.5$ and $n = 2$.

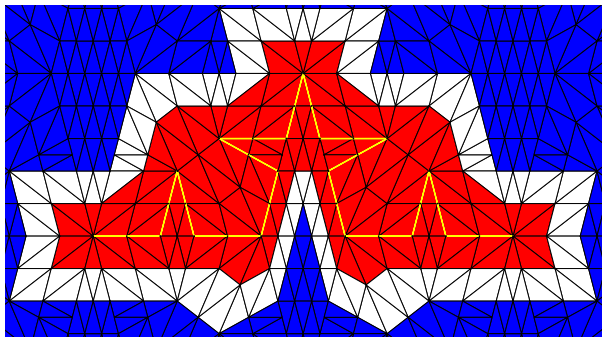

(c) This figure represents the regrouping of the predetermined transition triangles with the primary sidecar triangles. In this case, $\alpha = 2.5$ and $n = 2$.

Figure 3.1: A visualization of the first coloring scheme after regrouping the predefined triangles of ω_{TR} with ω_{SC}.

3.1.2 The Second Coloring. The second coloring of the mesh separates the mesh into eight colors based on the order in which the extension function is defined. We begin by separating the triangles into the three sets sets from the first coloring, namely ω_{SC}, ω_{TR}, and ω_{EX}. We further subdivide ω_{SC} (i.e., the red triangles of Figure 3.1(c)) into six sets.

(i) The first subset of ω_{SC}, denoted by ω_{SC_0}, are the magenta triangles of Figure 3.2. The extension function will first extend in these triangles.

(ii) The second subset of ω_{SC}, denoted by ω_{SC_1}, is the set of green triangles of Figure 3.2. The extension function extends to these triangles after one application of our affine extension process using the vertices of the prefractal Koch curve.

(iii) The third subset of ω_{SC}, denoted by ω_{SC_2}, is the set of dark gray triangles of Figure 3.2. The extension function extends to these triangles after two applications of our affine extension process using the vertices of the prefractal Koch curve.

(iv) The fourth subset of ω_{SC}, denoted by ω_{SC_3}, is the set of cyan triangles of Figure 3.2. The extension function extends to these triangles after three applications of our affine extension process using the vertices of the prefractal Koch curve.

(v) The fifth subset of ω_{SC}, denoted by ω_{SC_4}, is the set of yellow triangles of Figure 3.2. The extension function extends to these triangles after four applications of our affine extension process using the vertices of the prefractal Koch curve.

(vi) The sixth subset of ω_{SC}, denoted by ω_{SC_5}, is the set of brown triangles of Figure 3.2. The extension function extends to these triangles after five applications of our affine extension process using the vertices of the prefractal Koch curve.

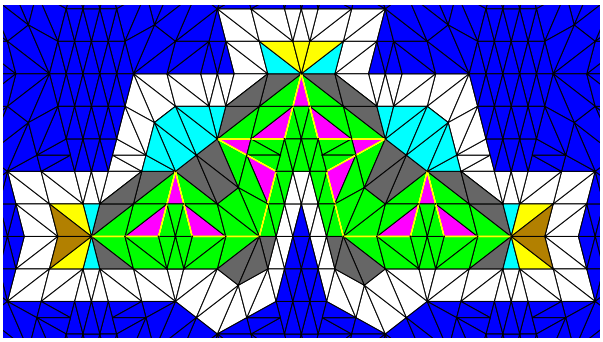

Figure 3.2: ω_{SC_0} is the set of magenta triangles; ω_{SC_1} is the set of green triangles; ω_{SC_2} is the set of dark gray triangles; ω_{SC_3} is the set of cyan triangles; ω_{SC_4} is the set of yellow triangles; and ω_{SC_5} is the set of brown triangles; ω_{TR} is the set of white triangles; ω_{EX} is the set of blue triangles.

We make the preceding statements precise in the following section.

We now have eight sets of triangles—namely ω_{SC_0}, ω_{SC_1}, ω_{SC_2}, ω_{SC_3}, ω_{SC_4}, ω_{SC_5}, ω_{TR}, and ω_{EX}—which make up ω; we note that

$$\omega_{SC} = \bigcup_{i=0}^{5} \omega_{SC_i} \qquad \text{and} \qquad \omega = \omega_{SC} \cup \omega_{TR} \cup \omega_{EX}.$$

We compute the extension in the following manner.

(i) Define the sets of triangles as described above.

(ii) Compute the values of the extension function on ω_{SC_i}.

(iii) Inherit the values of the extension function on ω_{EX} (this will be described in greater detail in the next section).

(iv) Compute the value of the extension function on ω_{TR} based on the values of $u_n^\star$ at the vertices of ω_{SC} and ω_{EX}.

3.2 Definition of the Extension Function

Now that we have a visual idea of the extension function, we make a rigorous definition of the extension. We will use the notation $\Pi_n u$ or $u_n^\star$ to refer to the extension function at iteration n.

3.2.1 Determining the Values of $u_n^\star$ at Vertices and Along Faces. Values at the vertices of the triangulation fall into one of three categories. Given a vertex X in the triangulation, either (i) $u_n^\star(X)$ is prescribed by the Hölder continuous function along K; (ii) $u_n^\star(X)$ is determined by the values of $u_n^\star$ at the vertices adjacent to X; or (iii) $u_n^\star(X)$ is inherited from the previous extension function.

Values of $u_n^\star$ which are part of category (i) are predetermined by the Hölder continuous function u on K. For any given n, there are exactly 4^n+1 vertices of the triangulation which have a value prescribed by u. The blue vertices of Figure 3.3 correspond to this category of vertices. After setting the values at vertices in category (i), we define $u_n^\star$ to be linearly affine along each edge of the Koch curve. This leads us to category (ii).

Values of $u_n^\star$ which are part of category (ii) are interpolated from the values of $u_n^\star$ at adjacent vertices. Vertices in this category are colored yellow in Figure 3.3.

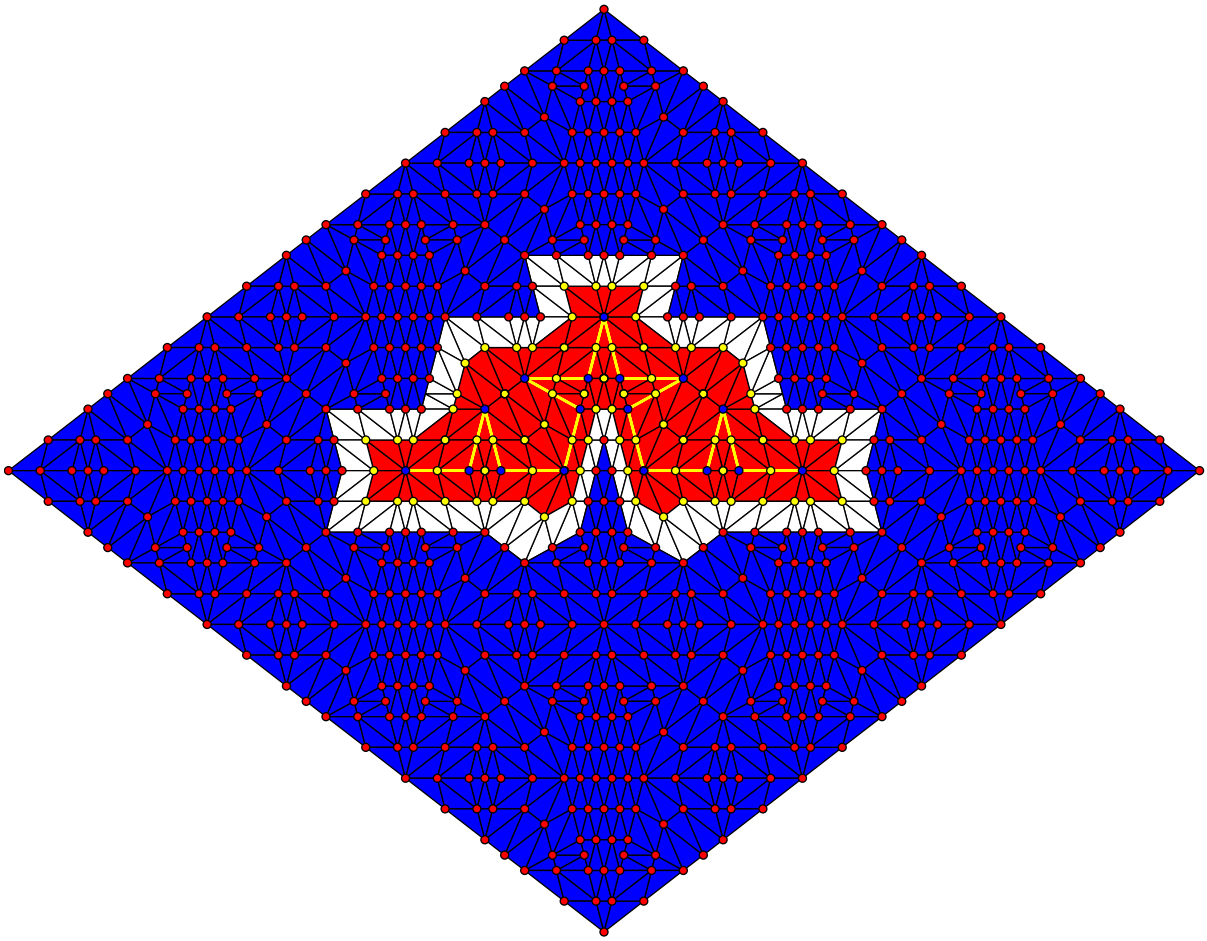

Figure 3.3: Values of $u_n^\star$ at the blue vertices are determined by the Hölder continuous function u. Values $u_n^\star$ at the red vertices are inherited from the previous extension function. Values of $u_n^\star$ at the yellow vertices are obtained through averaging the values of $u_n^\star$ at the known adjacent vertices. Notice how the vertex separation corresponds to the separation of the domain.

Finally, values of $u_n^\star$ which are part of category (iii) are inherited the previous extension function. Obtaining values of $u_n^\star$ therefore reduces to separating the domain as described in Section 3.1.1, identifying the vertices of the blue triangles with their location in the previous mesh, and then "lifting" the values $u_{n-1}^\star$ so that $u_{n-1}^\star(X) = u_n^\star(X)$ for every $X \in \omega_{EX}$. Vertices in which $u_n^\star$ is determined with this method are colored red in Figure 3.3.

As we determine the values of $u_n^\star$ at the vertices of $\mathcal{T}$, we define $u_n^\star$ to be linearly affine across each face once all three vertices of the face have a value of $u_n^\star$ prescribed. It is clear that this definition of $u_n^\star$ maintains continuity for each n. It is also clear that values of $u_n^\star$

in ω_{EX} are determined first because these values are inherited from the previous extension function $u^\star_{n-1}$; the values of $u^\star_n$ in ω_{SC} are the second to be determined using the affine process from above. Finally, the values of $u^\star_n$ on ω_{TR} are determined last, by using the values of $u^\star_n$ restricted to $\omega_{SC} \cup \omega_{EX}$.

3.2.2 The Initial Extension Function $u^\star_0$. We define the initial extension function $u^\star_0$ so that $u^\star_0(\partial\omega) = 0$. For the remaining vertices of $\mathcal{T}$, we set the values of $u^\star_n$ using the averaging process described in Section 3.2.1. This is the only extension function which disregards the coloring scheme provided by Section 3.1.1. Furthermore, define $u^\star_0(\Omega \setminus \omega) = 0$.

3.2.3 Subsequent $u^\star_n$. For all other extension functions $u^\star_n$, we construct the mesh as described in Sections 2.3.2 and 2.3.3 and then apply the process detailed in Section 3.2.1 to obtain values of $u^\star_n$ at each point of ω. As noted previously, this definition of $u^\star_n$ is constructs a well-defined continuous function at each vertex and across each edge in the triangulation of ω. We define $u^\star_n(\Omega \setminus \omega) = 0$ for n and hold $u^\star_n(\partial\omega) = 0$ at each iteration. Thus any extension affecting the values along the boundary are disregarded and redefined to satisfy this property.

In addition, some vertices (i.e., the hanging nodes) in the mesh will create crimps along faces of the triangulation. To avoid this irregularity in our method and preserve the linear affine property, we extend linearly along the edge through the two defined vertices to obtain the third. This process changes none of the process described above.

Chapter 4. Preliminary Definitions and Lemmas

This chapter states and proves the preliminary estimates on the Hölder seminorm necessary for the main result. As the definition of our extension function clearly implies continuity and bounded Hölder seminorm for $0 \leq n \leq 2$, we provide the following arguments and statements for $n \geq 3$. Sections 4.2 and 4.3 deal with bounding the seminorm over the various categories depicted in Figure 4.2.

4.1 Reference Triangles, Their Relationships, and Their Affine Function

For sake of ease, we define two types of triangles—Type 1 and Type 2—as shown in Figure 4.1. These triangles satisfy the relationships as described in Section 2.3.2; see Figure 2.5(b) for a visual representation of these relationships.

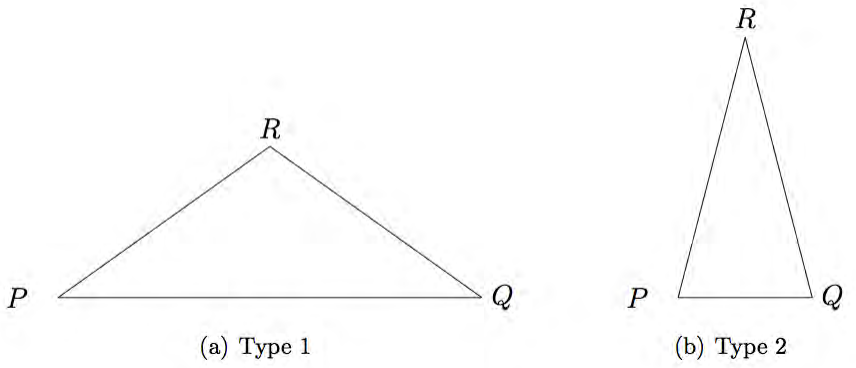

Figure 4.1: The Two Types of Triangles

In each of the following lemmas, we make use of five facts.

(i) Given two distinct points $X_1(x_1, y_1)$ and $X_2(x_2, y_2)$, the horizontal and vertical change between X_1 and X_2 is no greater than the total distance between X_1 and X_2.

(ii) Since $\alpha = 2 + 1/m$ for some $m \in \mathbb{N}$, we have $\sqrt{4 - (\alpha - 2)^2} \geq \sqrt{3}$, $\sqrt{4 - \alpha} \geq 1$, $\sqrt{\alpha} \leq 2$, and $\alpha - 2 \leq 1$.

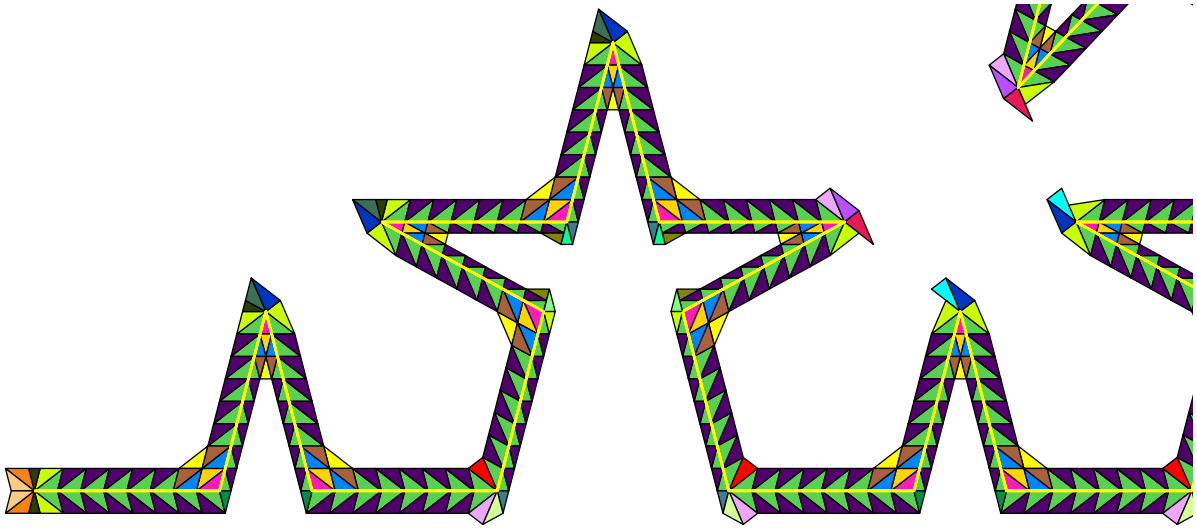

(a) This figure represents a complete classification of ω_{SC} for any prefractal in iteration $n \geq 3$. The triangles are first classified by shape, thus giving the two classes of triangles given by Figure 4.1. Within each class, we categorize the triangles by color to denote which calculations of the Hölder seminorm are similar. We repeat colors between the subcategories to limit the number of colors. This classification system will allow us to compute seminorm estimates in the limit for ω_{SC}.

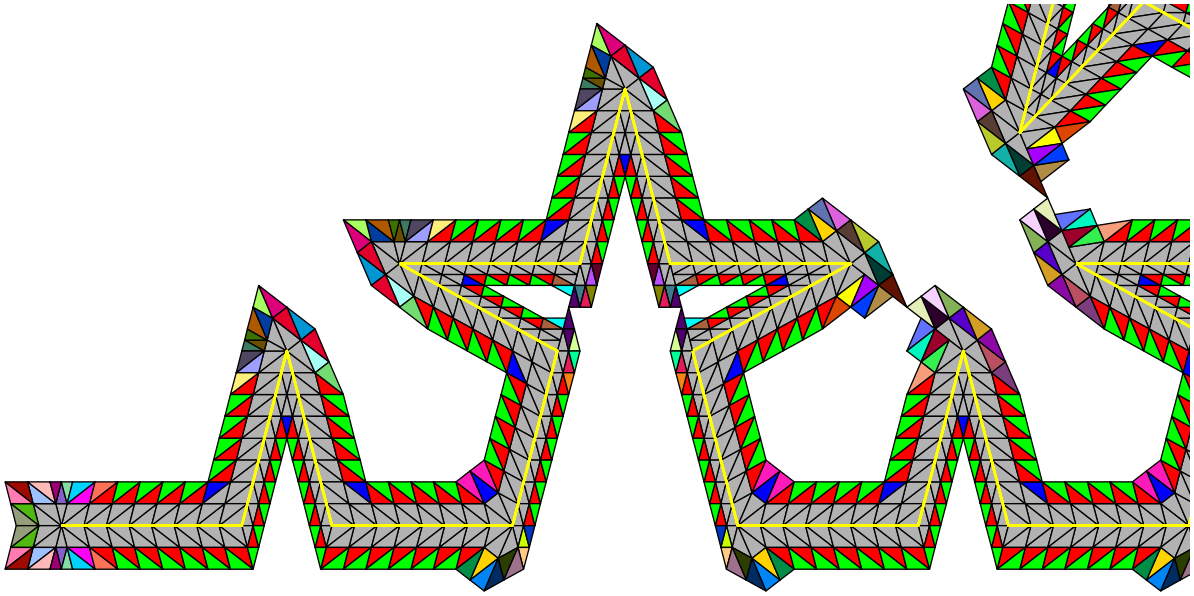

(b) This figure represents a complete classification of ω_{TR} for any prefractal in iteration $n \geq 3$. The triangles are first classified by shape, thus giving the two classes of triangles given by Figure 4.1. Within each class, we categorize the triangles by color to denote which calculations of the Hölder seminorm are similar. We repeat colors between the subcategories to limit the number of colors. This classification system will allow us to compute seminorm estimates in the limit for ω_{TR}.

Figure 4.2: A Complete Classification of ω_{SC} and ω_{TR} for $n \geq 3$

(iii) Both types of triangles are isosceles, hence $|P-R| = |Q-R|$ for both types of triangles.

(iv) Set $\theta = \cos^{-1}(\alpha/2 - 1)$. It is easy to see that $|P - R|$ of the outer most type 1 triangle satisfies

$$|P - R|^2 = \left(\frac{1}{2}\right)^2 + \left(\frac{\sqrt{4-(\alpha-2)^2}}{2\alpha}\right)^2.$$

Solving for $|P - R|$ implies $|P - R| = 1/\sqrt{\alpha}$. Thus

$$\sin(\theta/2) = \frac{\sqrt{4-(\alpha-2)^2}/2\alpha}{1/\sqrt{\alpha}} = \frac{\sqrt{4-\alpha}}{2}.$$

From the above we can also see that

$$\cos(\theta/2) = \frac{1/2}{1/\sqrt{\alpha}} = \frac{\sqrt{\alpha}}{2}.$$

(v) Since we only have two type of triangles in our mesh, we can use Figure 2.5(b) to determine the relationships. Considering the type two central triangle, we get $|P-R| = 1/\alpha$ and $|P-Q| = (\alpha-2)/\alpha$, so $|P-Q|/|R-P| = (\alpha-2)$, or $|P-Q| = (\alpha-2)|P-R|$. For the overall type 2 triangle, we have $|P - Q| = 1$ and $\cos(\theta/2) = |P - Q|/2|P - R|$. Plugging in $\cos(\theta/2)$ and solving for $|P - R|$ implies $|P - Q| = \sqrt{\alpha}|P - R|$.

Finally, we define two reference triangles—one for each type of triangle—with vertex P located at the origin, vertex Q located along the positive x-axis, and vertex R lying in the first quadrant; we call such a reference triangle T and it will be clear from context which type of triangle T refers too.

If T is type 1, it is clear that the coordinate of P are $(0, 0, u(P))$, that the coordinate of Q are $(|Q - P|, 0, u(Q))$, and that the coordinates of R are $(|Q - P|/2, |Q - P|\sin(\theta/2)/\sqrt{\alpha}, u(R))$. To construct the affine function, we create a plane using the three coordinates at the vertices. For this triangle, we have vectors $Q-P = (|Q-P|, 0, u(Q)-u(P))$ and $R - P = (|Q - P|/2, |Q - P|\sin(\theta/2)/\sqrt{\alpha}, u(R) - u(P))$. Crossing the vectors gives the

normal vector, and we have

$$\begin{aligned} N &= (Q-P)\times(R-P) \\ &= \left(\frac{|Q-P|\sin\left(\frac{\theta}{2}\right)(u(P)-u(Q))}{\sqrt{\alpha}}, -\frac{|Q-P|(2u(R)-u(Q)-u(P))}{2}, \frac{|Q-P|^2\sin\left(\frac{\theta}{2}\right)}{\sqrt{\alpha}} \right). \end{aligned}$$

Since a plane is given by $N\cdot X = N\cdot P$ where $X=(x,y,z)$ and P is any point on the plane, choosing P to be our point at the origin gives

$$\begin{aligned} \frac{|Q-P|\sin\left(\frac{\theta}{2}\right)(u(P)-u(Q))}{\sqrt{\alpha}}x - \frac{|Q-P|(2u(R)-u(Q)-u(P))}{2}y \\ + \frac{|Q-P|^2\sin\left(\frac{\theta}{2}\right)}{\sqrt{\alpha}}z = \frac{|Q-P|^2\sin\left(\frac{\theta}{2}\right)}{\sqrt{\alpha}}u(P). \end{aligned}$$

Solving for z and simplifying gives

$$z = u(P) + \left[\frac{u(Q)-u(P)}{|Q-P|}\right]x + \left[\frac{\sqrt{\alpha}(2u(R)-u(P)-u(Q))}{\sqrt{4-\alpha}|Q-P|}\right]y \tag{4.1}$$

as the affine function across Type 1 triangles.

If T is a type 2, we set P and Q as they were before, but change the middle coordinate of R to be $|Q-P|\sin(\theta/2)\sqrt{\alpha}/(\alpha-2)$. Following an analogous argument, we have that the affine function across the Type 2 triangle as

$$z = u(P) + \left[\frac{u(Q)-u(P)}{|Q-P|}\right]x + \left[\frac{(\alpha-2)(2u(R)-u(P)-u(Q))}{\sqrt{4-(\alpha-2)^2}|Q-P|}\right]y. \tag{4.2}$$

4.2 Seminorm Estimates on the Primary Sidecar Triangles

The following lemmas consider the Hölder seminorm on the sets of triangles defined by the classification system in Figure 4.2(a). As the need for convention will quickly arise, we make a couple definitions. We say a point Y is between X and Z in a prefractal if $X,Z\in V^n$, Y is some vertex in the triangulation along the prefractal Koch curve, and, as you trace along

the prefractal from X to Z, you cross the vertex Y. We say X is left of Y in a prefractal if X is a vertex between $(0,0)$ and Y; similarly, we say Y is right of X in a prefractal if Y is a vertex between X and $(1,0)$. Finally, we say a triangle T is above the prefractal K^n if one or more vertices of T are vertices along the Koch curve and the interior of T lies entirely in the upper half plane defined by the continuous line K^n for $x \in [0,1]$ and $y = 0$ otherwise. We say a triangle T is below the prefractal K^n if one or more vertices of T are vertices along the Koch curve and the interior of T lies entirely in the lower half plane defined by the continuous line K^n for $x \in [0,1]$ and $y = 0$ otherwise.

Lemma 1. *Let T be a primary sidecar triangle with vertices P, Q, and R as depicted by any green triangle of Figure 4.3. Let $\beta \in (0,1]$ and u be a $\beta-$Hölder continuous function*

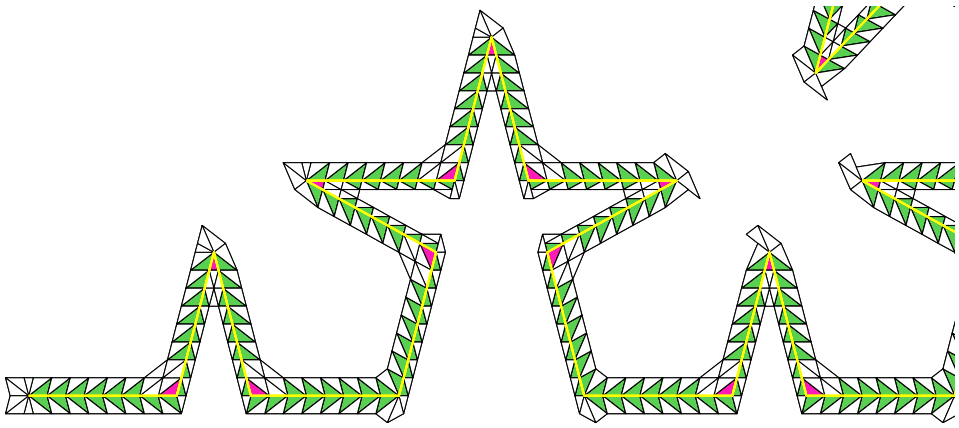

Figure 4.3: Cases for Lemma 1

defined on the vertices of the prefractal so that

$$\frac{|u(A) - u(B)|}{|A - B|^\beta} \leq |u|_{K,\beta}$$

for all $A, B \in V^n$. Then, for $n \geq 3$, $u_n^\star$ satisfies

$$\sup_{X,Y \in \mathcal{T}} \frac{|u_n^\star(X) - u_n^\star(Y)|}{|X - Y|^\beta} \leq 3(\alpha - 2)^{-1} |u|_{K,\beta}.$$

Proof. There are four cases to consider.

Case 1. This case considers type 1 triangles above K^n. Choose any triangle in this category and observe that two of the vertices lies along a segment of the prefractal which has exactly one pink type 1 triangle at the end. Label the vertex of V^n on this pink triangle as P_1 and the vertex at the other end of the segment P_2. Since $u_n^\star$ is affine along the segment set of K^n, each vertex X along this segment of the prefractal is a convex combination of $u(P_1)$ and $u(P_2)$, so that $u_n^\star(X)$ is defined as

$$u_n^\star(X) = \frac{k-i}{k}u(P_1) + \frac{i}{k}u(P_2),$$

where k is the number of elements along any segment of the prefractal and $i \in \{0, 1, \ldots, k\}$.

By symmetry in the estimates (as we will see momentarily), we further restrict our choice of T so that $u_n^\star(Q)$ and $u_n^\star(R)$ are defined by the process above. In this situation, we have

$$u_n^\star(Q) = \frac{k-i}{k}u(P_1) + \frac{i}{k}u(P_2), \qquad u_n^\star(R) = \frac{k-i+1}{k}u(P_1) + \frac{i-1}{k}u(P_2)$$

for $i \in \{3, 4, \ldots, k\}$. Moreover, since $u_n^\star(P)$ is defined as the average of adjacent $u_n^\star$ values, we immediately get that

$$u_n^\star(P) = \frac{1}{2}\left(u_n^\star(Q) + u_n^\star(R)\right) = \frac{2k-2i+1}{2k}u(P_1) + \frac{2i-1}{2k}u(P_2).$$

Choosing distinct $X_1, X_2 \in T$ with $X_1 = (x_1, y_1)$ and $X_2 = (x_2, y_2)$, the five facts of Section 4.1 and equation (4.1) gives

$$\begin{aligned}
\frac{|u_n^\star(X_1) - u_n^\star(X_2)|}{|X_1 - X_2|^\beta} &\leq \frac{|u_n^\star(P) - u_n^\star(Q)\|x_1 - x_2|}{|Q-P\|X_1 - X_2|^\beta} + \frac{\sqrt{\alpha}|2u_n^\star(R) - u_n^\star(P) - u_n^\star(Q)\|y_1 - y_2|}{\sqrt{4-\alpha}|Q-P\|X_1 - X_2|^\beta} \\
&\leq \frac{|u_n^\star(P) - u_n^\star(Q)\|x_1 - x_2|}{|Q-P\|X_1 - X_2|^\beta} + \frac{|4u_n^\star(R) - 2u_n^\star(P) - 2u_n^\star(Q)\|y_1 - y_2|}{\sqrt{4-\alpha}|Q-P\|X_1 - X_2|^\beta} \\
&\leq \frac{|u(P_1) - u(P_2)\|x_1 - x_2|}{2k|Q-P\|X_1 - X_2|^\beta} + \frac{3|u(P_1) - u(P_2)\|y_1 - y_2|}{k\sqrt{4-\alpha}|Q-P\|X_1 - X_2|^\beta}
\end{aligned} \tag{4.3}$$

Since $\alpha = 2 + 1/m$ for some $m \in \mathbb{N}$, we get that $1 \leq \sqrt{4-\alpha}$ and $\sqrt{2} \leq \sqrt{\alpha}$. Since type

1 triangles satisfy the relationship $|Q-P| = \sqrt{\alpha}|Q-R|$ and because there are exactly k segments of length $|Q-R|$ covering $|P_1-P_2|$, we immediately get that $|Q-P|$ and $|P_1-P_2|$ satisfy $|Q-P| = \sqrt{\alpha}|P_1-P_2|/k$. We also note that $|x_1-x_2|, |y_1-y_2| \leq |X_1-X_2| \leq |Q-P|$. The final observation we need is that $|A-B| = |A-B|^{\beta}|A-B|^{1-\beta}$. Using these facts and the hypotheses, (4.3) becomes

$$\begin{aligned}
\frac{|u_n^\star(X_1)-u_n^\star(X_2)|}{|X_1-X_2|^\beta} &\leq \frac{|u(P_1)-u(P_2)\|x_1-x_2|}{2\sqrt{\alpha}|P_1-P_2\|X_1-X_2|^\beta} + \frac{3|u(P_1)-u(P_2)\|y_1-y_2|}{\sqrt{\alpha}\sqrt{4-\alpha}|P_1-P_2\|X_1-X_2|^\beta} \\
&\leq \frac{|u(P_1)-u(P_2)\|x_1-x_2|}{2\sqrt{2}|P_1-P_2\|X_1-X_2|^\beta} + \frac{3|u(P_1)-u(P_2)\|y_1-y_2|}{\sqrt{2}|P_1-P_2\|X_1-X_2|^\beta} \\
&\leq \frac{|u(P_1)-u(P_2)|}{2\sqrt{2}|P_1-P_2|^\beta}\left(\frac{|x_1-x_2|}{|P_1-P_2|}\right)^{1-\beta}\left(\frac{|x_1-x_2|}{|X_1-X_2|}\right)^{\beta} \\
&\qquad + \frac{3|u(P_1)-u(P_2)|}{\sqrt{2}|P_1-P_2|^\beta}\left(\frac{|y_1-y_2|}{|P_1-P_2|}\right)^{1-\beta}\left(\frac{|y_1-y_2|}{|X_1-X_2|}\right)^{\beta} \\
&\leq \frac{|u(P_1)-u(P_2)|}{2\sqrt{2}|P_1-P_2|^\beta} + \frac{3|u(P_1)-u(P_2)|}{\sqrt{2}|P_1-P_2|^\beta} \\
&\leq \frac{1}{2\sqrt{2}}|u|_{K,\beta} + \frac{3}{\sqrt{2}}|u|_{K,\beta} \\
&= \frac{7}{2\sqrt{2}}|u|_{K,\beta} \\
&\leq 3(\alpha-2)^{-1}|u|_{K,\beta}.
\end{aligned}$$

As noted above, the symmetry of P and Q or $u(P)$ and $u(Q)$ inherent to the absolute values from above give the same upper bound from above if we instead had started with $u_n^\star(P)$ and $u_n^\star(Q)$.

Case 2. This case considers type 1 triangles below K^n. Using the same labeling scheme as in Case 1, only this time allowing $i \in \{1, 2, \ldots, k\}$, an identical argument gives

$$\frac{|u_n^\star(X_1)-u_n^\star(X_2)|}{|X_1-X_2|^\beta} \leq 3(\alpha-2)^{-1}|u|_{K,\beta}.$$

Case 3. This case considers type 2 triangles described in Figure 4.3 along a prefractal segment with a single pink type 2 triangle.

Begin by setting up an analogous labeling scheme as in Case 1 and consider an analogous restriction of T, namely that $u_n^\star(Q)$ and $u_n^\star(R)$ determine $u_n^\star(P)$. We immediately see that $u_n^\star(Q)$, $u_n^\star(R)$ and $u_n^\star(P)$ are defined in the same way. Thus

$$\begin{aligned}
u_n^\star(Q) &= \frac{k-i}{k}u(P_1) + \frac{i}{k}u(P_2),\\
u_n^\star(R) &= \frac{k-i+1}{k}u(P_1) + \frac{i-1}{k}u(P_2),\\
u_n^\star(P) &= \frac{2k-2i+1}{2k}u(P_1) + \frac{2i-1}{2k}u(P_2)
\end{aligned}$$

for $i \in \{3, 4, \ldots, k\}$.

Choosing distinct $X_1, X_2 \in T$ with $X_1 = (x_1, y_1)$ and $X_2 = (x_2, y_2)$, equation (4.2) gives

$$\begin{aligned}
\frac{|u_n^\star(X_1) - u_n^\star(X_2)|}{|X_1 - X_2|^\beta} &\leq \frac{|u_n^\star(P) - u_n^\star(Q)\|x_1 - x_2|}{|Q-P\|X_1 - X_2|^\beta} + \frac{(\alpha-2)|2u_n^\star(R) - u_n^\star(P) - u_n^\star(Q)\|y_1 - y_2|}{\sqrt{4-(\alpha-2)^2}|Q-P\|X_1 - X_2|^\beta}\\
&\leq \frac{|u_n^\star(P) - u_n^\star(Q)\|x_1 - x_2|}{|Q-P\|X_1 - X_2|^\beta} + \frac{|2u_n^\star(R) - u_n^\star(P) - u_n^\star(Q)\|y_1 - y_2|}{\sqrt{4-(\alpha-2)^2}|Q-P\|X_1 - X_2|^\beta}\\
&\leq \frac{|u(P_1) - u(P_2)\|x_1 - x_2|}{2k|Q-P\|X_1 - X_2|^\beta} + \frac{3|u(P_1) - u(P_2)\|y_1 - y_2|}{2k\sqrt{4-(\alpha-2)^2}|Q-P\|X_1 - X_2|^\beta}
\end{aligned}$$

Since $\alpha = 2 + 1/m$ for some $m \in \mathbb{N}$, we get that $\sqrt{3} \leq \sqrt{4-(\alpha-2)^2}$. Since type 2 triangles satisfy the relationship $|Q-P| = (\alpha-2)|Q-R|$ and because there are exactly k segments of length $|Q-R|$ covering $|P_1 - P_2|$, we immediately get that $|Q-P|$ and $|P_1-P_2|$ satisfy $|Q-P| = (\alpha-2)|P_1-P_2|/k$. We also note that $|x_1-x_2|, |y_1-y_2| \leq |X_1-X_2| \leq |Q-P|$. The final observation we need is that $|A-B| = |A-B|^\beta |A-B|^{1-\beta}$. Using these facts and the hypotheses, we have

$$\begin{aligned}
\frac{|u_n^\star(X_1) - u_n^\star(X_2)|}{|X_1 - X_2|^\beta} &\leq \frac{|u(P_1) - u(P_2)\|x_1 - x_2|}{2k|Q-P\|X_1 - X_2|^\beta} + \frac{\sqrt{3}|u(P_1) - u(P_2)\|y_1 - y_2|}{2k|Q-P\|X_1 - X_2|^\beta}\\
&\leq \frac{|u(P_1) - u(P_2)\|x_1 - x_2|}{2(\alpha-2)|P_1-P_2\|X_1 - X_2|^\beta} + \frac{\sqrt{3}|u(P_1) - u(P_2)\|y_1 - y_2|}{2(\alpha-2)|P_1-P_2\|X_1 - X_2|^\beta}\\
&\leq \frac{|u(P_1) - u(P_2)|}{2(\alpha-2)|P_1-P_2|^\beta} + \frac{\sqrt{3}|u(P_1) - u(P_2)|}{2(\alpha-2)|P_1-P_2|^\beta}
\end{aligned}$$

$$
\begin{aligned}
&\leq \frac{1}{2(\alpha-2)}|u|_{K,\beta} + \frac{\sqrt{3}}{2(\alpha-2)}|u|_{K,\beta} \\
&= \frac{1+\sqrt{3}}{2(\alpha-2)}|u|_{K,\beta} \\
&\leq 2(\alpha-2)^{-1}|u|_{K,\beta}.
\end{aligned}
$$

As noted above, the symmetry of P and Q inherent to the absolute values from above give the same upper bound if we instead had started with $u_n^\star(P)$ and $u_n^\star(Q)$.

Case 4. This case considers type 2 triangles described in Figure 4.3 along a prefractal segment with no type 2 pink triangle. For this case, we let P_1 be the vertex in V^n on the prefractal segment attached to the type 1 triangle and P_2 be the vertex at the other end of the segment. Using the same labeling scheme as in Case 3, only this time allowing $i \in \{1, 2, \ldots, k\}$, an identical argument gives

$$
\frac{|u_n^\star(X_1) - u_n^\star(X_2)|}{|X_1 - X_2|^\beta} \leq 2(\alpha-2)^{-1}|u|_{K,\beta}. \qquad \square
$$

Lemma 2. *Let T be a primary sidecar triangle with vertices P, Q, and R as depicted by any purple triangle of Figure 4.4. Let $\beta \in (0, 1]$ and u be a $\beta-$Hölder continuous function*

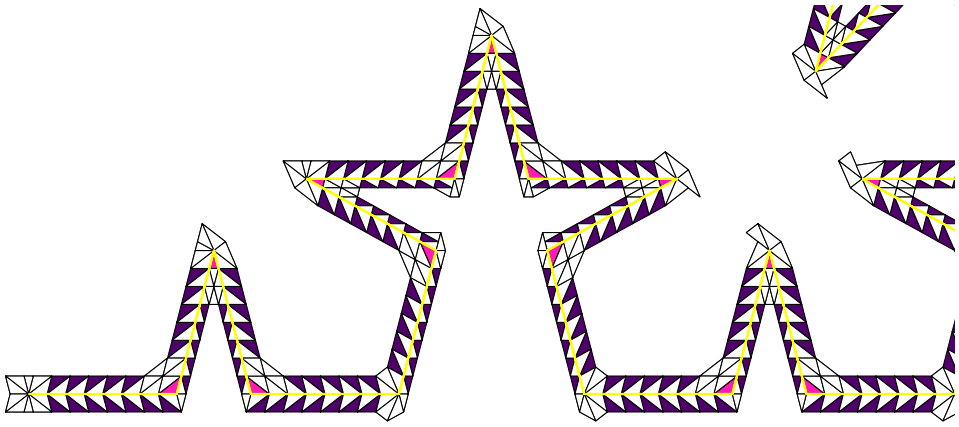

Figure 4.4: Cases for Lemma 2

defined on the vertices of the prefractal so that

$$\frac{|u(A)-u(B)|}{|A-B|^\beta} \le |u|_{K,\beta}$$

for all $A, B \in V^n$. *Then, for* $n \ge 3$, $u_n^\star$ *satisfies*

$$\sup_{X,Y\in\mathcal{T}} \frac{|u_n^\star(X)-u_n^\star(Y)|}{|X-Y|^\beta} \le 3(\alpha-2)^{-1}|u|_{K,\beta}.$$

Proof. There are four cases to consider. In each of the cases, we use the labeling system set up in Lemma 1.

Case 1. This case considers type 1 triangles T above K^n. We may, without loss of generality, further restrict our choice of T to triangles where $u_n^\star(Q)$ is determined by the prefractal segments. Using the labeling system of Lemma 1, we have

$$\begin{aligned}
u_n^\star(Q) &= \frac{k-i}{k}u(P_1) + \frac{i}{k}u(P_2),\\
u_n^\star(R) &= \frac{2k-2i-1}{2k}u(P_1) + \frac{2i+1}{2k}u(P_2),\\
u_n^\star(P) &= \frac{2k-2i+1}{2k}u(P_1) + \frac{2i-1}{2k}u(P_2)
\end{aligned}$$

for $i \in \{3, 4, \ldots, k-1\}$.

Choosing distinct $X_1, X_2 \in T$ with $X_1 = (x_1, y_1)$ and $X_2 = (x_2, y_2)$, equation (4.1) gives

$$\begin{aligned}
\frac{|u_n^\star(X_1)-u_n^\star(X_2)|}{|X_1-X_2|^\beta} &\le \frac{|u_n^\star(P)-u_n^\star(Q)\|x_1-x_2|}{|Q-P\|X_1-X_2|^\beta} + \frac{\sqrt{\alpha}|2u_n^\star(R)-u_n^\star(P)-u_n^\star(Q)\|y_1-y_2|}{\sqrt{4-\alpha}|Q-P\|X_1-X_2|^\beta}\\
&\le \frac{|u_n^\star(P)-u_n^\star(Q)\|x_1-x_2|}{|Q-P\|X_1-X_2|^\beta} + \frac{|4u_n^\star(R)-2u_n^\star(P)-2u_n^\star(Q)\|y_1-y_2|}{\sqrt{4-\alpha}|Q-P\|X_1-X_2|^\beta}\\
&\le \frac{|u(P_1)-u(P_2)\|x_1-x_2|}{2k|Q-P\|X_1-X_2|^\beta} + \frac{3|u(P_1)-u(P_2)\|y_1-y_2|}{k\sqrt{4-\alpha}|Q-P\|X_1-X_2|^\beta}\\
&\le \frac{|u(P_1)-u(P_2)\|x_1-x_2|}{2\sqrt{\alpha}|P_1-P_2\|X_1-X_2|^\beta} + \frac{3|u(P_1)-u(P_2)\|y_1-y_2|}{\sqrt{\alpha}\sqrt{4-\alpha}|P_1-P_2\|X_1-X_2|^\beta}\\
&\le \frac{|u(P_1)-u(P_2)\|x_1-x_2|}{2\sqrt{2}|P_1-P_2\|X_1-X_2|^\beta} + \frac{3|u(P_1)-u(P_2)\|y_1-y_2|}{\sqrt{2}|P_1-P_2\|X_1-X_2|^\beta}
\end{aligned}$$

$$
\begin{aligned}
&\leq \frac{|u(P_1) - u(P_2)|}{2\sqrt{2}|P_1 - P_2|^\beta} + \frac{3|u(P_1) - u(P_2)|}{\sqrt{2}|P_1 - P_2|^\beta} \\
&\leq \frac{1}{2\sqrt{2}}|u|_{K,\beta} + \frac{3}{\sqrt{2}}|u|_{K,\beta} \\
&= \frac{7}{2\sqrt{2}}|u|_{K,\beta} \\
&\leq 3(\alpha - 2)^{-1}|u|_{K,\beta}.
\end{aligned}
$$

Case 2. This case considers type 1 triangles below K^n. Using the same labeling scheme as in Lemma 1, only this time allowing $i \in \{1, 2, \ldots, k-1\}$, an identical argument gives

$$
\frac{|u_n^\star(X_1) - u_n^\star(X_2)|}{|X_1 - X_2|^\beta} \leq 3(\alpha - 2)^{-1}|u|_{K,\beta}.
$$

Case 3. This case considers type 2 triangles described in Figure 4.3 along a prefractal segment with a single pink type 2 triangle.

Begin by setting up an analogous labeling scheme as in Lemma 1 and consider an analogous restriction of T as in Case 1, namely that $u_n^\star(P)$ and $u_n^\star(R)$ are undetermined by the affine function along the prefractal segments. We immediately get

$$
\begin{aligned}
u_n^\star(Q) &= \frac{k-i}{k}u(P_1) + \frac{i}{k}u(P_2), \\
u_n^\star(R) &= \frac{k-i+1}{k}u(P_1) + \frac{i-1}{k}u(P_2), \\
u_n^\star(P) &= \frac{2k-2i+1}{2k}u(P_1) + \frac{2i-1}{2k}u(P_2)
\end{aligned}
$$

for $i \in \{3, 4, \ldots, k-1\}$.

Choosing distinct $X_1, X_2 \in T$ with $X_1 = (x_1, y_1)$ and $X_2 = (x_2, y_2)$, equation (4.2) gives

$$
\begin{aligned}
\frac{|u_n^\star(X_1) - u_n^\star(X_2)|}{|X_1 - X_2|^\beta} &\leq \frac{|u_n^\star(P) - u_n^\star(Q)\|x_1 - x_2|}{|Q - P\|X_1 - X_2|^\beta} + \frac{(\alpha-2)|2u_n^\star(R) - u_n^\star(P) - u_n^\star(Q)\|y_1 - y_2|}{\sqrt{4-(\alpha-2)^2}|Q-P\|X_1 - X_2|^\beta} \\
&\leq \frac{|u_n^\star(P) - u_n^\star(Q)\|x_1 - x_2|}{|Q - P\|X_1 - X_2|^\beta} + \frac{|2u_n^\star(R) - u_n^\star(P) - u_n^\star(Q)\|y_1 - y_2|}{\sqrt{4-(\alpha-2)^2}|Q-P\|X_1 - X_2|^\beta}
\end{aligned}
$$

$$
\begin{aligned}
&\leq \frac{|u(P_1)-u(P_2)||x_1-x_2|}{2k|Q-P||X_1-X_2|^\beta} + \frac{3|u(P_1)-u(P_2)||y_1-y_2|}{2k\sqrt{4-(\alpha-2)^2}|Q-P||X_1-X_2|^\beta} \\
&\leq \frac{|u(P_1)-u(P_2)||x_1-x_2|}{2k|Q-P||X_1-X_2|^\beta} + \frac{\sqrt{3}|u(P_1)-u(P_2)||y_1-y_2|}{2k|Q-P||X_1-X_2|^\beta} \\
&\leq \frac{|u(P_1)-u(P_2)||x_1-x_2|}{2(\alpha-2)|P_1-P_2||X_1-X_2|^\beta} + \frac{\sqrt{3}|u(P_1)-u(P_2)||y_1-y_2|}{2(\alpha-2)|P_1-P_2||X_1-X_2|^\beta} \\
&\leq \frac{|u(P_1)-u(P_2)|}{2(\alpha-2)|P_1-P_2|^\beta} + \frac{\sqrt{3}|u(P_1)-u(P_2)|}{2(\alpha-2)|P_1-P_2|^\beta} \\
&\leq \frac{1}{2(\alpha-2)}|u|_{K,\beta} + \frac{\sqrt{3}}{2(\alpha-2)}|u|_{K,\beta} \\
&= \frac{1+\sqrt{3}}{2(\alpha-2)}|u|_{K,\beta}.
\end{aligned}
$$

Case 4. This case considers type 2 triangles described in Figure 4.4 along a prefractal segment with no type 2 pink triangle. For this case, we let P_1 be the vertex in V^n on the prefractal segment attached to the type 1 triangle and P_2 be the vertex at the other end of the segment. Using the same labeling scheme as in Case 3, only this time allowing $i \in \{1, 2, \ldots, k-1\}$, an identical argument gives

$$
\frac{|u_n^\star(X_1)-u_n^\star(X_2)|}{|X_1-X_2|^\beta} \leq \frac{1+\sqrt{3}}{2(\alpha-2)}|u|_{K,\beta}. \qquad \square
$$

Lemma 3. *Let T be a primary sidecar triangle with vertices P, Q, and R as depicted by any pink triangle of Figure 4.5. Let $\beta \in (0,1]$ and u be a $\beta-$Hölder continuous function defined*

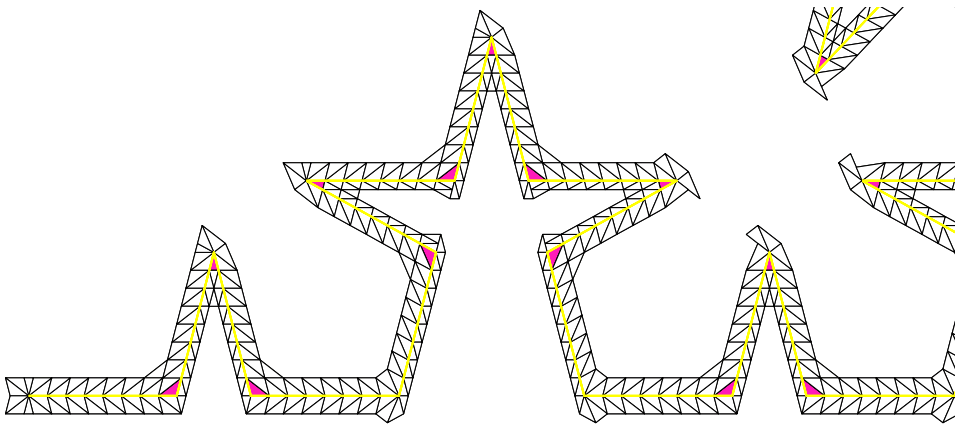

Figure 4.5: Cases for Lemma 3

on the vertices of the prefractal so that

$$\frac{|u(A) - u(B)|}{|A - B|^\beta} \leq |u|_{K,\beta}$$

for all $A, B \in V^n$. *Then, for* $n \geq 3$, $u_n^\star$ *satisfies*

$$\sup_{X,Y \in \mathcal{T}} \frac{|u_n^\star(X) - u_n^\star(Y)|}{|X - Y|^\beta} \leq 5(\alpha - 2)^{-1} |u|_{K,\beta}.$$

Proof. There are two cases for this lemma.

Case 1. This case considers the type 1 triangles. For any triangle T in this category, T has exactly one vertex in V^n, and we label this vertex P_2. Let the vertices of V^n immediately left and right of P_2 be labeled P_1 and P_3, respectively. If we label the vertices along the segments $\overline{P_1P_2}$ and $\overline{P_2P_3}$ starting from P_2 in a similar manner as before, we get

$$\begin{aligned} u_n^\star(R) &= u(P_2) \\ u_n^\star(P) &= \frac{k-1}{k} u(P_2) + \frac{1}{k} u(P_3) \\ u_n^\star(Q) &= \frac{k-1}{k} u(P_2) + \frac{1}{k} u(P_1). \end{aligned}$$

Choosing distinct $X_1, X_2 \in T$ with $X_1 = (x_1, y_1)$ and $X_2 = (x_2, y_2)$, equation (4.1) gives

$$\begin{aligned} \frac{|u_n^\star(X_1) - u_n^\star(X_2)|}{|X_1 - X_2|^\beta} &\leq \frac{|u_n^\star(P) - u_n^\star(Q)\|x_1 - x_2|}{|Q - P\|X_1 - X_2|^\beta} + \frac{\sqrt{\alpha}|2u_n^\star(R) - u_n^\star(P) - u_n^\star(Q)\|y_1 - y_2|}{\sqrt{4-\alpha}|Q - P\|X_1 - X_2|^\beta} \\ &\leq \frac{|u_n^\star(P) - u_n^\star(Q)\|x_1 - x_2|}{|Q - P\|X_1 - X_2|^\beta} + \frac{|4u_n^\star(R) - 2u_n^\star(P) - 2u_n^\star(Q)\|y_1 - y_2|}{\sqrt{4-\alpha}|Q - P\|X_1 - X_2|^\beta} \\ &\leq \frac{|u(P_1) - u(P_3)\|x_1 - x_2|}{k|Q - P\|X_1 - X_2|^\beta} + \frac{2|u(P_1) - u(P_2)\|y_1 - y_2|}{k\sqrt{4-\alpha}|Q - P\|X_1 - X_2|^\beta} \\ &\quad + \frac{2|u(P_2) - u(P_3)\|y_1 - y_2|}{k\sqrt{4-\alpha}|Q - P\|X_1 - X_2|^\beta} \end{aligned}$$

$$
\begin{aligned}
&\leq \frac{|u(P_1)-u(P_3)\|x_1-x_2|}{|P_1-P_3\|X_1-X_2|^\beta} + \frac{\sqrt{2}|u(P_1)-u(P_2)\|y_1-y_2|}{|P_1-P_2\|X_1-X_2|^\beta} \\
&\qquad + \frac{\sqrt{2}|u(P_2)-u(P_3)\|y_1-y_2|}{|P_2-P_3\|X_1-X_2|^\beta} \\
&\leq \frac{|u(P_1)-u(P_3)|}{|P_1-P_3|^\beta} + \frac{\sqrt{2}|u(P_1)-u(P_2)|}{|P_1-P_2|^\beta} + \frac{\sqrt{2}|u(P_2)-u(P_3)|}{|P_2-P_3|^\beta} \\
&\leq |u|_{K,\beta} + \sqrt{2}|u|_{K,\beta} + \sqrt{2}|u|_{K,\beta} \\
&= (1+2\sqrt{2})|u|_{K,\beta} \\
&\leq 5(\alpha-2)^{-1}|u|_{K,\beta}.
\end{aligned}
$$

Case 2. This case considers the type 2 triangles of Figure 4.5. Begin by setting up an analogous labeling scheme to Case 1. This scheme immediately gives $u_n^\star(R) = u(P_2)$ and

$$
u_n^\star(P) = \frac{k-1}{k}u(P_2) + \frac{1}{k}u(P_3), \qquad u_n^\star(Q) = \frac{k-1}{k}u(P_2) + \frac{1}{k}u(P_1).
$$

Choosing distinct $X_1, X_2 \in T$ with $X_1 = (x_1, y_1)$ and $X_2 = (x_2, y_2)$, equation (4.2) gives

$$
\begin{aligned}
\frac{|u_n^\star(X_1)-u_n^\star(X_2)|}{|X_1-X_2|^\beta} &\leq \frac{|u_n^\star(P)-u_n^\star(Q)\|x_1-x_2|}{|Q-P\|X_1-X_2|^\beta} + \frac{|2u_n^\star(R)-u_n^\star(P)-u_n^\star(Q)\|y_1-y_2|}{\sqrt{4-(\alpha-2)^2}|Q-P\|X_1-X_2|^\beta} \\
&\leq \frac{|u(P_1)-u(P_3)\|x_1-x_2|}{k|Q-P\|X_1-X_2|^\beta} + \frac{|u(P_1)-u(P_2)\|y_1-y_2|}{k\sqrt{3}|Q-P\|X_1-X_2|^\beta} \\
&\qquad + \frac{|u(P_2)-u(P_3)\|y_1-y_2|}{k\sqrt{3}|Q-P\|X_1-X_2|^\beta} \\
&\leq \frac{|u(P_1)-u(P_3)\|x_1-x_2|}{(\alpha-2)|P_1-P_2\|X_1-X_2|^\beta} + \frac{|u(P_1)-u(P_2)\|y_1-y_2|}{\sqrt{3}(\alpha-2)|P_1-P_2\|X_1-X_2|^\beta} \\
&\qquad + \frac{|u(P_2)-u(P_3)\|y_1-y_2|}{\sqrt{3}(\alpha-2)|P_2-P_3\|X_1-X_2|^\beta} \\
&\leq \frac{|u(P_1)-u(P_3)|}{(\alpha-2)|P_1-P_2|^\beta} + \frac{|u(P_1)-u(P_2)|}{\sqrt{3}(\alpha-2)|P_1-P_2|^\beta} + \frac{|u(P_2)-u(P_3)|}{\sqrt{3}(\alpha-2)|P_2-P_3|^\beta} \\
&\leq \frac{1}{\alpha-2}|u|_{K,\beta} + \frac{1}{\sqrt{3}(\alpha-2)}|u|_{K,\beta} + \frac{1}{\sqrt{3}(\alpha-2)}|u|_{K,\beta} \\
&= \frac{\sqrt{3}+2}{\sqrt{3}(\alpha-2)}|u|_{K,\beta}
\end{aligned}
$$

$$\leq 3(\alpha-2)^{-1}|u|_{K,\beta}. \qquad \square$$

Lemma 4. *Let T be a primary sidecar triangle with vertices P, Q, and R as depicted by any yellow triangle of Figure 4.6. Let $\beta \in (0,1]$ and u be a $\beta-$Hölder continuous function*

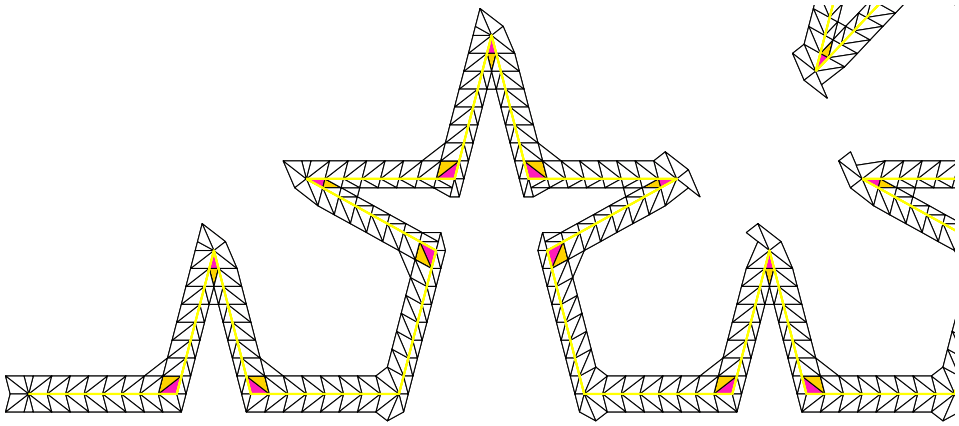

Figure 4.6: Cases for Lemma 4

defined on the vertices of the prefractal so that

$$\frac{|u(A)-u(B)|}{|A-B|^{\beta}} \leq |u|_{K,\beta}$$

for all $A, B \in V^n$. Then, for $n \geq 3$, $u_n^\star$ satisfies

$$\sup_{X,Y\in\mathcal{T}} \frac{|u_n^\star(X)-u_n^\star(Y)|}{|X-Y|^{\beta}} \leq 3(\alpha-2)^{-1}|u|_{K,\beta}.$$

Proof. There are two cases to consider.

Case 1. This case considers the yellow type 1 triangles of Figure 4.6. Using the labeling scheme from Lemma 3, we see that $u_n^\star(Q)$ and $u_n^\star(P)$ are given by the following convex combinations, respectively:

$$u_n^\star(Q) = \frac{k-1}{k}u(P_2) + \frac{1}{k}u(P_3), \qquad u_n^\star(P) = \frac{k-1}{k}u(P_2) + \frac{1}{k}u(P_1).$$

The value of $u_n^\star(R)$ is determined by a convex combination of four points, and is given by

$$u_n^\star(R) = \frac{3}{4k}u(P_1) + \frac{4k-6}{4k}u(P_2) + \frac{3}{4k}u(P_3).$$

Choosing distinct $X_1, X_2 \in T$ with $X_1 = (x_1, y_1)$ and $X_2 = (x_2, y_2)$, equation (4.1) gives

$$\begin{aligned}
\frac{|u_n^\star(X_1) - u_n^\star(X_2)|}{|X_1 - X_2|^\beta} &\leq \frac{|u_n^\star(P) - u_n^\star(Q)\|x_1 - x_2|}{|Q-P\|X_1 - X_2|^\beta} + \frac{|4u_n^\star(R) - 2u_n^\star(P) - 2u_n^\star(Q)\|y_1 - y_2|}{\sqrt{4-\alpha}|Q-P\|X_1 - X_2|^\beta} \\
&\leq \frac{|u(P_1) - u(P_3)\|x_1 - x_2|}{k|Q-P\|X_1 - X_2|^\beta} + \frac{|u(P_1) - u(P_2)\|y_1 - y_2|}{k\sqrt{4-\alpha}|Q-P\|X_1 - X_2|^\beta} \\
&\qquad + \frac{|u(P_2) - u(P_3)\|y_1 - y_2|}{k\sqrt{4-\alpha}|Q-P\|X_1 - X_2|^\beta} \\
&\leq \frac{|u(P_1) - u(P_3)\|x_1 - x_2|}{\sqrt{2}|P_1-P_2\|X_1 - X_2|^\beta} + \frac{|u(P_1) - u(P_2)\|y_1 - y_2|}{\sqrt{2}|P_1-P_2\|X_1 - X_2|^\beta} \\
&\qquad + \frac{|u(P_2) - u(P_3)\|y_1 - y_2|}{\sqrt{2}|P_2-P_3\|X_1 - X_2|^\beta} \\
&\leq \frac{|u(P_1) - u(P_3)|}{\sqrt{2}|P_1-P_2|^\beta} + \frac{|u(P_1) - u(P_2)|}{\sqrt{2}|P_1-P_2|^\beta} + \frac{|u(P_2) - u(P_3)|}{\sqrt{2}|P_2-P_3|^\beta} \\
&\leq \frac{1}{\sqrt{2}}|u|_{K,\beta} + \frac{1}{\sqrt{2}}|u|_{K,\beta} + \frac{1}{\sqrt{2}}|u|_{K,\beta} \\
&= \frac{3}{\sqrt{2}}|u|_{K,\beta} \\
&\leq 3(\alpha-2)^{-1}|u|_{K,\beta}.
\end{aligned}$$

Case 2. This case considers the yellow type 2 triangles of Figure 4.6. Using the labeling scheme from Lemma 3, we see that $u_n^\star(Q)$ and $u_n^\star(P)$ are given by the following convex combinations:

$$u_n^\star(Q) = \frac{k-1}{k}u(P_2) + \frac{1}{k}u(P_3), \qquad u_n^\star(P) = \frac{k-1}{k}u(P_2) + \frac{1}{k}u(P_1).$$

The value of $u_n^\star(R)$ is determined by a convex combination of four points, and is given by

$$u_n^\star(R) = \frac{3}{4k}u(P_1) + \frac{4k-6}{4k}u(P_2) + \frac{3}{4k}u(P_3).$$

Choosing distinct $X_1, X_2 \in T$ with $X_1 = (x_1, y_1)$ and $X_2 = (x_2, y_2)$, equation (4.2) gives

$$\begin{aligned}
\frac{|u_n^\star(X_1) - u_n^\star(X_2)|}{|X_1 - X_2|^\beta} &\leq \frac{|u_n^\star(P) - u_n^\star(Q)\|x_1 - x_2|}{|Q - P\|X_1 - X_2|^\beta} + \frac{|2u_n^\star(R) - u_n^\star(P) - u_n^\star(Q)\|y_1 - y_2|}{\sqrt{4 - (\alpha-2)^2}|Q - P\|X_1 - X_2|^\beta} \\
&\leq \frac{|u(P_1) - u(P_3)\|x_1 - x_2|}{k|Q - P\|X_1 - X_2|^\beta} + \frac{|u(P_1) - u(P_2)\|y_1 - y_2|}{2k\sqrt{3}|Q - P\|X_1 - X_2|^\beta} \\
&\qquad + \frac{|u(P_2) - u(P_3)\|y_1 - y_2|}{2k\sqrt{3}|Q - P\|X_1 - X_2|^\beta} \\
&\leq \frac{|u(P_1) - u(P_3)\|x_1 - x_2|}{(\alpha-2)|P_1 - P_2\|X_1 - X_2|^\beta} + \frac{|u(P_1) - u(P_2)\|y_1 - y_2|}{2\sqrt{3}(\alpha-2)|P_1 - P_2\|X_1 - X_2|^\beta} \\
&\qquad + \frac{|u(P_2) - u(P_3)\|y_1 - y_2|}{2\sqrt{3}(\alpha-2)|P_2 - P_3\|X_1 - X_2|^\beta} \\
&\leq \frac{|u(P_1) - u(P_3)|}{(\alpha-2)|P_1 - P_2|^\beta} + \frac{|u(P_1) - u(P_2)|}{2\sqrt{3}(\alpha-2)|P_1 - P_2|^\beta} + \frac{|u(P_2) - u(P_3)|}{2\sqrt{3}(\alpha-2)|P_2 - P_3|^\beta} \\
&\leq \frac{1}{\alpha-2}|u|_{K,\beta} + \frac{1}{2\sqrt{3}(\alpha-2)}|u|_{K,\beta} + \frac{1}{2\sqrt{3}(\alpha-2)}|u|_{K,\beta} \\
&= \frac{\sqrt{3}+1}{\sqrt{3}(\alpha-2)}|u|_{K,\beta} \\
&\leq 2(\alpha-2)^{-1}|u|_{K,\beta}.
\end{aligned}$$

□

Lemma 5. *Let T be a primary sidecar triangle with vertices P, Q, and R as depicted by any blue triangle of Figure 4.7. Let $\beta \in (0, 1]$ and u be a $\beta-$Hölder continuous function defined*

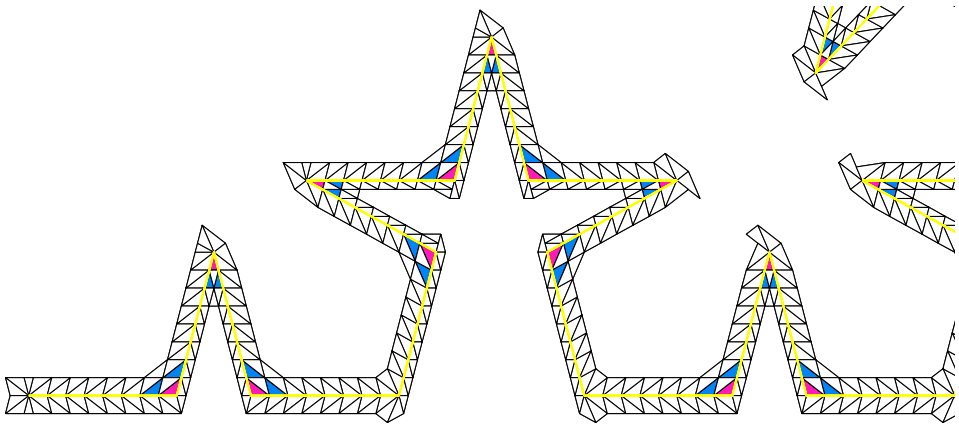

Figure 4.7: Cases for Lemma 5

on the vertices of the prefractal so that

$$\frac{|u(A)-u(B)|}{|A-B|^\beta} \le |u|_{K,\beta}$$

for all $A, B \in V^n$. *Then, for* $n \ge 3$, $u_n^\star$ *satisfies*

$$\sup_{X,Y\in\mathcal{T}} \frac{|u_n^\star(X)-u_n^\star(Y)|}{|X-Y|^\beta} \le 4(\alpha-2)^{-1}|u|_{K,\beta}.$$

Proof. There are two cases. We use the labeling scheme outlined in Lemma 3.

Case 1. This case considers the blue type 1 triangles T of Figure 4.7. By symmetry, we further restrict our choice of T to triangles where $u_n^\star(Q)$ and $u_n^\star(R)$ are defined by the affine function on the prefractal segments. In this case, we have

$$\begin{aligned}
u_n^\star(Q) &= \frac{k-2}{k}u(P_2) + \frac{2}{k}u(P_1),\\
u_n^\star(R) &= \frac{k-1}{k}u(P_2) + \frac{1}{k}u(P_1),\\
u_n^\star(P) &= \frac{3}{4k}u(P_1) + \frac{4k-6}{4k}u(P_2) + \frac{3}{4k}u(P_3).
\end{aligned}$$

Choosing distinct $X_1, X_2 \in T$ with $X_1 = (x_1, y_1)$ and $X_2 = (x_2, y_2)$, equation (4.1) gives

$$\begin{aligned}
\frac{|u_n^\star(X_1)-u_n^\star(X_2)|}{|X_1-X_2|^\beta} &\le \frac{|u_n^\star(P)-u_n^\star(Q)\|x_1-x_2|}{|Q-P\|X_1-X_2|^\beta} + \frac{|4u_n^\star(R)-2u_n^\star(P)-2u_n^\star(Q)\|y_1-y_2|}{\sqrt{4-\alpha}|Q-P\|X_1-X_2|^\beta}\\
&\le \frac{|u(P_1)-u(P_2)\|x_1-x_2|}{2k|Q-P\|X_1-X_2|^\beta} + \frac{3|u(P_1)-u(P_3)\|x_1-x_2|}{4k|Q-P\|X_1-X_2|^\beta}\\
&\qquad + \frac{3|u(P_1)-u(P_2)\|y_1-y_2|}{2k\sqrt{4-\alpha}|Q-P\|X_1-X_2|^\beta} + \frac{3|u(P_2)-u(P_3)\|y_1-y_2|}{2k\sqrt{4-\alpha}|Q-P\|X_1-X_2|^\beta}\\
&\le \frac{|u(P_1)-u(P_2)\|x_1-x_2|}{2\sqrt{2}|P_1-P_2\|X_1-X_2|^\beta} + \frac{3|u(P_1)-u(P_3)\|x_1-x_2|}{4|P_1-P_3\|X_1-X_2|^\beta}\\
&\qquad + \frac{3|u(P_1)-u(P_2)\|y_1-y_2|}{2\sqrt{2}|P_1-P_2\|X_1-X_2|^\beta} + \frac{3|u(P_2)-u(P_3)\|y_1-y_2|}{2\sqrt{2}|P_2-P_3\|X_1-X_2|^\beta}
\end{aligned}$$

$$
\begin{aligned}
&\leq \frac{|u(P_1)-u(P_2)|}{2\sqrt{2}|P_1-P_2|^\beta} + \frac{3|u(P_1)-u(P_3)|}{4|P_1-P_3|^\beta} + \frac{3|u(P_1)-u(P_2)|}{2\sqrt{2}|P_1-P_2|^\beta} \\
&\qquad + \frac{3|u(P_2)-u(P_3)|}{2\sqrt{2}|P_2-P_3|^\beta} \\
&\leq \frac{1}{2\sqrt{2}}|u|_{K,\beta} + \frac{3}{4}|u|_{K,\beta} + \frac{3}{2\sqrt{2}}|u|_{K,\beta} + \frac{3}{2\sqrt{2}}|u|_{K,\beta} \\
&= \frac{7\sqrt{2}+3}{4}|u|_{K,\beta} \\
&\leq 4(\alpha-2)^{-1}|u|_{K,\beta}.
\end{aligned}
$$

Case 2. This case considers the blue type 2 triangles T of Figure 4.7. By symmetry, we further restrict our choice of T to triangles where $u_n^\star(Q)$ and $u_n^\star(R)$ are defined by the affine function on the prefractal segments. In this case, we have

$$
\begin{aligned}
u_n^\star(Q) &= \frac{k-2}{k}u(P_2) + \frac{2}{k}u(P_1), \\
u_n^\star(R) &= \frac{k-1}{k}u(P_2) + \frac{1}{k}u(P_1), \\
u_n^\star(P) &= \frac{3}{4k}u(P_1) + \frac{4k-6}{4k}u(P_2) + \frac{3}{4k}u(P_3).
\end{aligned}
$$

Choosing distinct $X_1, X_2 \in T$ with $X_1 = (x_1, y_1)$ and $X_2 = (x_2, y_2)$, equation (4.2) gives

$$
\begin{aligned}
\frac{|u_n^\star(X_1)-u_n^\star(X_2)|}{|X_1-X_2|^\beta} &\leq \frac{|u_n^\star(P)-u_n^\star(Q)\|x_1-x_2|}{|Q-P\|X_1-X_2|^\beta} + \frac{|2u_n^\star(R)-u_n^\star(P)-u_n^\star(Q)\|y_1-y_2|}{\sqrt{4-(\alpha-2)^2}|Q-P\|X_1-X_2|^\beta} \\
&\leq \frac{|u(P_1)-u(P_2)\|x_1-x_2|}{2k|Q-P\|X_1-X_2|^\beta} + \frac{3|u(P_1)-u(P_3)\|x_1-x_2|}{4k|Q-P\|X_1-X_2|^\beta} \\
&\qquad + \frac{\sqrt{3}|u(P_1)-u(P_2)\|y_1-y_2|}{4k|Q-P\|X_1-X_2|^\beta} + \frac{\sqrt{3}|u(P_2)-u(P_3)\|y_1-y_2|}{4k|Q-P\|X_1-X_2|^\beta} \\
&\leq \frac{|u(P_1)-u(P_2)\|x_1-x_2|}{2(\alpha-2)|P_1-P_2\|X_1-X_2|^\beta} + \frac{3|u(P_1)-u(P_3)\|x_1-x_2|}{2\sqrt{2}|P_1-P_3\|X_1-X_2|^\beta} \\
&\qquad + \frac{\sqrt{3}|u(P_1)-u(P_2)\|y_1-y_2|}{4(\alpha-2)|P_1-P_2\|X_1-X_2|^\beta} + \frac{\sqrt{3}|u(P_2)-u(P_3)\|y_1-y_2|}{4(\alpha-2)|P_2-P_3\|X_1-X_2|^\beta} \\
&\leq \frac{|u(P_1)-u(P_2)|}{2(\alpha-2)|P_1-P_2|^\beta} + \frac{3|u(P_1)-u(P_3)|}{2\sqrt{2}|P_1-P_3|^\beta} \\
&\qquad + \frac{\sqrt{3}|u(P_1)-u(P_2)|}{4(\alpha-2)|P_1-P_2|^\beta} + \frac{\sqrt{3}|u(P_2)-u(P_3)|}{4(\alpha-2)|P_2-P_3|^\beta}
\end{aligned}
$$

$$\leq \frac{1}{2(\alpha-2)}|u|_{K,\beta} + \frac{3}{2\sqrt{2}(\alpha-2)}|u|_{K,\beta} + \frac{\sqrt{3}}{4(\alpha-2)}|u|_{K,\beta} + \frac{\sqrt{3}}{4(\alpha-2)}|u|_{K,\beta}$$
$$= \frac{4\sqrt{2}+3}{2\sqrt{6}(\alpha-2)}|u|_{K,\beta}$$
$$\leq 3(\alpha-2)^{-1}. \qquad \square$$

Lemma 6. *Let T be a primary sidecar triangle with vertices P, Q, and R as depicted by any brown triangle of Figure 4.8. Let $\beta \in (0,1]$ and u be a $\beta-$Hölder continuous function*

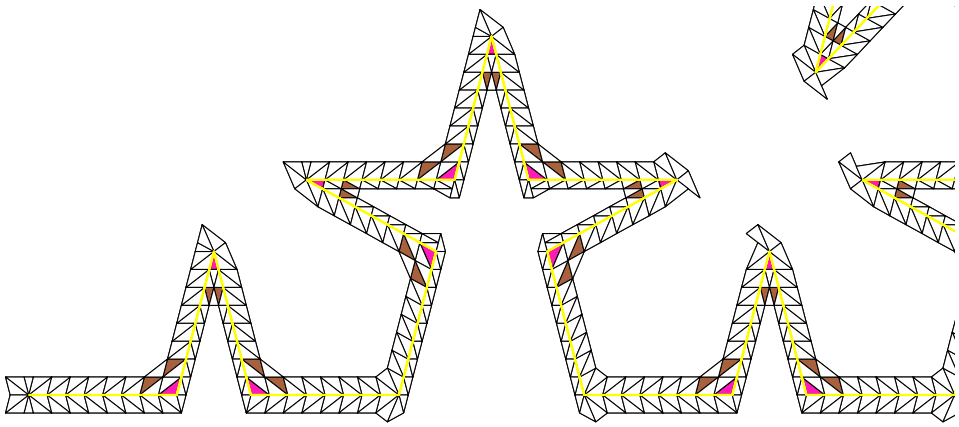

Figure 4.8: Cases for Lemma 6

defined on the vertices of the prefractal so that

$$\frac{|u(A)-u(B)|}{|A-B|^{\beta}} \leq |u|_{K,\beta}$$

for all $A, B \in V^n$. Then, for $n \geq 3$, $u_n^\star$ satisfies

$$\sup_{X,Y\in\mathcal{T}} \frac{|u_n^\star(X)-u_n^\star(Y)|}{|X-Y|^{\beta}} \leq 8(\alpha-2)^{-1}|u|_{K,\beta}.$$

Proof. There are two cases. We use the labeling scheme outlined in Lemma 3.

Case 1. This case considers the brown type 1 triangles T of Figure 4.8. By symmetry, we further restrict our choice of T to triangles where $u_n^\star(Q)$ is defined by the affine function on

the prefractal segments. In this case, we have

$$\begin{aligned}
u_n^\star(Q) &= \frac{k-2}{k}u(P_2) + \frac{2}{k}u(P_3),\\
u_n^\star(R) &= \frac{2k-5}{2k}u(P_2) + \frac{5}{2k}u(P_1),\\
u_n^\star(P) &= \frac{3}{4k}u(P_1) + \frac{4k-6}{4k}u(P_2) + \frac{3}{4k}u(P_3).
\end{aligned}$$

Choosing distinct $X_1, X_2 \in T$ with $X_1 = (x_1, y_1)$ and $X_2 = (x_2, y_2)$, equation (4.1) gives

$$\begin{aligned}
\frac{|u_n^\star(X_1) - u_n^\star(X_2)|}{|X_1 - X_2|^\beta} &\leq \frac{|u_n^\star(P) - u_n^\star(Q)\|x_1 - x_2|}{|Q-P\|X_1 - X_2|^\beta} + \frac{|4u_n^\star(R) - 2u_n^\star(P) - 2u_n^\star(Q)\|y_1 - y_2|}{\sqrt{4-\alpha}|Q-P\|X_1 - X_2|^\beta}\\
&\leq \frac{|u(P_2) - u(P_3)\|x_1 - x_2|}{2k|Q-P\|X_1 - X_2|^\beta} + \frac{3|u(P_1) - u(P_3)\|x_1 - x_2|}{4k|Q-P\|X_1 - X_2|^\beta}\\
&\qquad + \frac{11|u(P_2) - u(P_3)\|y_1 - y_2|}{2k\sqrt{4-\alpha}|Q-P\|X_1 - X_2|^\beta} + \frac{6|u(P_1) - u(P_2)\|y_1 - y_2|}{2k\sqrt{4-\alpha}|Q-P\|X_1 - X_2|^\beta}\\
&\leq \frac{|u(P_2) - u(P_3)\|x_1 - x_2|}{2\sqrt{2}|P_2 - P_3\|X_1 - X_2|^\beta} + \frac{3|u(P_1) - u(P_3)\|x_1 - x_2|}{4|P_1 - P_3\|X_1 - X_2|^\beta}\\
&\qquad + \frac{11|u(P_2) - u(P_3)\|y_1 - y_2|}{2\sqrt{2}|P_2 - P_3\|X_1 - X_2|^\beta} + \frac{6|u(P_1) - u(P_2)\|y_1 - y_2|}{2\sqrt{2}|P_1 - P_2\|X_1 - X_2|^\beta}\\
&\leq \frac{|u(P_2) - u(P_3)|}{2\sqrt{2}|P_2 - P_3|^\beta} + \frac{3|u(P_1) - u(P_3)|}{4|P_1 - P_3|^\beta} + \frac{11|u(P_2) - u(P_3)|}{2\sqrt{2}|P_2 - P_3|^\beta} + \frac{6|u(P_1) - u(P_2)|}{2\sqrt{2}|P_1 - P_2|^\beta}\\
&\leq \frac{1}{2\sqrt{2}}|u|_{K,\beta} + \frac{3}{4}|u|_{K,\beta} + \frac{11}{2\sqrt{2}}|u|_{K,\beta} + \frac{6}{2\sqrt{2}}|u|_{K,\beta}\\
&\leq \frac{15\sqrt{2}+3}{4}|u|_{K,\beta}\\
&\leq 8(\alpha-2)^{-1}|u|_{K,\beta}.
\end{aligned}$$

Case 2. This case considers the brown type 2 triangles T of Figure 4.8. By symmetry, we further restrict our choice of T to triangles where $u_n^\star(Q)$ is defined by the affine function on the prefractal segments. In this case, we have

$$\begin{aligned}
u_n^\star(Q) &= \frac{k-2}{k}u(P_2) + \frac{2}{k}u(P_3),\\
u_n^\star(R) &= \frac{2k-5}{2k}u(P_2) + \frac{5}{2k}u(P_1),
\end{aligned}$$

$$u_n^\star(P) = \frac{3}{4k}u(P_1) + \frac{4k-6}{4k}u(P_2) + \frac{3}{4k}u(P_3).$$

Choosing distinct $X_1, X_2 \in T$ with $X_1 = (x_1, y_1)$ and $X_2 = (x_2, y_2)$, equation (4.2) gives

$$\begin{aligned}
\frac{|u_n^\star(X_1) - u_n^\star(X_2)|}{|X_1 - X_2|^\beta} &\leq \frac{|u_n^\star(P) - u_n^\star(Q)\|x_1 - x_2|}{|Q-P\|X_1 - X_2|^\beta} + \frac{|2u_n^\star(R) - u_n^\star(P) - u_n^\star(Q)\|y_1 - y_2|}{\sqrt{4-(\alpha-2)^2}|Q-P\|X_1 - X_2|^\beta} \\
&\leq \frac{|u(P_1) - u(P_2)\|x_1 - x_2|}{2k|Q-P\|X_1 - X_2|^\beta} + \frac{3|u(P_1) - u(P_3)\|x_1 - x_2|}{4k|Q-P\|X_1 - X_2|^\beta} \\
&\quad + \frac{11|u(P_1) - u(P_3)\|y_1 - y_2|}{4k\sqrt{4-(\alpha-2)^2}|Q-P\|X_1 - X_2|^\beta} \\
&\quad + \frac{3|u(P_1) - u(P_2)\|y_1 - y_2|}{2k\sqrt{4-(\alpha-2)^2}|Q-P\|X_1 - X_2|^\beta} \\
&\leq \frac{|u(P_1) - u(P_2)\|x_1 - x_2|}{2(\alpha-2)|P_1-P_2\|X_1 - X_2|^\beta} + \frac{3|u(P_1) - u(P_3)\|x_1 - x_2|}{2\sqrt{2}(\alpha-2)|P_1-P_3\|X_1 - X_2|^\beta} \\
&\quad + \frac{11|u(P_1) - u(P_3)\|y_1 - y_2|}{2\sqrt{6}(\alpha-2)|P_1-P_3\|X_1 - X_2|^\beta} + \frac{\sqrt{3}|u(P_1) - u(P_2)\|y_1 - y_2|}{2(\alpha-2)|P_1-P_2\|X_1 - X_2|^\beta} \\
&\leq \frac{|u(P_1) - u(P_2)|}{2(\alpha-2)|P_1-P_2|^\beta} + \frac{3|u(P_1) - u(P_3)|}{2\sqrt{2}(\alpha-2)|P_1-P_3|^\beta} \\
&\quad + \frac{11|u(P_1) - u(P_3)|}{2\sqrt{6}(\alpha-2)|P_1-P_3|^\beta} + \frac{\sqrt{3}|u(P_1) - u(P_2)|}{2(\alpha-2)|P_1-P_2|^\beta} \\
&\leq \frac{1}{2(\alpha-2)}|u|_{K,\beta} + \frac{3}{2\sqrt{2}(\alpha-2)}|u|_{K,\beta} + \frac{11}{2\sqrt{6}(\alpha-2)}|u|_{K,\beta} + \frac{\sqrt{3}}{2(\alpha-2)}|u|_{K,\beta} \\
&= \frac{11+3\sqrt{2}+3\sqrt{3}+\sqrt{6}}{2\sqrt{6}}|u|_{K,\beta} \\
&\leq 5(\alpha-2)^{-1}|u|_{K,\beta}. \qquad \square
\end{aligned}$$

Lemma 7. *Let T be a primary sidecar triangle with vertices P, Q, and R as depicted by any yellow triangle of Figure 4.9. Let $\beta \in (0,1]$ and u be a $\beta-$Hölder continuous function defined on the vertices of the prefractal so that*

$$\frac{|u(A) - u(B)|}{|A-B|^\beta} \leq |u|_{K,\beta}$$

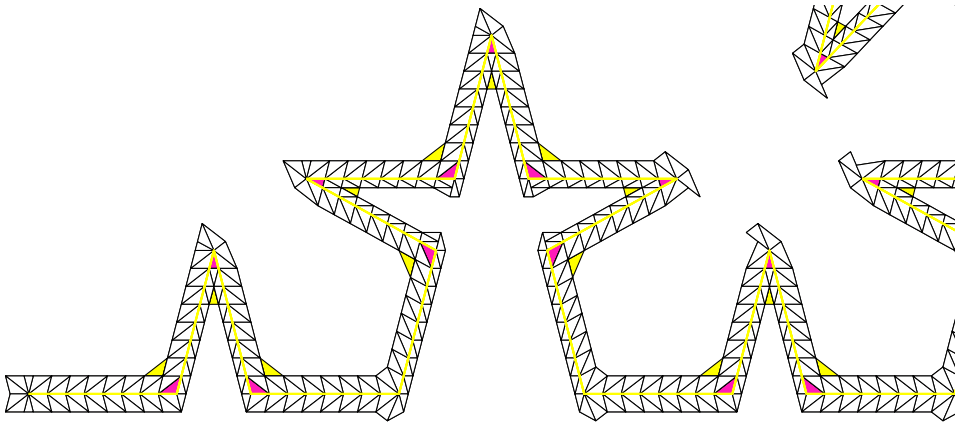

Figure 4.9: Cases for Lemma 7

for all $A, B \in V^n$. *Then, for* $n \geq 3$, $u_n^\star$ *satisfies*

$$\sup_{X,Y \in \mathcal{T}} \frac{|u_n^\star(X) - u_n^\star(Y)|}{|X - Y|^\beta} \leq 6(\alpha - 2)^{-1} |u|_{K,\beta}.$$

Proof. There are two cases. We use the labeling scheme outlined in Lemma 3.

Case 1. This case considers the yellow type 1 triangles T of Figure 4.9. By symmetry, we further restrict our choice of T to triangles where $u_n^\star(Q)$ is defined by the affine function on the prefractal segments. In this case, we have

$$\begin{aligned}
u_n^\star(P) &= \frac{2k-5}{2k} u(P_2) + \frac{5}{2k} u(P_3), \\
u_n^\star(Q) &= \frac{2k-5}{2k} u(P_2) + \frac{5}{2k} u(P_1), \\
u_n^\star(R) &= \frac{3}{4k} u(P_1) + \frac{4k-6}{4k} u(P_2) + \frac{3}{4k} u(P_3).
\end{aligned}$$

Choosing distinct $X_1, X_2 \in T$ with $X_1 = (x_1, y_1)$ and $X_2 = (x_2, y_2)$, equation (4.1) gives

$$\begin{aligned}
\frac{|u_n^\star(X_1) - u_n^\star(X_2)|}{|X_1 - X_2|^\beta} &\leq \frac{|u_n^\star(P) - u_n^\star(Q)\|x_1 - x_2|}{|Q - P\|X_1 - X_2|^\beta} + \frac{|4u_n^\star(R) - 2u_n^\star(P) - 2u_n^\star(Q)\|y_1 - y_2|}{\sqrt{4-\alpha}|Q - P\|X_1 - X_2|^\beta} \\
&\leq \frac{5|u(P_1) - u(P_3)\|x_1 - x_2|}{2k|Q - P\|X_1 - X_2|^\beta} + \frac{2|u(P_1) - u(P_2)\|y_1 - y_2|}{k|Q - P|\sqrt{4-\alpha}|X_1 - X_2|^\beta} \\
&\quad + \frac{2|u(P_2) - u(P_3)\|y_1 - y_2|}{k|Q - P|\sqrt{4-\alpha}|X_1 - X_2|^\beta}
\end{aligned}$$

$$
\begin{aligned}
&\leq \frac{5|u(P_1)-u(P_3)\|x_1-x_2|}{2|P_1-P_3\|X_1-X_2|^\beta} + \frac{\sqrt{2}|u(P_1)-u(P_2)\|y_1-y_2|}{|P_1-P_2\|X_1-X_2|^\beta} \\
&\qquad + \frac{\sqrt{2}|u(P_2)-u(P_3)\|y_1-y_2|}{|P_2-P_3\|X_1-X_2|^\beta} \\
&\leq \frac{5|u(P_1)-u(P_3)|}{2|P_1-P_3|^\beta} + \frac{\sqrt{2}|u(P_1)-u(P_2)|}{|P_1-P_2|^\beta} + \frac{\sqrt{2}|u(P_2)-u(P_3)|}{|P_2-P_3|^\beta} \\
&\leq \frac{5}{2}|u|_{K,\beta} + \sqrt{2}|u|_{K,\beta} + \sqrt{2}|u|_{K,\beta} \\
&= \frac{4\sqrt{2}+5}{2}|u|_{K,\beta} \\
&\leq 6(\alpha-2)^{-1}|u|_{K,\beta}.
\end{aligned}
$$

Case 2. This case considers the yellow type 2 triangles T of Figure 4.9. By symmetry, we further restrict our choice of T to triangles where $u_n^\star(Q)$ is defined by the affine function on the prefractal segments. In this case, we have

$$
\begin{aligned}
u_n^\star(P) &= \frac{2k-5}{2k}u(P_2) + \frac{5}{2k}u(P_3), \\
u_n^\star(Q) &= \frac{2k-5}{2k}u(P_2) + \frac{5}{2k}u(P_1), \\
u_n^\star(R) &= \frac{3}{4k}u(P_1) + \frac{4k-6}{4k}u(P_2) + \frac{3}{4k}u(P_3).
\end{aligned}
$$

Choosing distinct $X_1, X_2 \in T$ with $X_1 = (x_1, y_1)$ and $X_2 = (x_2, y_2)$, equation (4.2) gives

$$
\begin{aligned}
\frac{|u_n^\star(X_1)-u_n^\star(X_2)|}{|X_1-X_2|^\beta} &\leq \frac{|u_n^\star(P)-u_n^\star(Q)\|x_1-x_2|}{|Q-P\|X_1-X_2|^\beta} + \frac{|2u_n^\star(R)-u_n^\star(P)-u_n^\star(Q)\|y_1-y_2|}{\sqrt{4-(\alpha-2)^2}|Q-P\|X_1-X_2|^\beta} \\
&\leq \frac{5|u(P_1)-u(P_3)\|x_1-x_2|}{2k|Q-P\|X_1-X_2|^\beta} + \frac{|u(P_1)-u(P_2)\|y_1-y_2|}{k|Q-P|\sqrt{4-(\alpha-2)^2}|X_1-X_2|^\beta} \\
&\qquad + \frac{|u(P_2)-u(P_3)\|y_1-y_2|}{k|Q-P|\sqrt{4-(\alpha-2)^2}|X_1-X_2|^\beta} \\
&\leq \frac{5\sqrt{3}|u(P_1)-u(P_3)\|x_1-x_2|}{2(\alpha-2)|P_1-P_3\|X_1-X_2|^\beta} + \frac{|u(P_1)-u(P_2)\|y_1-y_2|}{\sqrt{3}(\alpha-2)|P_1-P_2\|X_1-X_2|^\beta} \\
&\qquad + \frac{|u(P_2)-u(P_3)\|y_1-y_2|}{\sqrt{3}(\alpha-2)|P_2-P_3\|X_1-X_2|^\beta}
\end{aligned}
$$

$$
\begin{aligned}
&\leq \frac{5\sqrt{3}|u(P_1)-u(P_3)|}{2(\alpha-2)|P_1-P_3|^\beta} + \frac{|u(P_1)-u(P_2)|}{\sqrt{3}(\alpha-2)|P_1-P_2|^\beta} + \frac{|u(P_2)-u(P_3)|}{\sqrt{3}(\alpha-2)|P_2-P_3|^\beta} \\
&\leq \frac{5\sqrt{3}}{2(\alpha-2)}|u|_{K,\beta} + \frac{1}{\sqrt{3}(\alpha-2)}|u|_{K,\beta} + \frac{1}{\sqrt{3}(\alpha-2)}|u|_{K,\beta} \\
&= \frac{19}{2\sqrt{3}(\alpha-2)}|u|_{K,\beta} \\
&\leq 6(\alpha-2)^{-1}|u|_{K,\beta}
\end{aligned}
$$

□

Lemma 8. *Let T be a primary sidecar triangle with vertices P, Q, and R as depicted by any green triangle of Figure 4.10. Let $\beta \in (0,1]$ and u be a $\beta-$Hölder continuous function*

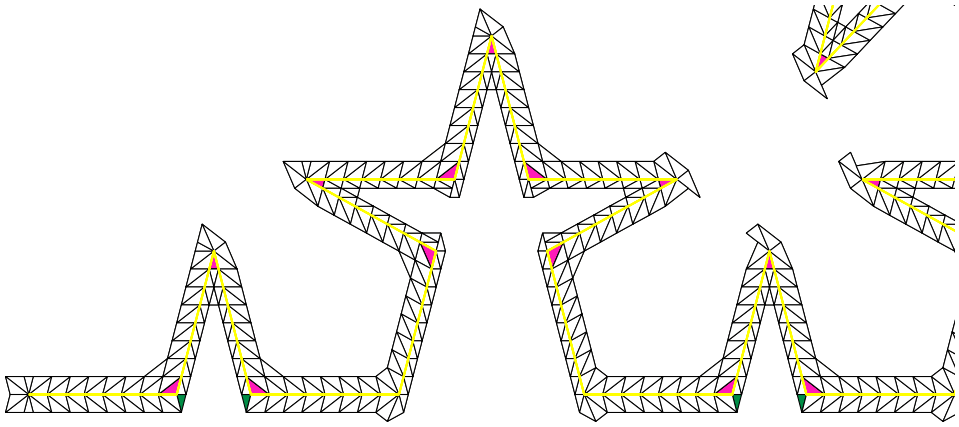

Figure 4.10: Cases for Lemma 8

defined on the vertices of the prefractal so that

$$\frac{|u(A)-u(B)|}{|A-B|^\beta} \leq |u|_{K,\beta}$$

for all $A, B \in V^n$. Then, for $n \geq 3$, $u_n^\star$ satisfies

$$\sup_{X,Y\in\mathcal{T}} \frac{|u_n^\star(X)-u_n^\star(Y)|}{|X-Y|^\beta} \leq 2(\alpha-2)^{-1}|u|_{K,\beta}.$$

Proof. We use the labeling scheme outlined in Lemma 3. This case considers the green type 2 triangles T of Figure 4.10. By symmetry, we further restrict our choice of T to triangles where $u_n^\star(Q)$ is defined by the affine function on the prefractal segments. In this case, we

have

$$\begin{aligned}
u_n^\star(Q) &= u(P_2),\\
u_n^\star(P) &= \frac{2k-1}{2k}u(P_2) + \frac{1}{2k}u(P_3),\\
u_n^\star(R) &= \frac{2k-1}{2k}u(P_2) + \frac{1}{2k}u(P_1).
\end{aligned}$$

Choosing distinct $X_1, X_2 \in T$ with $X_1 = (x_1, y_1)$ and $X_2 = (x_2, y_2)$, equation (4.2) gives

$$\begin{aligned}
\frac{|u_n^\star(X_1) - u_n^\star(X_2)|}{|X_1 - X_2|^\beta} &\leq \frac{|u_n^\star(P) - u_n^\star(Q)\|x_1 - x_2|}{|Q-P\|X_1 - X_2|^\beta} + \frac{|2u_n^\star(R) - u_n^\star(P) - u_n^\star(Q)\|y_1 - y_2|}{\sqrt{4-(\alpha-2)^2}|Q-P\|X_1 - X_2|^\beta}\\
&\leq \frac{|u(P_2) - u(P_3)\|x_1 - x_2|}{2k|Q-P\|X_1 - X_2|^\beta} + \frac{2|u(P_1) - u(P_2)\|y_1 - y_2|}{2k|Q-P|\sqrt{4-(\alpha-2)^2}|X_1 - X_2|^\beta}\\
&\qquad + \frac{|u(P_1) - u(P_3)\|y_1 - y_2|}{2k|Q-P|\sqrt{4-(\alpha-2)^2}|X_1 - X_2|^\beta}\\
&\leq \frac{\sqrt{3}|u(P_2) - u(P_3)\|x_1 - x_2|}{2(\alpha-2)|P_2 - P_3\|X_1 - X_2|^\beta} + \frac{2|u(P_1) - u(P_2)\|y_1 - y_2|}{2\sqrt{3}(\alpha-2)|P_1 - P_2\|X_1 - X_2|^\beta}\\
&\qquad + \frac{|u(P_1) - u(P_3)\|y_1 - y_2|}{2\sqrt{3}(\alpha-2)|P_1 - P_3\|X_1 - X_2|^\beta}\\
&\leq \frac{\sqrt{3}|u(P_2) - u(P_3)|}{2(\alpha-2)|P_2 - P_3|^\beta} + \frac{2|u(P_1) - u(P_2)|}{2\sqrt{3}(\alpha-2)|P_1 - P_2|^\beta} + \frac{|u(P_1) - u(P_3)|}{2\sqrt{3}(\alpha-2)|P_1 - P_3|^\beta}\\
&\leq \frac{\sqrt{3}}{2(\alpha-2)}|u|_{K,\beta} + \frac{2}{2\sqrt{3}(\alpha-2)}|u|_{K,\beta} + \frac{1}{2\sqrt{3}(\alpha-2)}|u|_{K,\beta}\\
&= \frac{\sqrt{3}}{(\alpha-2)}|u|_{K,\beta}\\
&\leq 2(\alpha-2)^{-1}|u|_{K,\beta}.
\end{aligned}$$

□

Lemma 9. *Let T be a primary sidecar triangle with vertices P, Q, and R as depicted by any red triangle of Figure 4.11. Let $\beta \in (0,1]$ and u be a $\beta-$Hölder continuous function defined on the vertices of the prefractal so that*

$$\frac{|u(A) - u(B)|}{|A-B|^\beta} \leq |u|_{K,\beta}$$

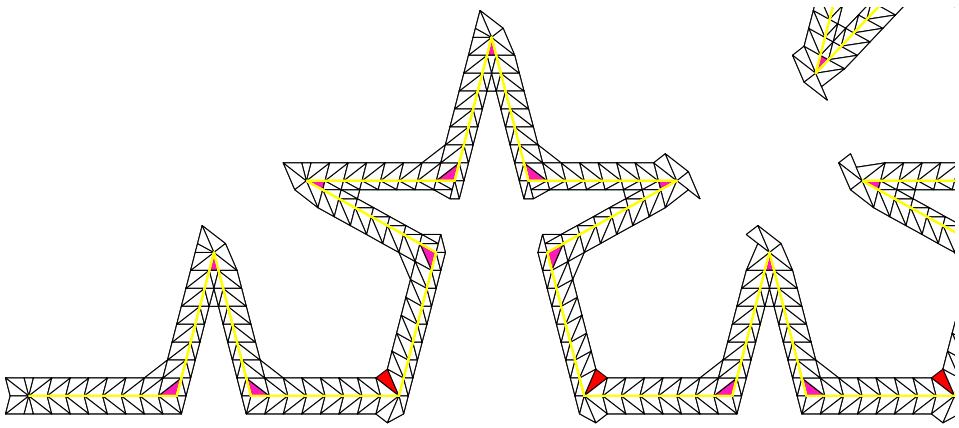

Figure 4.11: Cases for Lemma 9

for all $A, B \in V^n$. *Then, for* $n \geq 3$, $u_n^\star$ *satisfies*

$$\sup_{X,Y \in \mathcal{T}} \frac{|u_n^\star(X) - u_n^\star(Y)|}{|X - Y|^\beta} \leq 2(\alpha - 2)^{-1} |u|_{K,\beta}.$$

Proof. Let the vertex of T in V^n be labeled P_2. Label the vertex in V^n immediately left of P_2 as P_1 and the vertex immediately right of P_2 as P_3. Then

$$\begin{aligned}
u_n^\star(R) &= u(P_2), \\
u_n^\star(Q) &= \frac{2k-1}{2k} u(P_2) + \frac{1}{2k} u(P_1), \\
u_n^\star(P) &= \frac{2k-1}{2k} u(P_2) + \frac{1}{2k} u(P_3).
\end{aligned}$$

Choosing distinct $X_1, X_2 \in T$ with $X_1 = (x_1, y_1)$ and $X_2 = (x_2, y_2)$, equation (4.2) gives

$$\begin{aligned}
\frac{|u_n^\star(X_1) - u_n^\star(X_2)|}{|X_1 - X_2|^\beta} &\leq \frac{|u_n^\star(P) - u_n^\star(Q)\|x_1 - x_2|}{|Q - P\|X_1 - X_2|^\beta} + \frac{|2u_n^\star(R) - u_n^\star(P) - u_n^\star(Q)\|y_1 - y_2|}{\sqrt{4 - (\alpha - 2)^2}|Q - P\|X_1 - X_2|^\beta} \\
&\leq \frac{|u(P_1) - u(P_3)\|x_1 - x_2|}{2k|Q - P\|X_1 - X_2|^\beta} + \frac{2|u(P_1) - u(P_2)\|y_1 - y_2|}{2k|Q - P|\sqrt{4 - (\alpha - 2)^2}|X_1 - X_2|^\beta} \\
&\quad + \frac{|u(P_2) - u(P_3)\|y_1 - y_2|}{2k|Q - P|\sqrt{4 - (\alpha - 2)^2}|X_1 - X_2|^\beta}
\end{aligned}$$

$$
\begin{aligned}
&\leq \frac{\sqrt{3}|u(P_1)-u(P_3)\|x_1-x_2|}{2(\alpha-2)|P_1-P_3\|X_1-X_2|^\beta} + \frac{2|u(P_1)-u(P_2)\|y_1-y_2|}{2\sqrt{3}(\alpha-2)|P_1-P_2\|X_1-X_2|^\beta} \\
&\qquad + \frac{|u(P_2)-u(P_3)\|y_1-y_2|}{2\sqrt{3}(\alpha-2)|P_2-P_3\|X_1-X_2|^\beta} \\
&\leq \frac{\sqrt{3}|u(P_1)-u(P_3)|}{2(\alpha-2)|P_1-P_3|^\beta} + \frac{2|u(P_1)-u(P_2)|}{2\sqrt{3}(\alpha-2)|P_1-P_2|^\beta} + \frac{|u(P_2)-u(P_3)|}{2\sqrt{3}(\alpha-2)|P_2-P_3|^\beta} \\
&\leq \frac{\sqrt{3}}{2(\alpha-2)}|u|_{K,\beta} + \frac{2}{2\sqrt{3}(\alpha-2)}|u|_{K,\beta} + \frac{1}{2\sqrt{3}(\alpha-2)}|u|_{K,\beta} \\
&= \frac{\sqrt{3}}{(\alpha-2)}|u|_{K,\beta} \\
&\leq 2(\alpha-2)^{-1}|u|_{K,\beta}.
\end{aligned}
$$

□

Lemma 10. *Let T be a primary sidecar triangle with vertices P, Q, and R as depicted by any green triangle of Figure 4.12. Let $\beta \in (0,1]$ and u be a $\beta-$Hölder continuous function*

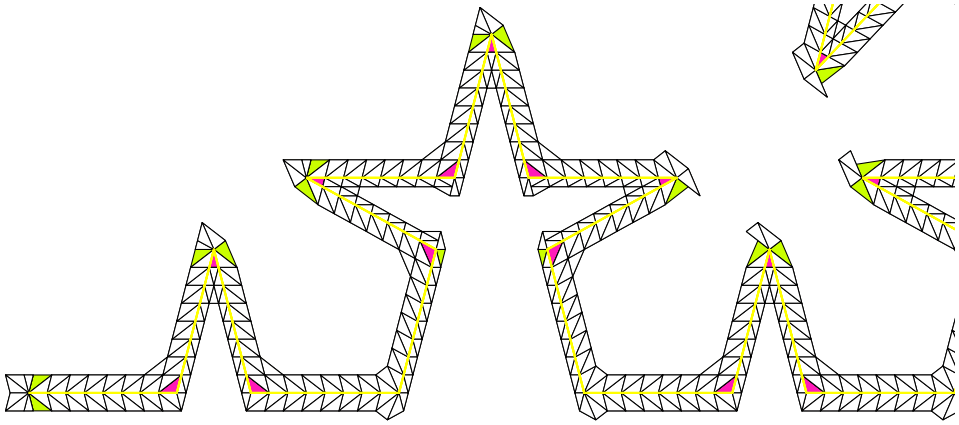

Figure 4.12: Cases for Lemma 10

defined on the vertices of the prefractal so that

$$\frac{|u(A)-u(B)|}{|A-B|^\beta} \leq |u|_{K,\beta}$$

for all $A, B \in V^n$. Then, for $n \geq 3$, $u_n^\star$ satisfies

$$\sup_{X,Y\in\mathcal{T}} \frac{|u_n^\star(X)-u_n^\star(Y)|}{|X-Y|^\beta} \leq 2(\alpha-2)^{-1}|u|_{K,\beta}.$$

Proof. There are four cases to consider.

Case 1. This cases considers the type 1 triangles at the ends of K^n; that is, have a vertex as $(0,0)$ or $(1,0)$. In this case, we let P_1 be one of these vertices, respectively, and P_2 be the vertex of V^n immediately right (respectively, left) of this vertex. Because of symmetry, we further restrict our attention to triangles where $u_n^\star(P)$ is determined by the affine function along the prefractal segments. This implies

$$\begin{aligned} u_n^\star(P) &= u(P_1), \\ u_n^\star(Q) &= \frac{2k-1}{2k}u(P_1) + \frac{1}{2k}u(P_2), \\ u_n^\star(R) &= \frac{4k-1}{4k}u(P_1) + \frac{1}{4k}u(P_2) \end{aligned}$$

Choosing distinct $X_1, X_2 \in T$ with $X_1 = (x_1, y_1)$ and $X_2 = (x_2, y_2)$, equation (4.1) gives

$$\begin{aligned} \frac{|u_n^\star(X_1) - u_n^\star(X_2)|}{|X_1 - X_2|^\beta} &\leq \frac{|u_n^\star(P) - u_n^\star(Q)\|x_1 - x_2|}{|Q-P\|X_1 - X_2|^\beta} + \frac{|4u_n^\star(R) - 2u_n^\star(P) - 2u_n^\star(Q)\|y_1 - y_2|}{\sqrt{4-\alpha}|Q-P\|X_1 - X_2|^\beta} \\ &\leq \frac{|u(P_1) - u(P_2)\|x_1 - x_2|}{2k|Q-P\|X_1 - X_2|^\beta} \\ &\leq \frac{|u(P_1) - u(P_2)\|x_1 - x_2|}{2\sqrt{2}|P_1 - P_2\|X_1 - X_2|^\beta} \\ &\leq \frac{|u(P_1) - u(P_2)|}{2\sqrt{2}|P_1 - P_2|^\beta} \\ &\leq \frac{1}{2\sqrt{2}}|u|_{K,\beta} \\ &\leq (\alpha-2)^{-1}|u|_{K,\beta}. \end{aligned}$$

Case 2. This case considers the type 2 triangles which have a vertex in common with a pink type 1 triangle. By a symmetrical argument, we further restrict our choice of T to triangles where $u_n^\star(Q)$ is determined by the affine function along the prefractal. We label the common vertex as P_2 and the vertex of V^n immediately left of P_2 as P_1. This implies

$$u_n^\star(Q) = u(P_2),$$

$$u_n^\star(R) = \frac{2k-1}{2k}u(P_2) + \frac{1}{2k}u(P_1),$$
$$u_n^\star(P) = \frac{4k-1}{4k}u(P_2) + \frac{1}{4k}u(P_1).$$

Choosing distinct $X_1, X_2 \in T$ with $X_1 = (x_1, y_1)$ and $X_2 = (x_2, y_2)$, equation (4.2) gives

$$\begin{aligned}
\frac{|u_n^\star(X_1) - u_n^\star(X_2)|}{|X_1 - X_2|^\beta} &\leq \frac{|u_n^\star(P) - u_n^\star(Q)\|x_1 - x_2|}{|Q-P\|X_1 - X_2|^\beta} + \frac{|2u_n^\star(R) - u_n^\star(P) - u_n^\star(Q)\|y_1 - y_2|}{\sqrt{4-(\alpha-2)^2}|Q-P\|X_1 - X_2|^\beta} \\
&\leq \frac{|u(P_1) - u(P_2)\|x_1 - x_2|}{4k|Q-P\|X_1 - X_2|^\beta} + \frac{3|u(P_1) - u(P_2)\|y_1 - y_2|}{4k\sqrt{4-(\alpha-2)^2}|Q-P\|X_1 - X_2|^\beta} \\
&\leq \frac{\sqrt{3}|u(P_1) - u(P_2)\|x_1 - x_2|}{4(\alpha-2)|P_1-P_2\|X_1 - X_2|^\beta} + \frac{3|u(P_1) - u(P_2)\|y_1 - y_2|}{4(\alpha-2)|P_1-P_2\|X_1 - X_2|^\beta} \\
&\leq \frac{\sqrt{3}|u(P_1) - u(P_2)|}{4(\alpha-2)|P_1-P_2|^\beta} + \frac{3|u(P_1) - u(P_2)|}{4(\alpha-2)|P_1-P_2|^\beta} \\
&\leq \frac{\sqrt{3}}{4(\alpha-2)}|u|_{K,\beta} + \frac{3}{4(\alpha-2)}|u|_{K,\beta} \\
&\leq \frac{3+\sqrt{3}}{4(\alpha-2)}|u|_{K,\beta} \\
&\leq 2(\alpha-2)^{-1}|u|_{K,\beta}.
\end{aligned}$$

Case 3. This case considers the type 1 triangles with a vertex in common with a pink type 1 triangle. By symmetry, we further restrict our choice in T to those where $u_n^\star(Q)$ is determined by the affine function along the prefractal. We label the common vertex as P_2, the vertex of V^n immediately left of P_2 as P_1, and the vertex of V^n immediately right of P_2 as P_3. This implies

$$u_n^\star(Q) = u(P_2),$$
$$u_n^\star(P) = \frac{2k-1}{2k}u(P_2) + \frac{1}{2k}u(P_1),$$
$$u_n^\star(R) = \frac{4k-1}{4k}u(P_2) + \frac{1}{4k}u(P_1).$$

Choosing distinct $X_1, X_2 \in T$ with $X_1 = (x_1, y_1)$ and $X_2 = (x_2, y_2)$, equation (4.1) gives

$$\begin{aligned}
\frac{|u_n^\star(X_1) - u_n^\star(X_2)|}{|X_1 - X_2|^\beta} &\leq \frac{|u_n^\star(P) - u_n^\star(Q)\|x_1 - x_2|}{|Q - P\|X_1 - X_2|^\beta} + \frac{|4u_n^\star(R) - 2u_n^\star(P) - 2u_n^\star(Q)\|y_1 - y_2|}{\sqrt{4-\alpha}|Q - P\|X_1 - X_2|^\beta} \\
&\leq \frac{|u(P_1) - u(P_2)\|x_1 - x_2|}{2k|Q - P\|X_1 - X_2|^\beta} \\
&\leq \frac{|u(P_1) - u(P_2)\|x_1 - x_2|}{2\sqrt{2}|P_1 - P_2\|X_1 - X_2|^\beta} \\
&\leq \frac{|u(P_1) - u(P_2)|}{2\sqrt{2}|P_1 - P_2|^\beta} \\
&\leq \frac{1}{2\sqrt{2}}|u|_{K,\beta} \\
&\leq (\alpha - 2)^{-1}|u|_{K,\beta}.
\end{aligned}$$

Case 4. This case considers the type 2 triangles with a vertex in common with a pink type 1 triangle. By symmetry, we further restrict our choice in T to those where $u_n^\star(Q)$ is determined by the affine function along the prefractal. We label the common vertex as P_2, the vertex of V^n immediately left of P_2 as P_1, and the vertex of V^n immediately right of P_2 as P_3. This implies

$$\begin{aligned}
u_n^\star(Q) &= u(P_2), \\
u_n^\star(R) &= \frac{2k-1}{2k}u(P_2) + \frac{1}{2k}u(P_3), \\
u_n^\star(P) &= \frac{4k-1}{4k}u(P_2) + \frac{1}{4k}u(P_3).
\end{aligned}$$

Choosing distinct $X_1, X_2 \in T$ with $X_1 = (x_1, y_1)$ and $X_2 = (x_2, y_2)$, equation (4.2) gives

$$\begin{aligned}
\frac{|u_n^\star(X_1) - u_n^\star(X_2)|}{|X_1 - X_2|^\beta} &\leq \frac{|u_n^\star(P) - u_n^\star(Q)\|x_1 - x_2|}{|Q - P\|X_1 - X_2|^\beta} + \frac{|2u_n^\star(R) - u_n^\star(P) - u_n^\star(Q)\|y_1 - y_2|}{\sqrt{4-(\alpha-2)^2}|Q - P\|X_1 - X_2|^\beta} \\
&\leq \frac{|u(P_2) - u(P_3)\|x_1 - x_2|}{4k|Q - P\|X_1 - X_2|^\beta} + \frac{3|u(P_2) - u(P_3)\|y_1 - y_2|}{4k\sqrt{4-(\alpha-2)^2}|Q - P\|X_1 - X_2|^\beta} \\
&\leq \frac{\sqrt{3}|u(P_2) - u(P_3)\|x_1 - x_2|}{4(\alpha-2)|Q - P\|X_1 - X_2|^\beta} + \frac{3|u(P_2) - u(P_3)\|y_1 - y_2|}{4(\alpha-2)|P_2 - P_3\|X_1 - X_2|^\beta}
\end{aligned}$$

$$
\begin{aligned}
&\leq \frac{\sqrt{3}|u(P_2) - u(P_3)|}{4(\alpha-2)|Q-P|^\beta} + \frac{3|u(P_2) - u(P_3)|}{4(\alpha-2)|P_2-P_3|^\beta} \\
&\leq \frac{\sqrt{3}}{4(\alpha-2)}|u|_{K,\beta} + \frac{3}{4(\alpha-2)}|u|_{K,\beta} \\
&\leq \frac{\sqrt{3}+3}{4(\alpha-2)}|u|_{K,\beta} \\
&\leq 2(\alpha-2)^{-1}|u|_{K,\beta}.
\end{aligned}
$$

□

Lemma 11. *Let T be a primary sidecar triangle with vertices P, Q, and R as depicted by any dark green triangle of Figure 4.13. Let $\beta \in (0,1]$ and u be a $\beta-$Hölder continuous*

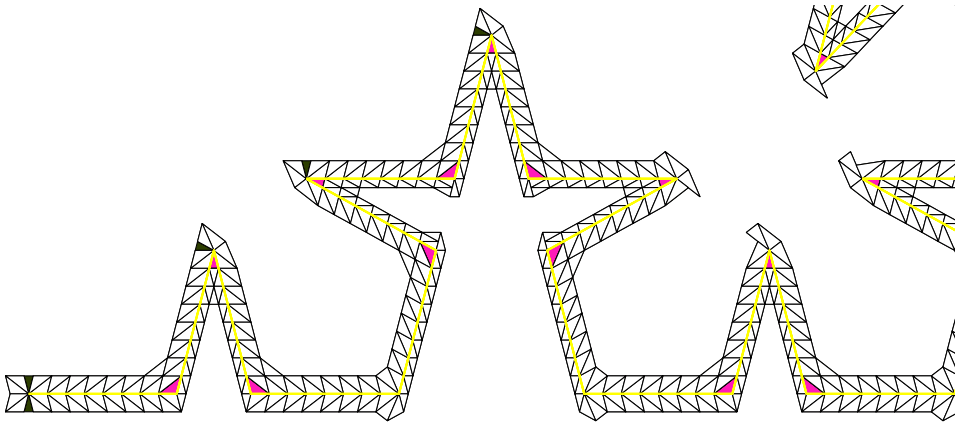

Figure 4.13: Cases for Lemma 11

function defined on the vertices of the prefractal so that

$$\frac{|u(A) - u(B)|}{|A-B|^\beta} \leq |u|_{K,\beta}$$

for all $A, B \in V^n$. Then, for $n \geq 3$, $u_n^\star$ satisfies

$$\sup_{X,Y \in \mathcal{T}} \frac{|u_n^\star(X) - u_n^\star(Y)|}{|X-Y|^\beta} \leq (\alpha-2)^{-1}|u|_{K,\beta}.$$

Proof. There are two cases. We use the labeling schemes from Lemma 10.

Case 1. This case deals with the dark green type 2 triangles at the ends of K^n. This implies

$$\begin{aligned}
u_n^\star(R) &= u(P_1),\\
u_n^\star(P) &= \frac{4k-1}{4k}u(P_1) + \frac{1}{4k}u(P_2),\\
u_n^\star(Q) &= \frac{8k-1}{8k}u(P_1) + \frac{1}{8k}u(P_2).
\end{aligned}$$

Choosing distinct $X_1, X_2 \in T$ with $X_1 = (x_1, y_1)$ and $X_2 = (x_2, y_2)$, equation (4.2) gives

$$\begin{aligned}
\frac{|u_n^\star(X_1) - u_n^\star(X_2)|}{|X_1 - X_2|^\beta} &\leq \frac{|u_n^\star(P) - u_n^\star(Q)\|x_1 - x_2|}{|Q-P\|X_1 - X_2|^\beta} + \frac{|2u_n^\star(R) - u_n^\star(P) - u_n^\star(Q)\|y_1 - y_2|}{\sqrt{4-(\alpha-2)^2}|Q-P\|X_1 - X_2|^\beta}\\
&\leq \frac{|u(P_1) - u(P_2)\|x_1 - x_2|}{8k|Q-P\|X_1 - X_2|^\beta} + \frac{3|u(P_1) - u(P_2)\|y_1 - y_2|}{8k|Q-P|\sqrt{4-(\alpha-2)^2}|X_1 - X_2|^\beta}\\
&\leq \frac{|u(P_1) - u(P_2)\|x_1 - x_2|}{8(\alpha-2)|P_1-P_2\|X_1 - X_2|^\beta} + \frac{\sqrt{3}|u(P_1) - u(P_2)\|y_1 - y_2|}{8(\alpha-2)|P_1-P_2\|X_1 - X_2|^\beta}\\
&\leq \frac{|u(P_1) - u(P_2)|}{8(\alpha-2)|P_1-P_2|^\beta} + \frac{\sqrt{3}|u(P_1) - u(P_2)|}{8(\alpha-2)|P_1-P_2|^\beta}\\
&\leq \frac{1}{8(\alpha-2)}|u|_{K,\beta} + \frac{\sqrt{3}}{8(\alpha-2)}|u|_{K,\beta}\\
&= \frac{1+\sqrt{3}}{8(\alpha-2)}|u|_{K,\beta}\\
&\leq (\alpha-2)^{-1}|u|_{K,\beta}.
\end{aligned}$$

Case 2. This case considers the type 2 triangles T with a vertex in V^n common to a pink type 2 triangle. By symmetry, we further restrict our choice of T to triangles defined by P_1 and P_2. We immediately get that

$$\begin{aligned}
u_n^\star(R) &= u(P_2),\\
u_n^\star(Q) &= \frac{4k-1}{4k}u(P_2) + \frac{1}{4k}u(P_1),\\
u_n^\star(P) &= \frac{8k-1}{8k}u(P_2) + \frac{1}{8k}u(P_1).
\end{aligned}$$

Choosing distinct $X_1, X_2 \in T$ with $X_1 = (x_1, y_1)$ and $X_2 = (x_2, y_2)$, equation (4.2) gives

$$\begin{aligned}
\frac{|u_n^\star(X_1) - u_n^\star(X_2)|}{|X_1 - X_2|^\beta} &\leq \frac{|u_n^\star(P) - u_n^\star(Q)\|x_1 - x_2|}{|Q - P\|X_1 - X_2|^\beta} + \frac{|2u_n^\star(R) - u_n^\star(P) - u_n^\star(Q)\|y_1 - y_2|}{\sqrt{4 - (\alpha - 2)^2}|Q - P\|X_1 - X_2|^\beta} \\
&\leq \frac{|u(P_1) - u(P_2)\|x_1 - x_2|}{8k|Q - P\|X_1 - X_2|^\beta} + \frac{3|u(P_1) - u(P_2)\|y_1 - y_2|}{8k|Q - P\|X_1 - X_2|^\beta} \\
&\leq \frac{|u(P_1) - u(P_2)\|x_1 - x_2|}{8(\alpha - 2)|P_1 - P_2\|X_1 - X_2|^\beta} + \frac{3|u(P_1) - u(P_2)\|y_1 - y_2|}{8(\alpha - 2)|P_1 - P_2\|X_1 - X_2|^\beta} \\
&\leq \frac{|u(P_1) - u(P_2)|}{8(\alpha - 2)|P_1 - P_2|^\beta} + \frac{3|u(P_1) - u(P_2)|}{8(\alpha - 2)|P_1 - P_2|^\beta} \\
&\leq \frac{1}{2(\alpha - 2)}|u|_{K,\beta} \\
&\leq (\alpha - 2)^{-1}|u|_{K,\beta}.
\end{aligned}$$

□

Lemma 12. *Let T be a primary sidecar triangle with vertices P, Q, and R as depicted by any brown triangle of Figure 4.14. Let $\beta \in (0, 1]$ and u be a $\beta-$Hölder continuous function*

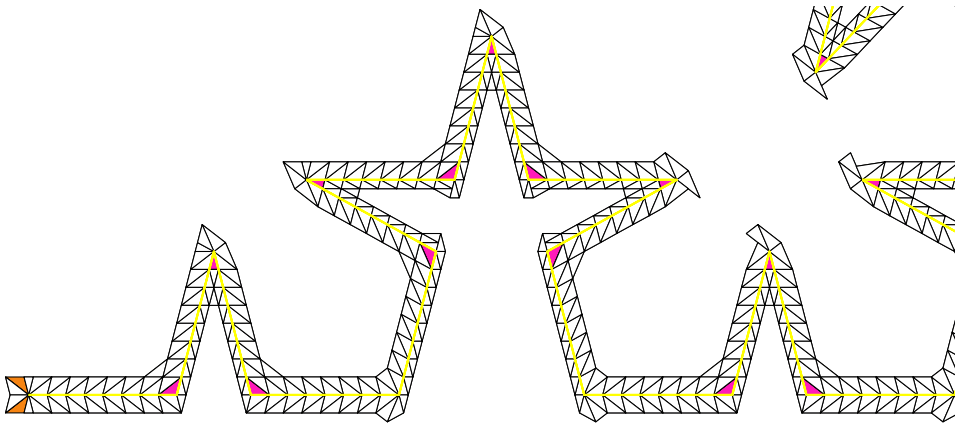

Figure 4.14: Cases for Lemma 12

defined on the vertices of the prefractal so that

$$\frac{|u(A) - u(B)|}{|A - B|^\beta} \leq |u|_{K,\beta}$$

for all $A, B \in V^n$. Then, for $n \geq 3$, $u_n^\star$ satisfies

$$\sup_{X,Y \in \mathcal{T}} \frac{|u_n^\star(X) - u_n^\star(Y)|}{|X - Y|^\beta} \leq (\alpha - 2)^{-1} |u|_{K,\beta}.$$

Proof. We use the labeling scheme outlined in Lemma 10. This case considers the type 1 triangles at the ends of K^n. By symmetry, we restrict our choice in T to those with $u_n^\star(Q)$ defined by the affine process along the segments of K^n. This gives

$$\begin{aligned}
u_n^\star(Q) &= u(P_1), \\
u_n^\star(R) &= \frac{8k-1}{8k} u(P_1) + \frac{1}{8k} u(P_2), \\
u_n^\star(P) &= \frac{16k-1}{16k} u(P_1) + \frac{1}{16k} u(P_2).
\end{aligned}$$

Choosing distinct $X_1, X_2 \in T$ with $X_1 = (x_1, y_1)$ and $X_2 = (x_2, y_2)$, equation (4.1) gives

$$\begin{aligned}
\frac{|u_n^\star(X_1) - u_n^\star(X_2)|}{|X_1 - X_2|^\beta} &\leq \frac{|u_n^\star(P) - u_n^\star(Q)\|x_1 - x_2|}{|Q - P\|X_1 - X_2|^\beta} + \frac{|4u_n^\star(R) - 2u_n^\star(P) - 2u_n^\star(Q)\|y_1 - y_2|}{\sqrt{4-\alpha}|Q - P\|X_1 - X_2|^\beta} \\
&\leq \frac{|u(P_1) - u(P_2)\|x_1 - x_2|}{16k|Q - P\|X_1 - X_2|^\beta} + \frac{3|u(P_1) - u(P_2)\|y_1 - y_2|}{8k|Q - P|\sqrt{4-\alpha}|X_1 - X_2|^\beta} \\
&\leq \frac{|u(P_1) - u(P_2)\|x_1 - x_2|}{16\sqrt{\alpha}|P_1 - P_2\|X_1 - X_2|^\beta} + \frac{3|u(P_1) - u(P_2)\|y_1 - y_2|}{8\sqrt{2}|P_1 - P_2\|X_1 - X_2|^\beta} \\
&\leq \frac{|u(P_1) - u(P_2)|}{16\sqrt{2}|P_1 - P_2|^\beta} + \frac{3|u(P_1) - u(P_2)|}{8\sqrt{2}|P_1 - P_2|^\beta} \\
&\leq \frac{1}{16\sqrt{2}} |u|_{K,\beta} + \frac{3}{8\sqrt{2}} |u|_{K,\beta} \\
&= \frac{7}{16\sqrt{2}} |u|_{K,\beta} \\
&\leq (\alpha - 2)^{-1} |u|_{K,\beta}.
\end{aligned}$$

□

Lemma 13. *Let T be a primary sidecar triangle with vertices P, Q, and R as depicted by any beige triangle of Figure 4.15. Let $\beta \in (0, 1]$ and u be a $\beta-$Hölder continuous function*

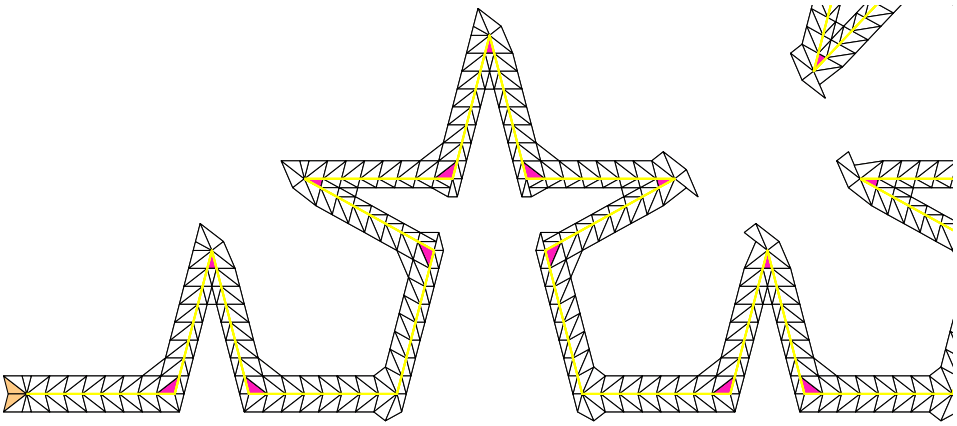

Figure 4.15: Cases for Lemma 13

defined on the vertices of the prefractal so that

$$\frac{|u(A) - u(B)|}{|A - B|^\beta} \leq |u|_{K,\beta}$$

for all $A, B \in V^n$. *Then, for* $n \geq 3$, $u_n^\star$ *satisfies*

$$\sup_{X,Y \in \mathcal{T}} \frac{|u_n^\star(X) - u_n^\star(Y)|}{|X - Y|^\beta} \leq (\alpha - 2)^{-1} |u|_{K,\beta}.$$

Proof. We use the labeling scheme outlined in Lemma 10. By symmetry, we restrict our choice in T to those with $u_n^\star(P)$ defined by the affine process along the segments of K^n. This gives

$$\begin{aligned} u_n^\star(P) &= u(P_1), \\ u_n^\star(Q) &= \frac{16k - 1}{16k} u(P_1) + \frac{1}{16k} u(P_2), \\ u_n^\star(R) &= \frac{32k - 1}{32k} u(P_1) + \frac{1}{32k} u(P_2). \end{aligned}$$

Choosing distinct $X_1, X_2 \in T$ with $X_1 = (x_1, y_1)$ and $X_2 = (x_2, y_2)$, equation (4.1) gives

$$\frac{|u_n^\star(X_1) - u_n^\star(X_2)|}{|X_1 - X_2|^\beta} \leq \frac{|u_n^\star(P) - u_n^\star(Q)\|x_1 - x_2|}{|Q - P\|X_1 - X_2|^\beta} + \frac{|4u_n^\star(R) - 2u_n^\star(P) - 2u_n^\star(Q)\|y_1 - y_2|}{\sqrt{4 - \alpha}|Q - P\|X_1 - X_2|^\beta}$$

$$
\begin{aligned}
&\leq \frac{|u(P_1) - u(P_2)\|x_1 - x_2|}{16k|Q - P\|X_1 - X_2|^\beta} \\
&\leq \frac{|u(P_1) - u(P_2)\|x_1 - x_2|}{16\sqrt{\alpha}|P_1 - P_2\|X_1 - X_2|^\beta} \\
&\leq \frac{|u(P_1) - u(P_2)|}{16\sqrt{2}|P_1 - P_2|^\beta} \\
&\leq \frac{1}{16\sqrt{2}}|u|_{K,\beta} \\
&\leq (\alpha - 2)^{-1}|u|_{K,\beta}.
\end{aligned}
$$

□

Lemma 14. *Let T be a primary sidecar triangle with vertices P, Q, and R as depicted by any dark green triangle of Figure 4.16. Let $\beta \in (0, 1]$ and u be a $\beta-$Hölder continuous*

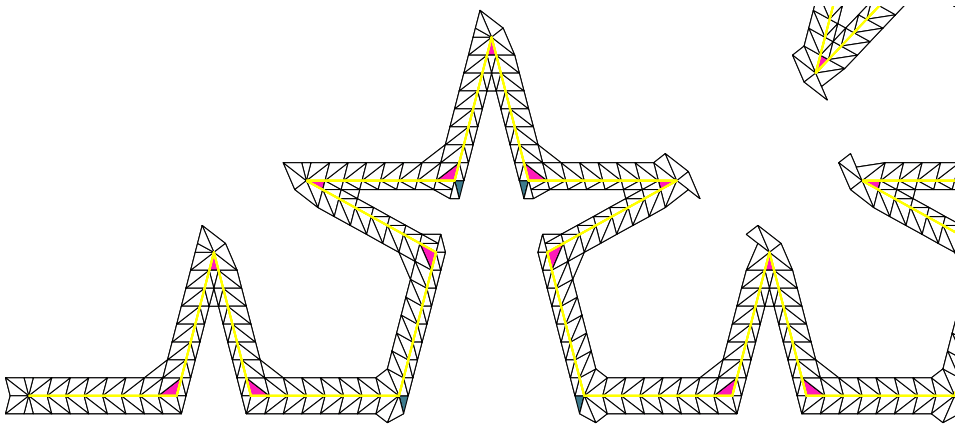

Figure 4.16: Cases for Lemma 14

function defined on the vertices of the prefractal so that

$$\frac{|u(A) - u(B)|}{|A - B|^\beta} \leq |u|_{K,\beta}$$

for all $A, B \in V^n$. Then, for $n \geq 3$, $u_n^\star$ satisfies

$$\sup_{X,Y \in \mathcal{T}} \frac{|u_n^\star(X) - u_n^\star(Y)|}{|X - Y|^\beta} \leq (\alpha - 2)^{-1}|u|_{K,\beta}.$$

Proof. We let the vertex of the green triangle in V^n be labeled P_2 with the vertices of V^n immediately right and left of P_2 labeled as P_1 and P_3 respectively. By symmetry, we further

restrict T to those which have $u_n^\star(Q)$ defined by the affine function on the segments of K^n. Then we have

$$\begin{aligned} u_n^\star(Q) &= u(P_2), \\ u_n^\star(P) &= \frac{2k-1}{2k}u(P_2) + \frac{1}{2k}u(P_3), \\ u_n^\star(R) &= \frac{4k-1}{4k}u(P_2) + \frac{1}{4k}u(P_3). \end{aligned}$$

Choosing distinct $X_1, X_2 \in T$ with $X_1 = (x_1, y_1)$ and $X_2 = (x_2, y_2)$, equation (4.2) gives

$$\begin{aligned} \frac{|u_n^\star(X_1) - u_n^\star(X_2)|}{|X_1 - X_2|^\beta} &\leq \frac{|u_n^\star(P) - u_n^\star(Q)\|x_1 - x_2|}{|Q - P\|X_1 - X_2|^\beta} + \frac{|2u_n^\star(R) - u_n^\star(P) - u_n^\star(Q)\|y_1 - y_2|}{\sqrt{4-(\alpha-2)^2}|Q - P\|X_1 - X_2|^\beta} \\ &\leq \frac{|u(P_2) - u(P_3)\|x_1 - x_2|}{2k|Q - P\|X_1 - X_2|^\beta} \\ &\leq \frac{|u(P_2) - u(P_3)\|x_1 - x_2|}{2(\alpha-2)|P_2 - P_3\|X_1 - X_2|^\beta} \\ &\leq \frac{|u(P_2) - u(P_3)|}{2(\alpha-2)|P_2 - P_3|^\beta} \\ &\leq \frac{1}{2(\alpha-2)}|u|_{K,\beta} \\ &\leq (\alpha-2)^{-1}|u|_{K,\beta}. \end{aligned}$$

□

Lemma 15. *Let T be a primary sidecar triangle with vertices P, Q, and R as depicted by any purple triangle of Figure 4.17. Let $\beta \in (0, 1]$ and u be a $\beta-$Hölder continuous function defined on the vertices of the prefractal so that*

$$\frac{|u(A) - u(B)|}{|A - B|^\beta} \leq |u|_{K,\beta}$$

for all $A, B \in V^n$. Then, for $n \geq 3$, $u_n^\star$ satisfies

$$\sup_{X,Y \in \mathcal{T}} \frac{|u_n^\star(X) - u_n^\star(Y)|}{|X - Y|^\beta} \leq (\alpha-2)^{-1}|u|_{K,\beta}.$$

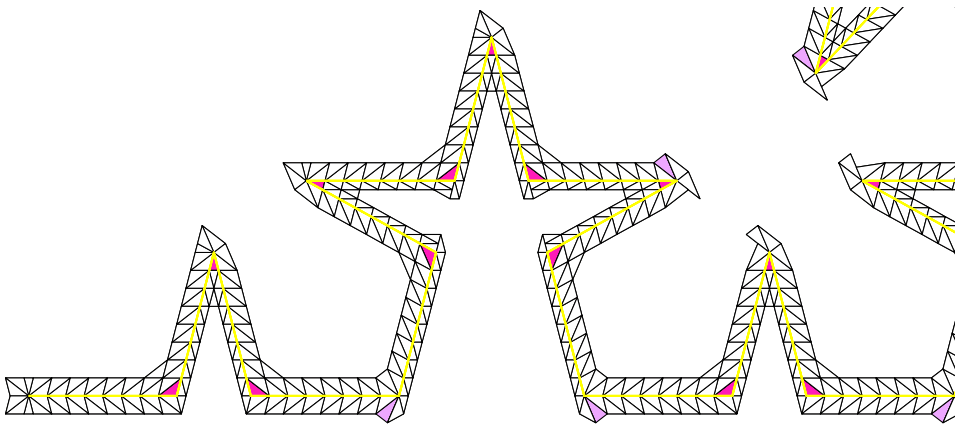

Figure 4.17: Cases for Lemma 15

Proof. We demonstrate the bound for the bound for the lilac triangle with the left most vertex of V^n attached to any such triangle; the other work analogously. If we let this vertex of V^n be P_2 and the vertex of V^n immediately left of this vertex as P_1, we have

$$\begin{aligned}
u_n^\star(R) &= u(P_2), \\
u_n^\star(P) &= \frac{2k-1}{2k}u(P_2) + \frac{1}{2k}u(P_1) \\
u_n^\star(Q) &= \frac{4k-1}{4k}u(P_2) + \frac{1}{4k}u(P_1).
\end{aligned}$$

Choosing distinct $X_1, X_2 \in T$ with $X_1 = (x_1, y_1)$ and $X_2 = (x_2, y_2)$, equation (4.2) gives

$$\begin{aligned}
\frac{|u_n^\star(X_1) - u_n^\star(X_2)|}{|X_1 - X_2|^\beta} &\leq \frac{|u_n^\star(P) - u_n^\star(Q)\|x_1 - x_2|}{|Q - P\|X_1 - X_2|^\beta} + \frac{|2u_n^\star(R) - u_n^\star(P) - u_n^\star(Q)\|y_1 - y_2|}{\sqrt{4-(\alpha-2)^2}|Q-P\|X_1 - X_2|^\beta} \\
&\leq \frac{|u(P_1) - u(P_2)\|x_1 - x_2|}{4k|Q - P\|X_1 - X_2|^\beta} + \frac{3|u(P_1) - u(P_2)\|y_1 - y_2|}{2k\sqrt{4-(\alpha-2)^2}|Q-P\|X_1 - X_2|^\beta} \\
&\leq \frac{|u(P_1) - u(P_2)\|x_1 - x_2|}{4(\alpha-2)|P_1 - P_2\|X_1 - X_2|^\beta} + \frac{\sqrt{3}|u(P_1) - u(P_2)\|y_1 - y_2|}{4(\alpha-2)|P_1 - P_2\|X_1 - X_2|^\beta} \\
&\leq \frac{|u(P_1) - u(P_2)|}{4(\alpha-2)|P_1 - P_2|^\beta} + \frac{\sqrt{3}|u(P_1) - u(P_2)|}{4(\alpha-2)|P_1 - P_2|^\beta} \\
&\leq \frac{1}{4(\alpha-2)}|u|_{K,\beta} + \frac{\sqrt{3}}{4(\alpha-2)}|u|_{K,\beta} \\
&= \frac{1+\sqrt{3}}{4(\alpha-2)}|u|_{K,\beta}
\end{aligned}$$

$$\leq (\alpha - 2)^{-1}|u|_{K,\beta}. \qquad \square$$

Lemma 16. *Let T be a primary sidecar triangle with vertices P, Q, and R as depicted by any pale green triangle of Figure 4.18. Let $\beta \in (0, 1]$ and u be a $\beta-$Hölder continuous*

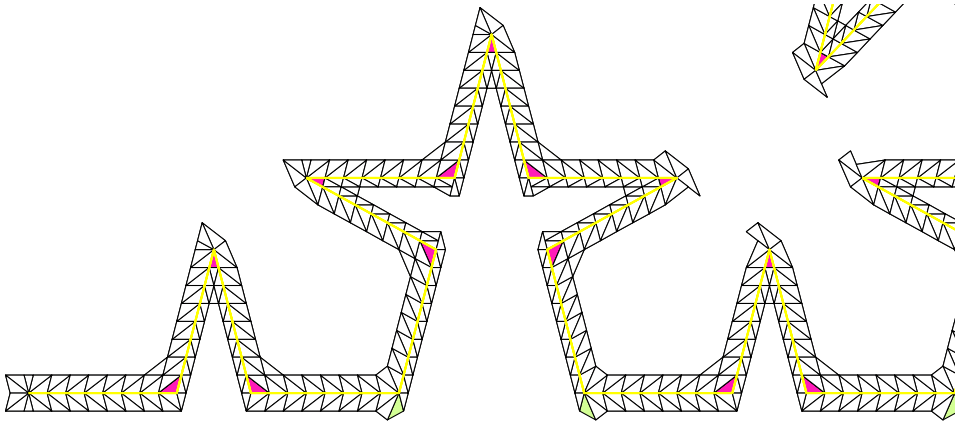

Figure 4.18: Cases for Lemma 16

function defined on the vertices of the prefractal so that

$$\frac{|u(A) - u(B)|}{|A - B|^{\beta}} \leq |u|_{K,\beta}$$

for all $A, B \in V^n$. Then, for $n \geq 3$, $u_n^\star$ satisfies

$$\sup_{X,Y \in \mathcal{T}} \frac{|u_n^\star(X) - u_n^\star(Y)|}{|X - Y|^{\beta}} \leq 2(\alpha - 2)^{-1}|u|_{K,\beta}.$$

Proof. Once again, we demonstrate the bound for the left most pale green triangle as the rest are shown similarly. We label in a similar manner to Lemma 16, except we also define P_3 as the vertex immediately right of P_2 in V^n. This gives

$$\begin{aligned}
u_n^\star(P) &= u(P_2), \\
u_n^\star(Q) &= \frac{4k-1}{4k}u(P_2) + \frac{1}{4k}u(P_1), \\
u_n^\star(R) &= \frac{4k-1}{4k}u(P_2) + \frac{1}{4k}u(P_3).
\end{aligned}$$

Choosing distinct $X_1, X_2 \in T$ with $X_1 = (x_1, y_1)$ and $X_2 = (x_2, y_2)$, equation (4.1) gives

$$\begin{aligned}
\frac{|u_n^\star(X_1) - u_n^\star(X_2)|}{|X_1 - X_2|^\beta} &\leq \frac{|u_n^\star(P) - u_n^\star(Q)\|x_1 - x_2|}{|Q - P\|X_1 - X_2|^\beta} + \frac{|4u_n^\star(R) - 2u_n^\star(P) - 2u_n^\star(Q)\|y_1 - y_2|}{\sqrt{4-\alpha}|Q - P\|X_1 - X_2|^\beta} \\
&\leq \frac{|u(P_1) - u(P_2)\|x_1 - x_2|}{4k|Q - P\|X_1 - X_2|^\beta} + \frac{|u(P_1) - u(P_3)\|y_1 - y_2|}{2k|Q - P|\sqrt{4-\alpha}|X_1 - X_2|^\beta} \\
&\qquad + \frac{|u(P_2) - u(P_3)\|y_1 - y_2|}{2k|Q - P|\sqrt{4-\alpha}|X_1 - X_2|^\beta} \\
&\leq \frac{|u(P_1) - u(P_2)\|x_1 - x_2|}{4\sqrt{2}|P_1 - P_2\|X_1 - X_2|^\beta} + \frac{|u(P_1) - u(P_3)\|y_1 - y_2|}{2|P_1 - P_3\|X_1 - X_2|^\beta} \\
&\qquad + \frac{|u(P_2) - u(P_3)\|y_1 - y_2|}{2\sqrt{2}|P_2 - P_3\|X_1 - X_2|^\beta} \\
&\leq \frac{|u(P_1) - u(P_2)|}{4\sqrt{2}|P_1 - P_2|^\beta} + \frac{|u(P_1) - u(P_3)|}{2|P_1 - P_3|^\beta} + \frac{|u(P_2) - u(P_3)|}{2\sqrt{2}|P_2 - P_3|^\beta} \\
&\leq \frac{1}{4\sqrt{2}}|u|_{K,\beta} + \frac{1}{2}|u|_{K,\beta} + \frac{1}{2\sqrt{2}}|u|_{K,\beta} \\
&= \frac{3 + 2\sqrt{2}}{4\sqrt{2}}|u|_{K,\beta} \\
&\leq 2(\alpha - 2)^{-1}|u|_{K,\beta}.
\end{aligned}$$

□

Lemma 17. *Let T be a primary sidecar triangle with vertices P, Q, and R as depicted by any dark blue triangle of Figure 4.19. Let $\beta \in (0, 1]$ and u be a $\beta-$Hölder continuous*

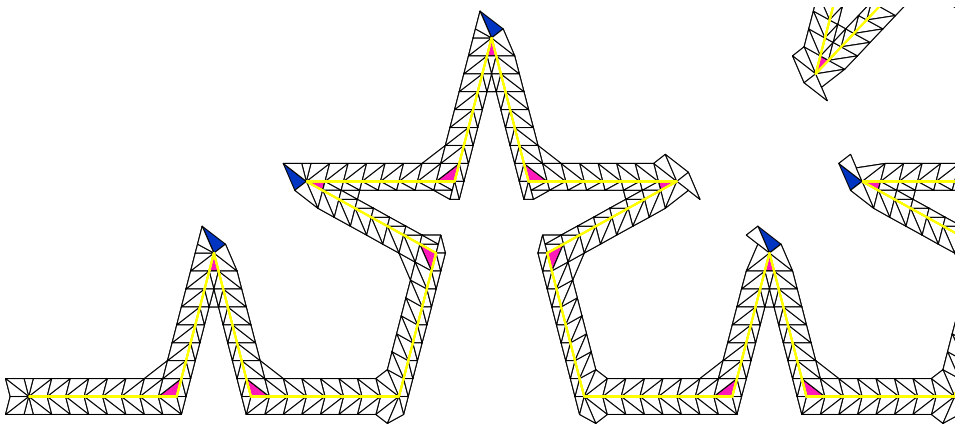

Figure 4.19: Cases for Lemma 17

function defined on the vertices of the prefractal so that

$$\frac{|u(A) - u(B)|}{|A - B|^\beta} \leq |u|_{K,\beta}$$

for all $A, B \in V^n$. *Then, for* $n \geq 3$, $u_n^\star$ *satisfies*

$$\sup_{X,Y \in \mathcal{T}} \frac{|u_n^\star(X) - u_n^\star(Y)|}{|X - Y|^\beta} \leq (\alpha - 2)^{-1} |u|_{K,\beta}.$$

Proof. As with the previous lemmas, we prove the bound for the left most blue triangle as the others follow in an analogous manner. In this case, we let the vertex of V^n be P_2 and the vertices immediately left and right of P_2 in V^n be P_1 and P_3, respectively. It is easy to check that

$$\begin{aligned}
u_n^\star(P) &= u(P_2), \\
u_n^\star(Q) &= \frac{4k-1}{4k} u(P_2) + \frac{1}{4k} u(P_3), \\
u_n^\star(R) &= \frac{8k-1}{8k} u(P_2) + \frac{1}{8k} u(P_3).
\end{aligned}$$

Choosing distinct $X_1, X_2 \in T$ with $X_1 = (x_1, y_1)$ and $X_2 = (x_2, y_2)$, equation (4.2) gives

$$\begin{aligned}
\frac{|u_n^\star(X_1) - u_n^\star(X_2)|}{|X_1 - X_2|^\beta} &\leq \frac{|u_n^\star(P) - u_n^\star(Q)\|x_1 - x_2|}{|Q - P\|X_1 - X_2|^\beta} + \frac{|2u_n^\star(R) - u_n^\star(P) - u_n^\star(Q)\|y_1 - y_2|}{\sqrt{4 - (\alpha-2)^2}|Q - P\|X_1 - X_2|^\beta} \\
&\leq \frac{|u(P_2) - u(P_3)\|x_1 - x_2|}{4k|Q - P\|X_1 - X_2|^\beta} \\
&\leq \frac{|u(P_2) - u(P_3)\|x_1 - x_2|}{4(\alpha-2)|P_2 - P_3\|X_1 - X_2|^\beta} \\
&\leq \frac{|u(P_2) - u(P_3)|}{4(\alpha-2)|P_2 - P_3|^\beta} \\
&\leq \frac{1}{4(\alpha-2)} |u|_{K,\beta} \\
&\leq (\alpha-2)^{-1} |u|_{K,\beta}.
\end{aligned}$$

□

Lemma 18. *Let T be a primary sidecar triangle with vertices P, Q, and R as depicted by any dark green triangle of Figure 4.20. Let $\beta \in (0,1]$ and u be a $\beta-$Hölder continuous*

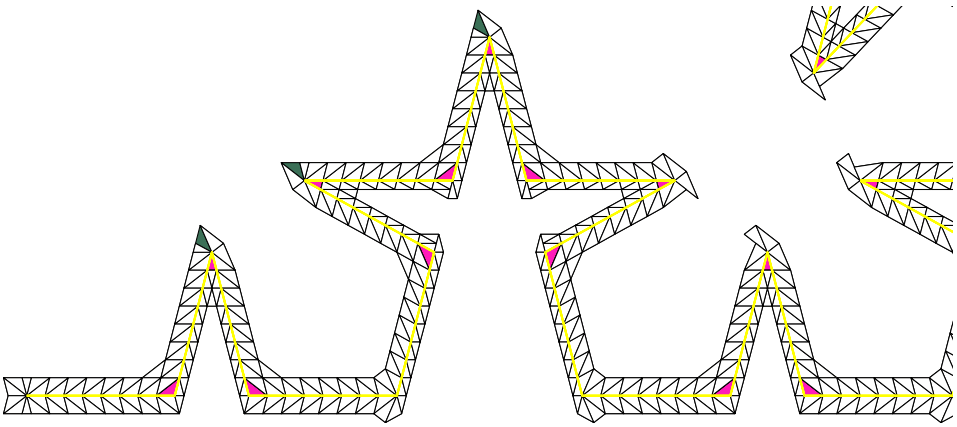

Figure 4.20: Cases for Lemma 18

function defined on the vertices of the prefractal so that

$$\frac{|u(A)-u(B)|}{|A-B|^{\beta}} \leq |u|_{K,\beta}$$

for all $A, B \in V^n$. Then, for $n \geq 3$, $u_n^\star$ satisfies

$$\sup_{X,Y\in\mathcal{T}} \frac{|u_n^\star(X)-u_n^\star(Y)|}{|X-Y|^{\beta}} \leq (\alpha-2)^{-1}|u|_{K,\beta}.$$

Proof. We prove the statement for the left most triangle. Let P_2 be the vertex of V^n in common with T and assume P_1 and P_3 are the vertices of V^n immediately left and right of P_2. Then

$$\begin{aligned}
u_n^\star(P) &= u(P_2),\\
u_n^\star(Q) &= \frac{8k-1}{8k}u(P_2) + \frac{1}{8k}u(P_3),\\
u_n^\star(R) &= \frac{8k-1}{8k}u(P_2) + \frac{1}{8k}u(P_1).
\end{aligned}$$

Choosing distinct $X_1, X_2 \in T$ with $X_1 = (x_1, y_1)$ and $X_2 = (x_2, y_2)$, equation (4.1) gives

$$\begin{aligned}
\frac{|u_n^\star(X_1) - u_n^\star(X_2)|}{|X_1 - X_2|^\beta} &\leq \frac{|u_n^\star(P) - u_n^\star(Q)\|x_1 - x_2|}{|Q - P\|X_1 - X_2|^\beta} + \frac{|4u_n^\star(R) - 2u_n^\star(P) - 2u_n^\star(Q)\|y_1 - y_2|}{\sqrt{4-\alpha}|Q - P\|X_1 - X_2|^\beta} \\
&\leq \frac{|u(P_2) - u(P_3)\|x_1 - x_2|}{8k|Q - P\|X_1 - X_2|^\beta} + \frac{|u(P_1) - u(P_2)\|y_1 - y_2|}{4k|Q - P|\sqrt{4-\alpha}|X_1 - X_2|^\beta} \\
&\qquad + \frac{|u(P_1) - u(P_3)\|y_1 - y_2|}{4k|Q - P|\sqrt{4-\alpha}|X_1 - X_2|^\beta} \\
&\leq \frac{|u(P_2) - u(P_3)\|x_1 - x_2|}{8\sqrt{2}|P_2 - P_3\|X_1 - X_2|^\beta} + \frac{|u(P_1) - u(P_2)\|y_1 - y_2|}{4\sqrt{2}|P_1 - P_2\|X_1 - X_2|^\beta} \\
&\qquad + \frac{|u(P_1) - u(P_3)\|y_1 - y_2|}{4|P_1 - P_3\|X_1 - X_2|^\beta} \\
&\leq \frac{|u(P_2) - u(P_3)|}{8\sqrt{2}|P_2 - P_3|^\beta} + \frac{|u(P_1) - u(P_2)|}{4\sqrt{2}|P_1 - P_2|^\beta} + \frac{|u(P_1) - u(P_3)|}{4|P_1 - P_3|^\beta} \\
&\leq \frac{1}{8\sqrt{2}}|u|_{K,\beta} + \frac{1}{4\sqrt{2}}|u|_{K,\beta} + \frac{1}{4}|u|_{K,\beta} \\
&= \frac{3 + 2\sqrt{2}}{8\sqrt{2}}|u|_{K,\beta} \\
&\leq (\alpha - 2)^{-1}|u|_{K,\beta}.
\end{aligned}$$

□

Lemma 19. *Let T be a primary sidecar triangle with vertices P, Q, and R as depicted by any purple triangle of Figure 4.21. Let $\beta \in (0, 1]$ and u be a $\beta-$Hölder continuous function*

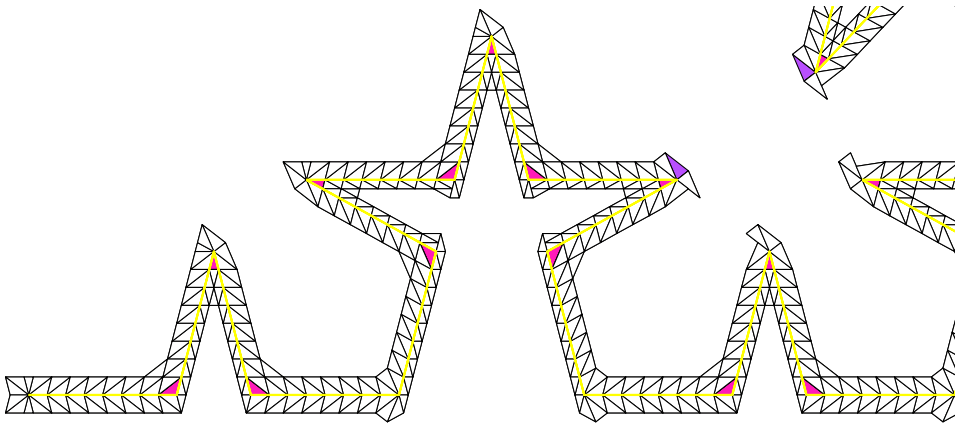

Figure 4.21: Cases for Lemma 19

defined on the vertices of the prefractal so that

$$\frac{|u(A)-u(B)|}{|A-B|^\beta} \leq |u|_{K,\beta}$$

for all $A, B \in V^n$. *Then, for* $n \geq 3$, $u_n^\star$ *satisfies*

$$\sup_{X,Y\in\mathcal{T}} \frac{|u_n^\star(X)-u_n^\star(Y)|}{|X-Y|^\beta} \leq (\alpha-2)^{-1}|u|_{K,\beta}.$$

Proof. By symmetry, we restrict our choice of T so that $u_n^\star(P)$ is defined by the affine process along the segments of the prefractal. We let P_2 be the point in V^n on T, P_1 be the point immediately left of P_2 in V^n, and P_3 be the point immediately right of P_2 in V^n. In this instance, we have

$$\begin{aligned}
u_n^\star(P) &= u(P_2),\\
u_n^\star(R) &= \frac{4k-1}{4k}u(P_2) + \frac{1}{4k}u(P_1),\\
u_n^\star(Q) &= \frac{8k-1}{8k}u(P_2) + \frac{1}{8k}u(P_1).
\end{aligned}$$

Choosing distinct $X_1, X_2 \in T$ with $X_1 = (x_1, y_1)$ and $X_2 = (x_2, y_2)$, equation (4.2) gives

$$\begin{aligned}
\frac{|u_n^\star(X_1)-u_n^\star(X_2)|}{|X_1-X_2|^\beta} &\leq \frac{|u_n^\star(P)-u_n^\star(Q)\|x_1-x_2|}{|Q-P\|X_1-X_2|^\beta} + \frac{|2u_n^\star(R)-u_n^\star(P)-u_n^\star(Q)\|y_1-y_2|}{\sqrt{4-(\alpha-2)^2}|Q-P\|X_1-X_2|^\beta}\\
&\leq \frac{|u(P_1)-u(P_2)\|x_1-x_2|}{8k|Q-P\|X_1-X_2|^\beta} + \frac{3|u(P_1)-u(P_2)\|y_1-y_2|}{8k\sqrt{4-(\alpha-2)^2}|Q-P\|X_1-X_2|^\beta}\\
&\leq \frac{|u(P_1)-u(P_2)\|x_1-x_2|}{8(\alpha-2)|P_1-P_2\|X_1-X_2|^\beta} + \frac{\sqrt{3}|u(P_1)-u(P_2)\|y_1-y_2|}{8(\alpha-2)|P_1-P_2\|X_1-X_2|^\beta}\\
&\leq \frac{|u(P_1)-u(P_2)|}{8(\alpha-2)|P_1-P_2|^\beta} + \frac{\sqrt{3}|u(P_1)-u(P_2)|}{8(\alpha-2)|P_1-P_2|^\beta}\\
&\leq \frac{1}{8(\alpha-2)}|u|_{K,\beta} + \frac{\sqrt{3}}{8(\alpha-2)}|u|_{K,\beta}\\
&= \frac{\sqrt{3}+1}{8(\alpha-2)}|u|_{K,\beta}
\end{aligned}$$

$$\leq (\alpha - 2)^{-1}|u|_{K,\beta}. \qquad \square$$

Lemma 20. *Let T be a primary sidecar triangle with vertices P, Q, and R as depicted by any dark red triangle of Figure 4.22. Let $\beta \in (0, 1]$ and u be a $\beta-$Hölder continuous function*

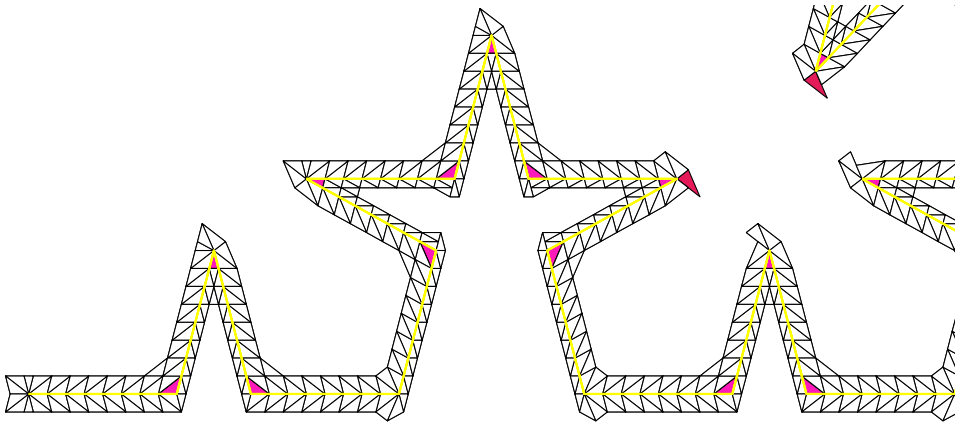

Figure 4.22: Cases for Lemma 20

defined on the vertices of the prefractal so that

$$\frac{|u(A) - u(B)|}{|A - B|^{\beta}} \leq |u|_{K,\beta}$$

for all $A, B \in V^n$. Then, for $n \geq 3$, $u_n^\star$ satisfies

$$\sup_{X,Y \in \mathcal{T}} \frac{|u_n^\star(X) - u_n^\star(Y)|}{|X - Y|^{\beta}} \leq (\alpha - 2)^{-1}|u|_{K,\beta}.$$

Proof. By symmetry, we show the result when $u_n^\star(Q)$ is defined by the affine process along the prefractal. Using the labeling scheme of Lemma 19, we have

$$\begin{aligned} u_n^\star(Q) &= u(P_2), \\ u_n^\star(P) &= \frac{8k-1}{8k}u(P_2) + \frac{1}{8k}u(P_1), \\ u_n^\star(R') &= \frac{4k-1}{4k}u(P_2) + \frac{1}{4k}u(P_3), \end{aligned}$$

where R' is the point in the center of the segment $\overline{QR}$. Since we define $u_n^\star$ to be affine along each edge, we can parameterize $u_n^\star$ along $\overline{QR}$ as $u_n^\star(t) = u_n^\star(Q)(1-t) + u_n^\star(R')t$ where $t = 0$ corresponds to $u_n^\star(Q)$ and $t = 1$ corresponds to $u_n^\star(R')$. Defining $u_n^\star(R)$ at $t = 2$, we have

$$u_n^\star(R) = u_n^\star(2) = 2u_n^\star(R') - u_n^\star(Q) = \frac{2k-1}{2k}u(P_2) + \frac{1}{2k}u(P_3).$$

Choosing distinct $X_1, X_2 \in T$ with $X_1 = (x_1, y_1)$ and $X_2 = (x_2, y_2)$, equation (4.2) gives

$$\begin{aligned}
\frac{|u_n^\star(X_1) - u_n^\star(X_2)|}{|X_1 - X_2|^\beta} &\leq \frac{|u_n^\star(P) - u_n^\star(Q)\|x_1 - x_2|}{|Q-P\|X_1 - X_2|^\beta} + \frac{|2u_n^\star(R) - u_n^\star(P) - u_n^\star(Q)\|y_1 - y_2|}{\sqrt{4-(\alpha-2)^2}|Q-P\|X_1 - X_2|^\beta} \\
&\leq \frac{|u(P_1) - u(P_2)\|x_1 - x_2|}{8k|Q-P\|X_1 - X_2|^\beta} + \frac{|u(P_1) - u(P_2)\|y_1 - y_2|}{8k\sqrt{4-(\alpha-2)^2}|Q-P\|X_1 - X_2|^\beta} \\
&\qquad + \frac{|u(P_2) - u(P_3)\|y_1 - y_2|}{k\sqrt{4-(\alpha-2)^2}|Q-P\|X_1 - X_2|^\beta} \\
&\leq \frac{|u(P_1) - u(P_2)\|x_1 - x_2|}{8(\alpha-2)|P_1-P_2\|X_1 - X_2|^\beta} + \frac{|u(P_1) - u(P_2)\|y_1 - y_2|}{8\sqrt{3}(\alpha-2)|P_1-P_2\|X_1 - X_2|^\beta} \\
&\qquad + \frac{|u(P_2) - u(P_3)\|y_1 - y_2|}{\sqrt{3}(\alpha-2)|P_2-P_3\|X_1 - X_2|^\beta} \\
&\leq \frac{|u(P_1) - u(P_2)|}{8(\alpha-2)|P_1-P_2|^\beta} + \frac{|u(P_1) - u(P_2)|}{8\sqrt{3}(\alpha-2)|P_1-P_2|^\beta} + \frac{|u(P_2) - u(P_3)|}{\sqrt{3}(\alpha-2)|P_2-P_3|^\beta} \\
&\leq \frac{1}{8(\alpha-2)}|u|_{K,\beta} + \frac{1}{8\sqrt{3}(\alpha-2)}|u|_{K,\beta} + \frac{1}{\sqrt{3}(\alpha-2)}|u|_{K,\beta} \\
&= \frac{1+3\sqrt{3}}{8(\alpha-2)}|u|_{K,\beta} \\
&\leq (\alpha-2)^{-1}|u|_{K,\beta}.
\end{aligned}$$

□

Lemma 21. *Let T be a primary sidecar triangle with vertices P, Q, and R as depicted by any cyan triangle of Figure 4.23. Let $\beta \in (0,1]$ and u be a $\beta-$Hölder continuous function defined on the vertices of the prefractal so that*

$$\frac{|u(A) - u(B)|}{|A-B|^\beta} \leq |u|_{K,\beta}$$

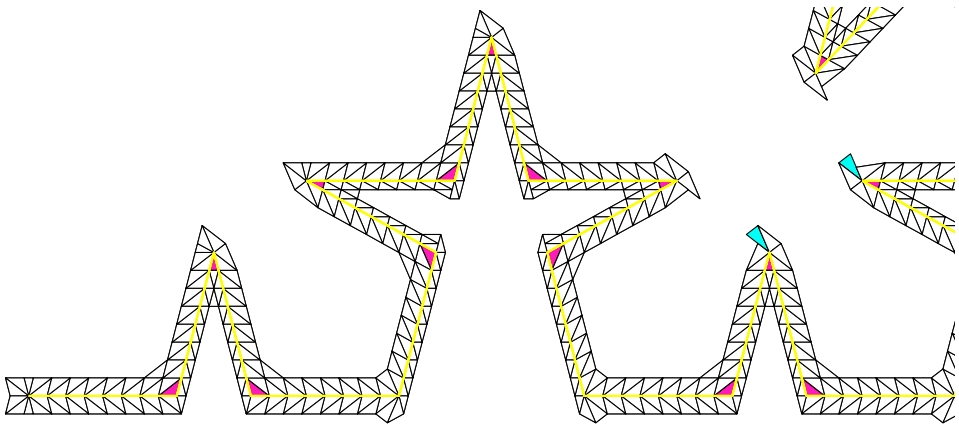

Figure 4.23: Cases for Lemma 21

for all $A, B \in V^n$. *Then, for* $n \geq 3$, $u_n^\star$ *satisfies*

$$\sup_{X,Y \in \mathcal{T}} \frac{|u_n^\star(X) - u_n^\star(Y)|}{|X - Y|^\beta} \leq (\alpha - 2)^{-1} |u|_{K,\beta}.$$

Proof. We show the result for the first cyan triangle, as the other work analogously. Let the vertex of T in V^n be P_2, the vertex in V^n immediately left of P_2 be P_1, and P_3 be the vertex of V^n immediately right of P_2. We have

$$\begin{aligned}
u_n^\star(R) &= u(P_2), \\
u_n^\star(P) &= \frac{8k-1}{8k} u(P_2) + \frac{1}{8k} u(P_3), \\
u_n^\star(Q') &= \frac{4k-1}{4k} u(P_2) + \frac{1}{4k} u(P_1)
\end{aligned}$$

where Q' is the vertex in the center of the segment of QR. In a manner similar to determining $u_n^\star(R)$ of Lemma 20, we see that

$$u_n^\star(Q) = \frac{2k-1}{2k} u(P_2) + \frac{1}{2k} u(P_1).$$

Choosing distinct $X_1, X_2 \in T$ with $X_1 = (x_1, y_1)$ and $X_2 = (x_2, y_2)$, equation (4.2) gives

$$\begin{aligned}
\frac{|u_n^\star(X_1) - u_n^\star(X_2)|}{|X_1 - X_2|^\beta} &\leq \frac{|u_n^\star(P) - u_n^\star(Q)\|x_1 - x_2|}{|Q - P\|X_1 - X_2|^\beta} + \frac{|2u_n^\star(R) - u_n^\star(P) - u_n^\star(Q)\|y_1 - y_2|}{\sqrt{4 - (\alpha-2)^2}|Q - P\|X_1 - X_2|^\beta} \\
&\leq \frac{3|u(P_1) - u(P_2)\|x_1 - x_2|}{8k|Q - P\|X_1 - X_2|^\beta} + \frac{|u(P_1) - u(P_3)\|x_1 - x_2|}{8k|Q - P\|X_1 - X_2|^\beta} \\
&\qquad + \frac{|u(P_1) - u(P_2)\|y_1 - y_2|}{2k\sqrt{3}|Q - P\|X_1 - X_2|^\beta} + \frac{|u(P_2) - u(P_3)\|y_1 - y_2|}{8k\sqrt{3}|Q - P\|X_1 - X_2|^\beta} \\
&\leq \frac{3|u(P_1) - u(P_2)\|x_1 - x_2|}{8(\alpha-2)|P_1 - P_2\|X_1 - X_2|^\beta} + \frac{|u(P_1) - u(P_3)\|x_1 - x_2|}{8|P_1 - P_3\|X_1 - X_2|^\beta} \\
&\qquad + \frac{|u(P_1) - u(P_2)\|y_1 - y_2|}{2\sqrt{3}(\alpha-2)|P_1 - P_2\|X_1 - X_2|^\beta} \\
&\qquad\qquad + \frac{|u(P_2) - u(P_3)\|y_1 - y_2|}{8\sqrt{3}(\alpha-2)|P_2 - P_3\|X_1 - X_2|^\beta} \\
&\leq \frac{3|u(P_1) - u(P_2)|}{8(\alpha-2)|P_1 - P_2|^\beta} + \frac{|u(P_1) - u(P_3)|}{8|P_1 - P_3|^\beta} \\
&\qquad + \frac{|u(P_1) - u(P_2)|}{2\sqrt{3}(\alpha-2)|P_1 - P_2|^\beta} + \frac{|u(P_2) - u(P_3)|}{8\sqrt{3}(\alpha-2)|P_2 - P_3|^\beta} \\
&\leq \frac{3}{8(\alpha-2)}|u|_{K,\beta} + \frac{1}{8}|u|_{K,\beta} + \frac{1}{2\sqrt{3}(\alpha-2)}|u|_{K,\beta} + \frac{1}{8\sqrt{3}(\alpha-2)}|u|_{K,\beta} \\
&= \frac{\sqrt{3}(\alpha+1)+5}{8\sqrt{3}(\alpha-2)}|u|_{K,\beta} \\
&\leq (\alpha-2)^{-1}|u|_{K,\beta}. \qquad \square
\end{aligned}$$

Lemma 22. *Let T be a primary sidecar triangle with vertices P, Q, and R as depicted by any green triangle of Figure 4.24. Let $\beta \in (0, 1]$ and u be a $\beta-$Hölder continuous function defined on the vertices of the prefractal so that*

$$\frac{|u(A) - u(B)|}{|A - B|^\beta} \leq |u|_{K,\beta}$$

for all $A, B \in V^n$. Then, for $n \geq 3$, $u_n^\star$ satisfies

$$\sup_{X,Y \in \mathcal{T}} \frac{|u_n^\star(X) - u_n^\star(Y)|}{|X - Y|^\beta} \leq 2(\alpha-2)^{-1}|u|_{K,\beta}.$$

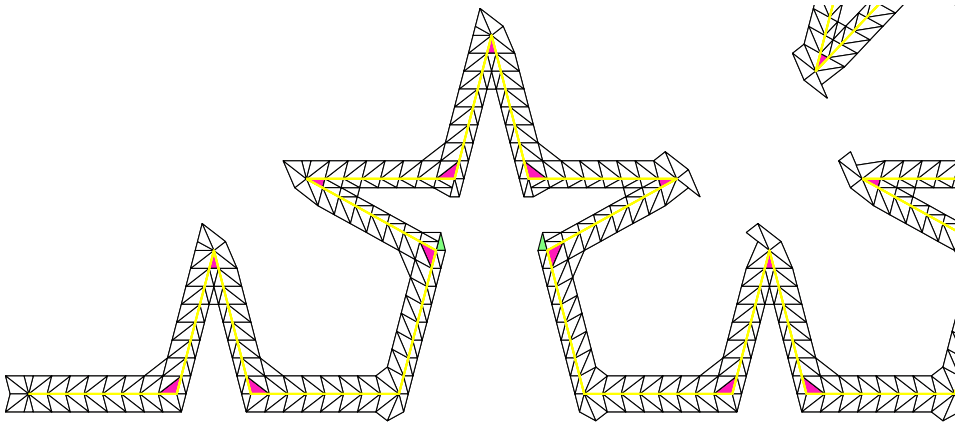

Figure 4.24: Cases for Lemma 22

Proof. By a symmetrical argument, we only consider the first such green triangle of Figure 4.24. If we label the vertex of T in V^n as P_2 and the vertices immediately left and right of P_2 in V^n as P_1 and P_3, respectively, we have

$$\begin{aligned} u_n^\star(P) &= u(P_2), \\ u_n^\star(Q) &= \frac{4k-1}{4k}u(P_2) + \frac{1}{4k}u(P_1), \\ u_n^\star(R') &= \frac{2k-1}{2k}u(P_2) + \frac{1}{2k}u(P_3) \end{aligned}$$

where R' is the point in the center of the segment $\overline{PR}$. Since the value of $u_n^\star$ is linearly affine along $\overline{PR}$, we have that

$$u_n^\star(R) = \frac{k-1}{k}u(P_2) + \frac{1}{k}u(P_3).$$

Choosing distinct $X_1, X_2 \in T$ with $X_1 = (x_1, y_1)$ and $X_2 = (x_2, y_2)$, equation (4.2) gives

$$\begin{aligned} \frac{|u_n^\star(X_1) - u_n^\star(X_2)|}{|X_1 - X_2|^\beta} &\leq \frac{|u_n^\star(P) - u_n^\star(Q)\|x_1 - x_2|}{|Q-P\|X_1 - X_2|^\beta} + \frac{|2u_n^\star(R) - u_n^\star(P) - u_n^\star(Q)\|y_1 - y_2|}{\sqrt{4-(\alpha-2)^2}|Q-P\|X_1 - X_2|^\beta} \\ &\leq \frac{|u(P_1) - u(P_2)\|x_1 - x_2|}{4k|Q-P\|X_1 - X_2|^\beta} + \frac{7|u(P_2) - u(P_3)\|y_1 - y_2|}{4\sqrt{3}k|Q-P\|X_1 - X_2|^\beta} \\ &\quad + \frac{|u(P_1) - u(P_3)\|y_1 - y_2|}{4k|Q-P\|X_1 - X_2|^\beta} \end{aligned}$$

$$
\begin{aligned}
&\leq \frac{|u(P_1)-u(P_2)\|x_1-x_2|}{4(\alpha-2)|P_1-P_2\|X_1-X_2|^\beta} + \frac{7|u(P_2)-u(P_3)\|y_1-y_2|}{4\sqrt{3}(\alpha-2)|P_2-P_3\|X_1-X_2|^\beta} \\
&\qquad + \frac{|u(P_1)-u(P_3)\|y_1-y_2|}{4|P_1-P_3\|X_1-X_2|^\beta} \\
&\leq \frac{|u(P_1)-u(P_2)|}{4(\alpha-2)|P_1-P_2|^\beta} + \frac{7|u(P_2)-u(P_3)|}{4\sqrt{3}(\alpha-2)|P_2-P_3|^\beta} + \frac{|u(P_1)-u(P_3)|}{4|P_1-P_3|^\beta} \\
&\leq \frac{1}{4(\alpha-2)}|u|_{K,\beta} + \frac{7}{4\sqrt{3}(\alpha-2)}|u|_{K,\beta} + \frac{1}{4}|u|_{K,\beta} \\
&= \frac{\sqrt{3}(\alpha-1)+7}{4\sqrt{3}(\alpha-2)}|u|_{K,\beta} \\
&\leq 2(\alpha-2)^{-1}|u|_{K,\beta}.
\end{aligned}
$$

□

Lemma 23. *Let T be a primary sidecar triangle with vertices P, Q, and R as depicted by any green triangle of Figure 4.25. Let $\beta \in (0,1]$ and u be a $\beta-$Hölder continuous function*

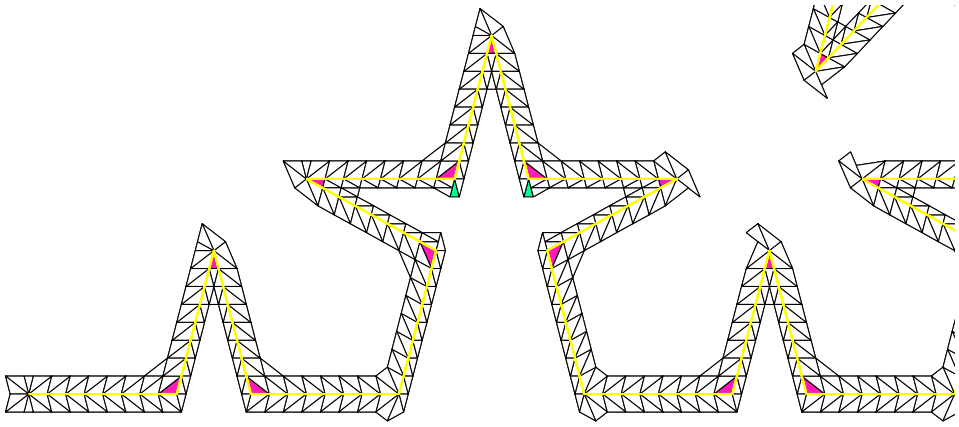

Figure 4.25: Cases for Lemma 23

defined on the vertices of the prefractal so that

$$\frac{|u(A)-u(B)|}{|A-B|^\beta} \leq |u|_{K,\beta}$$

for all $A, B \in V^n$. Then, for $n \geq 3$, $u_n^\star$ satisfies

$$\sup_{X,Y\in\mathcal{T}} \frac{|u_n^\star(X)-u_n^\star(Y)|}{|X-Y|^\beta} \leq 3(\alpha-2)^{-1}|u|_{K,\beta}.$$

Proof. By a symmetrical arguments, we will prove the upper bound for the first green triangle of Figure 4.25. If we label the vertex of T in V^n as P_2 and the vertices of V^n immediately left and right of P_2 as P_1 and P_3, respectively, then we have

$$\begin{aligned} u_n^\star(R) &= u(P_2), \\ u_n^\star(Q) &= \frac{4k-1}{4k}u(P_2) + \frac{1}{4k}u(P_3), \\ u_n^\star(P') &= \frac{2k-1}{2k}u(P_2) + \frac{1}{2k}u(P_1) \end{aligned}$$

where P' is the point in the center of the segment $\overline{PR}$. Since $u_n^\star$ is affine along $\overline{PR}$, we have

$$u_n^\star(P) = \frac{k-1}{k}u(P_2) + \frac{1}{k}u(P_1).$$

Choosing distinct $X_1, X_2 \in T$ with $X_1 = (x_1, y_1)$ and $X_2 = (x_2, y_2)$, equation (4.2) gives

$$\begin{aligned} \frac{|u_n^\star(X_1) - u_n^\star(X_2)|}{|X_1 - X_2|^\beta} &\leq \frac{|u_n^\star(P) - u_n^\star(Q)\|x_1 - x_2|}{|Q-P\|X_1 - X_2|^\beta} + \frac{|2u_n^\star(R) - u_n^\star(P) - u_n^\star(Q)\|y_1 - y_2|}{\sqrt{4-(\alpha-2)^2}|Q-P\|X_1 - X_2|^\beta} \\ &\leq \frac{3|u(P_1) - u(P_2)\|x_1 - x_2|}{4k|Q-P\|X_1 - X_2|^\beta} + \frac{|u(P_1) - u(P_3)\|x_1 - x_2|}{4k|Q-P\|X_1 - X_2|^\beta} \\ &\qquad + \frac{|u(P_1) - u(P_2)\|y_1 - y_2|}{\sqrt{3}k|Q-P\|X_1 - X_2|^\beta} + \frac{|u(P_2) - u(P_3)\|y_1 - y_2|}{4\sqrt{3}k|Q-P\|X_1 - X_2|^\beta} \\ &\leq \frac{3|u(P_1) - u(P_2)\|x_1 - x_2|}{4(\alpha-2)|P_1-P_2\|X_1 - X_2|^\beta} + \frac{|u(P_1) - u(P_3)\|x_1 - x_2|}{4|P_1-P_3\|X_1 - X_2|^\beta} \\ &\qquad + \frac{|u(P_1) - u(P_2)\|y_1 - y_2|}{\sqrt{3}(\alpha-2)|P_1-P_2\|X_1 - X_2|^\beta} + \frac{|u(P_2) - u(P_3)\|y_1 - y_2|}{4\sqrt{3}(\alpha-2)|P_2-P_3\|X_1 - X_2|^\beta} \\ &\leq \frac{3|u(P_1) - u(P_2)|}{4(\alpha-2)|P_1-P_2|^\beta} + \frac{|u(P_1) - u(P_3)|}{4|P_1-P_3|^\beta} \\ &\qquad + \frac{|u(P_1) - u(P_2)|}{\sqrt{3}(\alpha-2)|P_1-P_2|^\beta} + \frac{|u(P_2) - u(P_3)|}{4\sqrt{3}(\alpha-2)|P_2-P_3|^\beta} \\ &\leq \frac{3}{4(\alpha-2)}|u|_{K,\beta} + \frac{1}{4}|u|_{K,\beta} + \frac{1}{\sqrt{3}(\alpha-2)}|u|_{K,\beta} + \frac{1}{4\sqrt{3}(\alpha-2)}|u|_{K,\beta} \\ &= \frac{\sqrt{3}(\alpha+1)+5}{4(\alpha-2)}|u|_{K,\beta} \\ &\leq 3(\alpha-2)^{-1}|u|_{K,\beta}. \end{aligned}$$

□

Lemma 24. *Let T be a primary sidecar triangle with vertices P, Q, and R as depicted by any dark green triangle of Figure 4.26. Let $\beta \in (0,1]$ and u be a $\beta-$Hölder continuous*

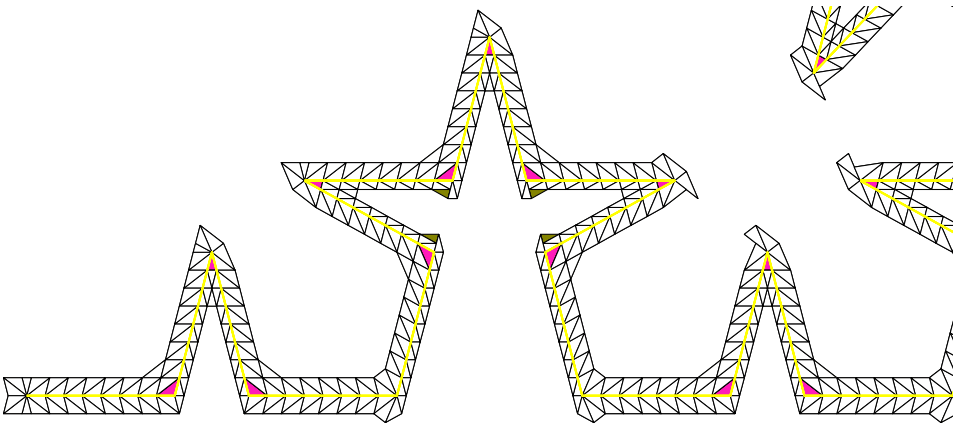

Figure 4.26: Cases for Lemma 24

function defined on the vertices of the prefractal so that

$$\frac{|u(A)-u(B)|}{|A-B|^{\beta}} \leq |u|_{K,\beta}$$

for all $A, B \in V^n$. Then, for $n \geq 3$, $u_n^\star$ satisfies

$$\sup_{X,Y\in\mathcal{T}} \frac{|u_n^\star(X)-u_n^\star(Y)|}{|X-Y|^{\beta}} \leq 2(\alpha-2)^{-1}|u|_{K,\beta}.$$

Proof. We consider only the first forest green triangle, as the other work similarly. Find the vertex of T closest to a vertex of V^n and label this vertex of V^n as P_2. We label the vertices of V^n immediately left and right of P_2 as P_1 and P_3, respectively. By previous arguments, we have

$$\begin{aligned}
u_n^\star(P) &= \frac{2k-1}{2k}u(P_2) + \frac{1}{2k}u(P_3),\\
u_n^\star(Q) &= \frac{k-1}{k}u(P_2) + \frac{1}{k}u(P_3),\\
u_n^\star(R) &= \frac{2k-3}{2k}u(P_2) + \frac{3}{2k}u(P_3).
\end{aligned}$$

Choosing distinct $X_1, X_2 \in T$ with $X_1 = (x_1, y_1)$ and $X_2 = (x_2, y_2)$, equation (4.2) gives

$$\begin{aligned}
\frac{|u_n^\star(X_1) - u_n^\star(X_2)|}{|X_1 - X_2|^\beta} &\leq \frac{|u_n^\star(P) - u_n^\star(Q)\|x_1 - x_2|}{|Q - P\|X_1 - X_2|^\beta} + \frac{|2u_n^\star(R) - u_n^\star(P) - u_n^\star(Q)\|y_1 - y_2|}{\sqrt{4 - (\alpha-2)^2}|Q - P\|X_1 - X_2|^\beta} \\
&\leq \frac{|u(P_2) - u(P_3)\|x_1 - x_2|}{2k|Q - P\|X_1 - X_2|^\beta} + \frac{3|u(P_2) - u(P_3)\|x_1 - x_2|}{2\sqrt{3}k|Q - P\|X_1 - X_2|^\beta} \\
&\leq \frac{|u(P_2) - u(P_3)\|x_1 - x_2|}{2(\alpha-2)|P_2 - P_3\|X_1 - X_2|^\beta} + \frac{3|u(P_2) - u(P_3)\|x_1 - x_2|}{2\sqrt{3}(\alpha-2)|P_2 - P_3\|X_1 - X_2|^\beta} \\
&\leq \frac{|u(P_2) - u(P_3)|}{2(\alpha-2)|P_2 - P_3|^\beta} + \frac{3|u(P_2) - u(P_3)|}{2\sqrt{3}(\alpha-2)|P_2 - P_3|^\beta} \\
&\leq \frac{1}{2(\alpha-2)}|u|_{K,\beta} + \frac{3}{2\sqrt{3}(\alpha-2)}|u|_{K,\beta} \\
&= \frac{\sqrt{3}+3}{2\sqrt{3}(\alpha-2)}|u|_{K,\beta} \\
&\leq 2(\alpha-2)^{-1}|u|_{K,\beta}.
\end{aligned}$$

□

We summarize the results of the Lemmas 1 – 24 in Table 4.1.

Table 4.1: A Table of Upper Bounds on ω_{SC}.

Lemma	**Upper Bound**	**Reference Label**
1	$3(\alpha-2)^{-1}\|u\|_{K,\beta}$	1
2	$3(\alpha-2)^{-1}\|u\|_{K,\beta}$	2
3	$5(\alpha-2)^{-1}\|u\|_{K,\beta}$	3
4	$3(\alpha-2)^{-1}\|u\|_{K,\beta}$	4
5	$4(\alpha-2)^{-1}\|u\|_{K,\beta}$	5
6	$8(\alpha-2)^{-1}\|u\|_{K,\beta}$	6
7	$6(\alpha-2)^{-1}\|u\|_{K,\beta}$	7
8	$2(\alpha-2)^{-1}\|u\|_{K,\beta}$	8
9	$2(\alpha-2)^{-1}\|u\|_{K,\beta}$	9
10	$2(\alpha-2)^{-1}\|u\|_{K,\beta}$	10
11	$(\alpha-2)^{-1}\|u\|_{K,\beta}$	11
12	$(\alpha-2)^{-1}\|u\|_{K,\beta}$	12
13	$(\alpha-2)^{-1}\|u\|_{K,\beta}$	13
14	$(\alpha-2)^{-1}\|u\|_{K,\beta}$	14
15	$(\alpha-2)^{-1}\|u\|_{K,\beta}$	15
16	$2(\alpha-2)^{-1}\|u\|_{K,\beta}$	16
17	$(\alpha-2)^{-1}\|u\|_{K,\beta}$	17
18	$(\alpha-2)^{-1}\|u\|_{K,\beta}$	18
19	$(\alpha-2)^{-1}\|u\|_{K,\beta}$	19
20	$(\alpha-2)^{-1}\|u\|_{K,\beta}$	20
21	$(\alpha-2)^{-1}\|u\|_{K,\beta}$	21
22	$2(\alpha-2)^{-1}\|u\|_{K,\beta}$	22
23	$3(\alpha-2)^{-1}\|u\|_{K,\beta}$	23
24	$2(\alpha-2)^{-1}\|u\|_{K,\beta}$	24

Thus the seminorm in ω_{SC} is bounded above by $8(\alpha-2)^{-1}|u|_{S,\beta}$.

4.3 Seminorm Estimates on the Transition Triangles

Before going any further, we further subdivide ω_{TR} into two global sets, namely $\omega_{TR_{SC}}$ and $\omega_{TR_{TR}}$. The first of these sets, $\omega_{TR_{SC}}$, denotes the transition triangles of iteration n which lie entirely within ω_{SC} of iteration $n-1$ while the second of these, $\omega_{TR_{TR}}$, is the set of remaining transition triangles, i.e., $\omega_{TR_{TR}} = \omega_{TR} \setminus \omega_{TR_{SC}}$. Table 4.2 contains the bounds for both sets of triangles, where a $*$ in the first column denotes a triangle in $\omega_{TR_{TR}}$.

Lemma 25. *Let $\mathcal{T}^n$ be the triangulation of ω for the extension function $u_n^\star$ and $C_{MTR_{SC}}$ be the maximum transition triangle constant within $\omega_{TR_{SC}}$ of Table 4.2. Then*

$$\frac{|u_n^\star(X) - u_n^\star(Y)|}{|X-Y|^\beta} \leq C_{MTR_{SC}}$$

for any X and Y is a single triangle $T \in \omega_{EX}$ of $\mathcal{T}^n$.

Proof. Let $T \in \omega_{EX}$ be the triangle containing X and Y. If $T \in \omega_{SC} \cup \omega_{TR}$. Let m be the iteration where the value of $u_n^\star(T)$ was last set; that is, $u_m^\star(X) \neq u_{m-1}^\star(X)$ for some $X \in T$ but $u_m^\star(X) = u_{m+i}^\star(X)$ for all $X \in T$ and $i \in \{1, \ldots, n-m\}$. Let T_m be the triangle from the triangulation $\mathcal{T}^m$ containing T. It follows from the construction of the extension function over ω that $T_m \in \omega_{SC} \cup \omega_{TR_{SC}}$ for the triangulation $\mathcal{T}^m$. Thus

$$\frac{|u_m^\star(A) - u_m^\star(B)|}{|A-B|^\beta} \leq C_{MTR_{SC}}$$

for all $A, B \in T_m$. Since $T \subset T_m$, the previous observation then implies

$$\frac{|u_m^\star(X) - u_m^\star(Y)|}{|X-Y|^\beta} \leq C_{MTR_{SC}}$$

for all $X, Y \in T_m$. Thus

$$\frac{|u_n^\star(X) - u_n^\star(Y)|}{|X-Y|^\beta} = \frac{|u_m^\star(X) - u_m^\star(Y)|}{|X-Y|^\beta} \leq C_{MTR_{SC}}$$

for all $X, Y \in T_m$. □

Lemma 26. *Let T be a transition triangle with vertices P, Q, and R as depicted by any gray transition triangle of Figure 4.27. Let $\beta \in (0, 1]$ and u be a $\beta-$Hölder continuous function*

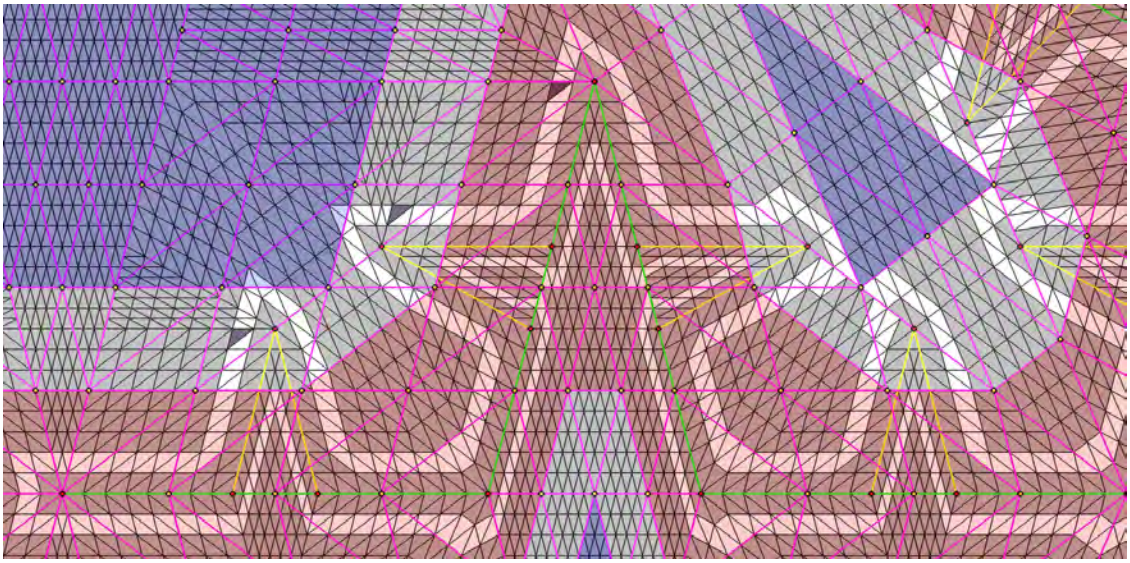

Figure 4.27: Cases for Lemma 25 are given by the charcoal triangles in the white band. In this figure, the yellow points are vertices of the mesh in iteration $n-1$; the red points are points along the prefractal of iteration n; the green line represents the prefractal in iteration $n-1$; the green line—with the appropriate modifications as shown with the yellow line—is the prefractal of iteration n; the pink grid lines denote the mesh from iteration $n-1$ which are further separated into ω_{SC}, ω_{TR}, and ω_{EX} as denoted by the red, white, and blue shading, respectively; and the black grid lines denote the mesh from the current iteration.

defined on the vertices of the prefractal so that

$$\frac{|u(A) - u(B)|}{|A-B|^\beta} \leq |u|_{K,\beta}$$

for all $A, B \in V^n$. Then, for $n \geq 3$, $u_n^\star$ satisfies

$$\sup_{X,Y \in \mathcal{T}} \frac{|u_n^\star(X) - u_n^\star(Y)|}{|X - Y|^\beta} \leq 9000(\alpha - 2)^{-2n} |u|_{K,\beta}.$$

Proof. The first case is the charcoal triangle in the red region, i.e., $T \in \omega_{TR_{SC}}$. We begin by labeling the vertices of V^n from left to right as A_i, where $i \in \{1, 2, \ldots, 4^n + 1\}$. By considering the reference triangle T, the algorithm provided for determining the values at the vertices of the triangulation implies $u_n^\star(P) = u_{n-1}^\star(P)$ and $u_n^\star(R) = u_{n-1}^\star(R)$, while

$$u_n^\star(Q) = \frac{4k-1}{4k} u(A_3) + \frac{1}{4k} u(A_2).$$

Observe that our algorithm for determining the values at the vertices of $\mathcal{T}^n$ imply $u(A_i) = u_n^\star(A_i)$ for all i. We further restrict our choice of T to the left most charcoal colored triangle of Figure 4.27.

Choosing distinct $X_1, X_2 \in T$ with $X_1 = (x_1, y_1)$ and $X_2 = (x_2, y_2)$, equation (4.1) gives

$$\begin{aligned}
\frac{|u_n^\star(X_1) - u_n^\star(X_2)|}{|X_1 - X_2|^\beta} &\leq \frac{|u_n^\star(P) - u_n^\star(Q)\|x_1 - x_2|}{|Q - P\|X_1 - X_2|^\beta} + \frac{|4u_n^\star(R) - 2u_n^\star(P) - 2u_n^\star(Q)\|y_1 - y_2|}{\sqrt{4-\alpha}|Q - P\|X_1 - X_2|^\beta} \\
&\leq \frac{|u(A_3) - u_n^\star(P)\|x_1 - x_2|}{|Q - P\|X_1 - X_2|^\beta} + \frac{|u(A_3) - u(A_2)\|x_1 - x_2|}{4k|Q - P\|X_1 - X_2|^\beta} \\
&\quad + \frac{2|u_n^\star(R) - u(A_3)\|y_1 - y_2|}{|Q - P\|X_1 - X_2|^\beta} + \frac{2|u_n^\star(R) - u_n^\star(P)\|y_1 - y_2|}{|Q - P\|X_1 - X_2|^\beta} \\
&\quad + \frac{|u(A_2) - u(A_3)\|y_1 - y_2|}{2k|Q - P\|X_1 - X_2|^\beta} \\
&\leq \frac{|u(A_3) - u_n^\star(P)\|x_1 - x_2|}{|Q - P\|X_1 - X_2|^\beta} + \frac{2|u_n^\star(R) - u(A_3)\|y_1 - y_2|}{|Q - P\|X_1 - X_2|^\beta} \\
&\quad + 500(\alpha - 2)^{-(n+1)} |u|_{K,\beta} + \frac{3}{4\sqrt{2}} |u|_{K,\beta}
\end{aligned}$$

Now let $A \in V^n$ be any vertex of V^{n-1}. Then

$$\begin{aligned}
&\leq \frac{|u(A_3) - u_n^\star(A)\|x_1 - x_2|}{|Q-P\|X_1 - X_2|^\beta} + \frac{|u(A) - u_n^\star(P)\|x_1 - x_2|}{|Q-P\|X_1 - X_2|^\beta} + \frac{2|u_n^\star(A) - u(A_3)\|y_1 - y_2|}{|Q-P\|X_1 - X_2|^\beta} \\
&\quad + \frac{2|u_n^\star(R) - u(A)\|y_1 - y_2|}{|Q-P\|X_1 - X_2|^\beta} + 500(\alpha-2)^{-(n+1)}|u|_{K,\beta} + \frac{3}{4\sqrt{2}}|u|_{K,\beta} \\
&\leq \frac{|u(P) - u_n^\star(A)\|x_1 - x_2|}{|Q-P\|X_1 - X_2|^\beta} + \frac{2|u_n^\star(R) - u(A)\|y_1 - y_2|}{|Q-P\|X_1 - X_2|^\beta} + 524(\alpha-2)^{-(n+1)}|u|_{K,\beta} \\
&\quad + \frac{3}{4\sqrt{2}}|u|_{K,\beta} \\
&\leq 2820(\alpha-2)^{-2n}|u|_{K,\beta} + 5640(\alpha-2)^{-2n}|u|_{K,\beta} + \frac{3}{4\sqrt{2}}|u|_{K,\beta} + 524(\alpha-2)^{-(n+1)}|u|_{K,\beta} \\
&\leq 9000(\alpha-2)^{-2n}|u|_{K,\beta}.
\end{aligned}$$

Because the mesh is self-similar, we immediately get that the seminorm of all charcoal triangles of the larger mesh are also bounded by $9000(\alpha-2)^{-2n}|u|_{K,\beta}$. □

Lemma 27. *Let T be a transition triangle with vertices P, Q, and R as depicted by any pink transition triangle of Figure 4.28. Let $\beta \in (0,1]$ and u be a $\beta-$Hölder continuous function defined on the vertices of the prefractal so that*

$$\frac{|u(A) - u(B)|}{|A-B|^\beta} \leq |u|_{K,\beta}$$

for all $A, B \in V^n$. Then, for $n \geq 3$, $u_n^\star$ satisfies

$$\sup_{X,Y \in \mathcal{T}} \frac{|u_n^\star(X) - u_n^\star(Y)|}{|X-Y|^\beta} \leq 9000(\alpha-2)^{-2n}|u|_{K,\beta}.$$

Proof. Let us consider the left most pink colored triangle of Figure 4.28. We begin by labeling the vertices of V^n from left to right in sequential order as A_i, where $i \in \{1, 2, \ldots, 4^n + 1\}$. By considering the reference triangle T, the algorithm provided for determining the values

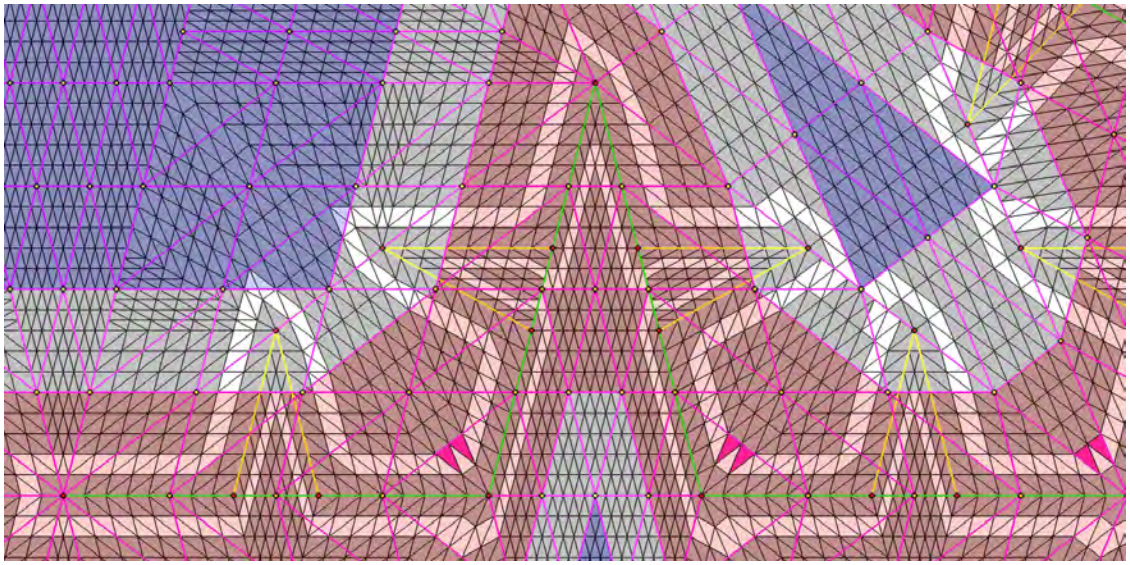

Figure 4.28: Cases for Lemma 26 are given by the pink triangles in the white band. In this figure, the yellow points are vertices of the mesh in iteration $n-1$; the red points are points along the prefractal of iteration n; the green line represents the prefractal in iteration $n-1$; the green line—with the appropriate modifications as shown with the yellow line—is the prefractal of iteration n; the pink grid lines denote the mesh from iteration $n-1$ which are further separated into ω_{SC}, ω_{TR}, and ω_{EX} as denoted by the red, white, and blue shading, respectively; and the black grid lines denote the mesh from the current iteration.

at the vertices of the triangulation implies $u_n^\star(P) = u_{n-1}^\star(P)$ and $u_n^\star(Q) u_{n-1}^\star(Q)$, while

$$u_n^\star(R) = \frac{2k-1}{2k} u(A_5) + \frac{1}{2k} u(A_4).$$

We also recall that $u(A_i) = u_n^\star(A_i)$ for all i.

Choosing distinct $X_1, X_2 \in T$ with $X_1 = (x_1, y_1)$ and $X_2 = (x_2, y_2)$, equation (4.1) gives

$$\begin{aligned}
\frac{u_n^\star(X_1) - u_n^\star(X_2)|}{|X_1 - X_2|^\beta} &\leq \frac{|u_n^\star(P) - u_n^\star(Q)\|x_1 - x_2|}{|Q-P\|X_1 - X_2|^\beta} + \frac{|2u_n^\star(R) - u_n^\star(P) - u_n^\star(Q)\|y_1 - y_2|}{\sqrt{4-(\alpha-2)^2}|Q-P\|X_1 - X_2|^\beta} \\
&\leq \frac{|u_n^\star(P) - u_n^\star(Q)\|x_1 - x_2|}{|Q-P\|X_1 - X_2|^\beta} + \frac{|u_n^\star(A_5) - u_n^\star(Q)\|y_1 - y_2|}{\sqrt{3}|Q-P\|X_1 - X_2|^\beta} \\
&\quad + \frac{|u_n^\star(P) - u_n^\star(A_5)\|y_1 - y_2|}{\sqrt{3}|Q-P\|X_1 - X_2|^\beta} + \frac{|u_n^\star(A_4) - u_n^\star(A_5)\|y_1 - y_2|}{2k\sqrt{3}|Q-P\|X_1 - X_2|^\beta} \\
&\leq \frac{21}{4} C |u|_{K,\beta} \\
&\leq 42(\alpha-2)^{-2} |u|_{K,\beta}
\end{aligned}$$

where C is the largest multiple of $|u|_{K,\beta}$ in Table 4.1 (i.e., $c = 8(\alpha-2)^{-1}$); to complete these steps, we used the fact that every triangles in the mesh is—at some iteration—in ω_{SC}, thus the seminorm of that triangle is bounded above by the bounds of Table 4.1 and that the following relations hold:

(i) $0 < |P - A_5| \leq 2|Q - P|(\alpha-2)^{-1}$,

(ii) $0 < |Q - A_5| \leq 2|Q - P|(\alpha-2)^{-1}$,

(iii) $\sqrt{\alpha}(\alpha-2)k^{-1}|A_4 - A_5| = |Q - P|$.

Since the roles of P and Q are symmetric in equation (4.1), we see that the seminorm on the remaining pink triangles of Figure 4.28 are also bounded above by $42(\alpha-2)^{-2}|u|_{K,\beta}$. Because the mesh is self-similar, we immediately get that the seminorm of all pink triangles of the larger mesh are also bounded by $42(\alpha-2)^{-2}|u|_{K,\beta}$. □

The methods employed to prove Lemma 26 and 27 can be used provide the seminorm estimates for the remainder of the transition triangles of Figure 4.2(b). These results are summarized in Figures 4.29 – 4.41 and Table 4.2.

Table 4.2: This table is broken into two categories, namely $\omega_{TR_{SC}}$ and $\omega_{TR_{TR}}$. Triangles in $\omega_{TR_{TR}}$ are denoted by an $*$ in column one.

Figure	**Triangle Color**	**An Upper Bound on $\lvert u\rvert_{K,\beta}$**	**Reference Label**
4.29	Red	$205(\alpha-2)^{-(n+1)}\lvert u\rvert_{K,\beta}$	1
4.29	Yellow	$205(\alpha-2)^{-(n+1)}\lvert u\rvert_{K,\beta}$	2
4.29	Cyan	$205(\alpha-2)^{-2}\lvert u\rvert_{K,\beta}$	3
4.29	Magenta	$42(\alpha-2)^{-2}\lvert u\rvert_{K,\beta}$	4
4.29	Green	$37(\alpha-2)^{-2}\lvert u\rvert_{K,\beta}$	5
4.29	Blue	$44(\alpha-2)^{-2}\lvert u\rvert_{K,\beta}$	6
4.30	Red	$80(\alpha-2)^{-2}\lvert u\rvert_{K,\beta}$	7
4.30	Yellow	$50(\alpha-2)^{-2}\lvert u\rvert_{K,\beta}$	8
4.30	Cyan	$48(\alpha-2)^{-2}\lvert u\rvert_{K,\beta}$	9
4.30	Magenta	$80(\alpha-2)^{-2}\lvert u\rvert_{K,\beta}$	10
4.30	Green	$40(\alpha-2)^{-2}\lvert u\rvert_{K,\beta}$	11
4.30	Blue	$42(\alpha-2)^{-2}\lvert u\rvert_{K,\beta}$	12
4.31	Red	$42(\alpha-2)^{-2}\lvert u\rvert_{K,\beta}$	13
4.31	Yellow	$50(\alpha-2)^{-2}\lvert u\rvert_{K,\beta}$	14
4.31	Cyan	$36(\alpha-2)^{-2}\lvert u\rvert_{K,\beta}$	15
4.31	Magenta	$32(\alpha-2)^{-2}\lvert u\rvert_{K,\beta}$	16
4.31	Green	$32(\alpha-2)^{-2}\lvert u\rvert_{K,\beta}$	17
4.31	Blue	$48(\alpha-2)^{-2}\lvert u\rvert_{K,\beta}$	18
4.32	Red	$40(\alpha-2)^{-2}\lvert u\rvert_{K,\beta}$	19
4.32	Yellow	$56(\alpha-2)^{-2}\lvert u\rvert_{K,\beta}$	20
4.32	Cyan	$48(\alpha-2)^{-2}\lvert u\rvert_{K,\beta}$	21

Continued on next page

Table 4.2 – *Continued from previous page*

Figure	**Triangle Color**	**An Upper Bound on $\|u\|_{K,\beta}$**	**Reference Label**
4.32	Magenta	$40(\alpha-2)^{-2}\|u\|_{K,\beta}$	22
4.32	Green	$40(\alpha-2)^{-2}\|u\|_{K,\beta}$	23
4.32	Blue	$40(\alpha-2)^{-2}\|u\|_{K,\beta}$	24
4.33	Red	$48(\alpha-2)^{-2}\|u\|_{K,\beta}$	25
4.33	Yellow	$112(\alpha-2)^{-2}\|u\|_{K,\beta}$	26
4.33	Cyan	$88(\alpha-2)^{-2}\|u\|_{K,\beta}$	27
4.33	Magenta	$88(\alpha-2)^{-2}\|u\|_{K,\beta}$	28
4.33	Green	$72(\alpha-2)^{-2}\|u\|_{K,\beta}$	29
4.33	Blue	$72(\alpha-2)^{-2}\|u\|_{K,\beta}$	30
4.34	Red	$24(\alpha-2)^{-2}\|u\|_{K,\beta}$	31
4.34	Yellow	$32(\alpha-2)^{-2}\|u\|_{K,\beta}$	32
4.34	Cyan	$72(\alpha-2)^{-2}\|u\|_{K,\beta}$	33
4.34	Magenta	$32(\alpha-2)^{-2}\|u\|_{K,\beta}$	34
4.34	Green	$48(\alpha-2)^{-2}\|u\|_{K,\beta}$	35
4.34	Blue	$56(\alpha-2)^{-2}\|u\|_{K,\beta}$	36
4.35	Red	not applicable	not applicable
4.35	Yellow	not applicable	not applicable
4.35	Cyan	$72(\alpha-2)^{-2}\|u\|_{K,\beta}$	37
4.35	Magenta	not applicable	not applicable
4.35	Green	not applicable	not applicable
4.35	Blue	not applicable	not applicable
4.36	Red	not applicable	not applicable
4.36	Yellow	not applicable	not applicable

Continued on next page

Table 4.2 – *Continued from previous page*

Figure	**Triangle Color**	**An Upper Bound on $\lvert u\rvert_{K,\beta}$**	**Reference Label**
4.36	Cyan	not applicable	not applicable
4.36	Magenta	not applicable	not applicable
4.36	Green	$49(\alpha-2)^{-2}\lvert u\rvert_{K,\beta}$	38
4.36	Blue	not applicable	not applicable
4.37	Red	not applicable	not applicable
4.37	Yellow	not applicable	not applicable
4.37	Cyan	not applicable	not applicable
4.37	Magenta	not applicable	not applicable
4.37	Green	not applicable	not applicable
4.37	Blue	$14(\alpha-2)^{-2}\lvert u\rvert_{K,\beta}$	39
4.38	Red	not applicable	not applicable
4.38	Yellow	$80(\alpha-2)^{-2}\lvert u\rvert_{K,\beta}$	40
4.38	Cyan	$37(\alpha-2)^{-2}\lvert u\rvert_{K,\beta}$	41
4.38	Magenta	$80(\alpha-2)^{-2}\lvert u\rvert_{K,\beta}$	42
4.38	Green	$53(\alpha-2)^{-2}\lvert u\rvert_{K,\beta}$	43
4.38	Blue	$41(\alpha-2)^{-2}\lvert u\rvert_{K,\beta}$	44
4.39	Red	$80(\alpha-2)^{-2}\lvert u\rvert_{K,\beta}$	45
4.39	Yellow	$76(\alpha-2)^{-2}\lvert u\rvert_{K,\beta}$	46
4.39	Cyan	$81(\alpha-2)^{-2}\lvert u\rvert_{K,\beta}$	47
4.39	Magenta	$76(\alpha-2)^{-2}\lvert u\rvert_{K,\beta}$	48
4.39	Green	$32(\alpha-2)^{-2}\lvert u\rvert_{K,\beta}$	49
4.39	Blue	$50(\alpha-2)^{-2}\lvert u\rvert_{K,\beta}$	50
4.40	Red	$50(\alpha-2)^{-2}\lvert u\rvert_{K,\beta}$	51

Continued on next page

Table 4.2 – *Continued from previous page*

Figure	**Triangle Color**	**An Upper Bound on $\lvert u\rvert_{K,\beta}$**	**Reference Label**
4.40	Yellow	not applicable	not applicable
4.40	Cyan	$80(\alpha-2)^{-2}\lvert u\rvert_{K,\beta}$	52
4.40	Magenta	not applicable	not applicable
4.40	Green	not applicable	not applicable
4.40	Blue	not applicable	not applicable
4.41	Red	not applicable	not applicable
4.41	Yellow	not applicable	not applicable
4.41	Cyan	not applicable	not applicable
4.41	Magenta	not applicable	not applicable
4.41	Green	not applicable	not applicable
4.41	Blue	not applicable	not applicable
4.29 *	Red	not applicable	not applicable
4.29 *	Yellow	not applicable	not applicable
4.29 *	Cyan	not applicable	not applicable
4.29 *	Magenta	not applicable	not applicable
4.29 *	Green	$5125\lvert u\rvert_{K,\beta}(\alpha-2)^{-2n}$	53
4.29 *	Blue	not applicable	not applicable
4.30 *	Red	not applicable	not applicable
4.30 *	Yellow	not applicable	not applicable
4.30 *	Cyan	$6125\lvert u\rvert_{K,\beta}(\alpha-2)^{-2n}$	54
4.30 *	Magenta	not applicable	not applicable
4.30 *	Green	not applicable	not applicable
4.30 *	Blue	not applicable	not applicable

Continued on next page

Table 4.2 – *Continued from previous page*

Figure	**Triangle Color**	**An Upper Bound on $\|u\|_{K,\beta}$**	**Reference Label**
4.31 *	Red	not applicable	not applicable
4.31 *	Yellow	not applicable	not applicable
4.31 *	Cyan	not applicable	not applicable
4.31 *	Magenta	not applicable	not applicable
4.31 *	Green	not applicable	not applicable
4.31 *	Blue	not applicable	not applicable
4.32 *	Red	not applicable	not applicable
4.32 *	Yellow	not applicable	not applicable
4.32 *	Cyan	not applicable	not applicable
4.32 *	Magenta	not applicable	not applicable
4.32 *	Green	not applicable	not applicable
4.32 *	Blue	not applicable	not applicable
4.33 *	Red	not applicable	not applicable
4.33 *	Yellow	not applicable	not applicable
4.33 *	Cyan	not applicable	not applicable
4.33 *	Magenta	not applicable	not applicable
4.33 *	Green	not applicable	not applicable
4.33 *	Blue	not applicable	not applicable
4.34 *	Red	not applicable	not applicable
4.34 *	Yellow	not applicable	not applicable
4.34 *	Cyan	not applicable	not applicable
4.34 *	Magenta	not applicable	not applicable
4.34 *	Green	not applicable	not applicable

Continued on next page

Table 4.2 – *Continued from previous page*

Figure	**Triangle Color**	**An Upper Bound on $\lvert u\rvert_{K,\beta}$**	**Reference Label**
4.34 *	Blue	not applicable	not applicable
4.35 *	Red	$5125\lvert u\rvert_{K,\beta}(\alpha-2)^{-2n}$	55
4.35 *	Yellow	$5125\lvert u\rvert_{K,\beta}(\alpha-2)^{-2n}$	56
4.35 *	Cyan	not applicable	not applicable
4.35 *	Magenta	$5125\lvert u\rvert_{K,\beta}(\alpha-2)^{-2n}$	57
4.35 *	Green	$6150\lvert u\rvert_{K,\beta}(\alpha-2)^{-2n}$	58
4.35 *	Blue	$4100\lvert u\rvert_{K,\beta}(\alpha-2)^{-2n}$	59
4.36 *	Red	$2050\lvert u\rvert_{K,\beta}(\alpha-2)^{-2n}$	60
4.36 *	Yellow	$4100\lvert u\rvert_{K,\beta}(\alpha-2)^{-2n}$	61
4.36 *	Cyan	$4100\lvert u\rvert_{K,\beta}(\alpha-2)^{-2n}$	62
4.36 *	Magenta	$5125\lvert u\rvert_{K,\beta}(\alpha-2)^{-2n}$	63
4.36 *	Green	$7175\lvert u\rvert_{K,\beta}(\alpha-2)^{-2n}$	64
4.36 *	Blue	$6150\lvert u\rvert_{K,\beta}(\alpha-2)^{-2n}$	65
4.37 *	Red	$6150\lvert u\rvert_{K,\beta}(\alpha-2)^{-2n}$	66
4.37 *	Yellow	$6150\lvert u\rvert_{K,\beta}(\alpha-2)^{-2n}$	67
4.37 *	Cyan	$4100\lvert u\rvert_{K,\beta}(\alpha-2)^{-2n}$	68
4.37 *	Magenta	$5125\lvert u\rvert_{K,\beta}(\alpha-2)^{-2n}$	69
4.37 *	Green	$6150\lvert u\rvert_{K,\beta}(\alpha-2)^{-2n}$	70
4.37 *	Blue	$2050\lvert u\rvert_{K,\beta}(\alpha-2)^{-2n}$	71
4.38 *	Red	$7175\lvert u\rvert_{K,\beta}(\alpha-2)^{-2n}$	72
4.38 *	Yellow	$10250\lvert u\rvert_{K,\beta}(\alpha-2)^{-2n}$	73
4.38 *	Cyan	$5125\lvert u\rvert_{K,\beta}(\alpha-2)^{-2n}$	74
4.38 *	Magenta	$8200\lvert u\rvert_{K,\beta}(\alpha-2)^{-2n}$	75

Continued on next page

Table 4.2 – *Continued from previous page*

Figure	**Triangle Color**	**An Upper Bound on $\lvert u\rvert_{K,\beta}$**	**Reference Label**
4.38 *	Green	$7175\lvert u\rvert_{K,\beta}(\alpha-2)^{-2n}$	76
4.38 *	Blue	$6150\lvert u\rvert_{K,\beta}(\alpha-2)^{-2n}$	77
4.39 *	Red	$10250\lvert u\rvert_{K,\beta}(\alpha-2)^{-2n}$	78
4.39 *	Yellow	$10250\lvert u\rvert_{K,\beta}(\alpha-2)^{-2n}$	79
4.39 *	Cyan	$11275\lvert u\rvert_{K,\beta}(\alpha-2)^{-2n}$	80
4.39 *	Magenta	$10250\lvert u\rvert_{K,\beta}(\alpha-2)^{-2n}$	81
4.39 *	Green	$9225\lvert u\rvert_{K,\beta}(\alpha-2)^{-2n}$	82
4.39 *	Blue	$7175\lvert u\rvert_{K,\beta}(\alpha-2)^{-2n}$	83
4.40 *	Red	$7175\lvert u\rvert_{K,\beta}(\alpha-2)^{-2n}$	84
4.40 *	Yellow	$10250\lvert u\rvert_{K,\beta}(\alpha-2)^{-2n}$	85
4.40 *	Cyan	$10250\lvert u\rvert_{K,\beta}(\alpha-2)^{-2n}$	86
4.40 *	Magenta	$10250\lvert u\rvert_{K,\beta}(\alpha-2)^{-2n}$	87
4.40 *	Green	$10250\lvert u\rvert_{K,\beta}(\alpha-2)^{-2n}$	88
4.40 *	Blue	$5125\lvert u\rvert_{K,\beta}(\alpha-2)^{-2n}$	89
4.41 *	Red	$5125\lvert u\rvert_{K,\beta}(\alpha-2)^{-2n}$	90
4.41 *	Yellow	$10250\lvert u\rvert_{K,\beta}(\alpha-2)^{-2n}$	91
4.41 *	Cyan	$10250\lvert u\rvert_{K,\beta}(\alpha-2)^{-2n}$	92
4.41 *	Magenta	$6150\lvert u\rvert_{K,\beta}(\alpha-2)^{-2n}$	93
4.41 *	Green	$10250\lvert u\rvert_{K,\beta}(\alpha-2)^{-2n}$	94
4.41 *	Blue	$6150\lvert u\rvert_{K,\beta}(\alpha-2)^{-2n}$	95

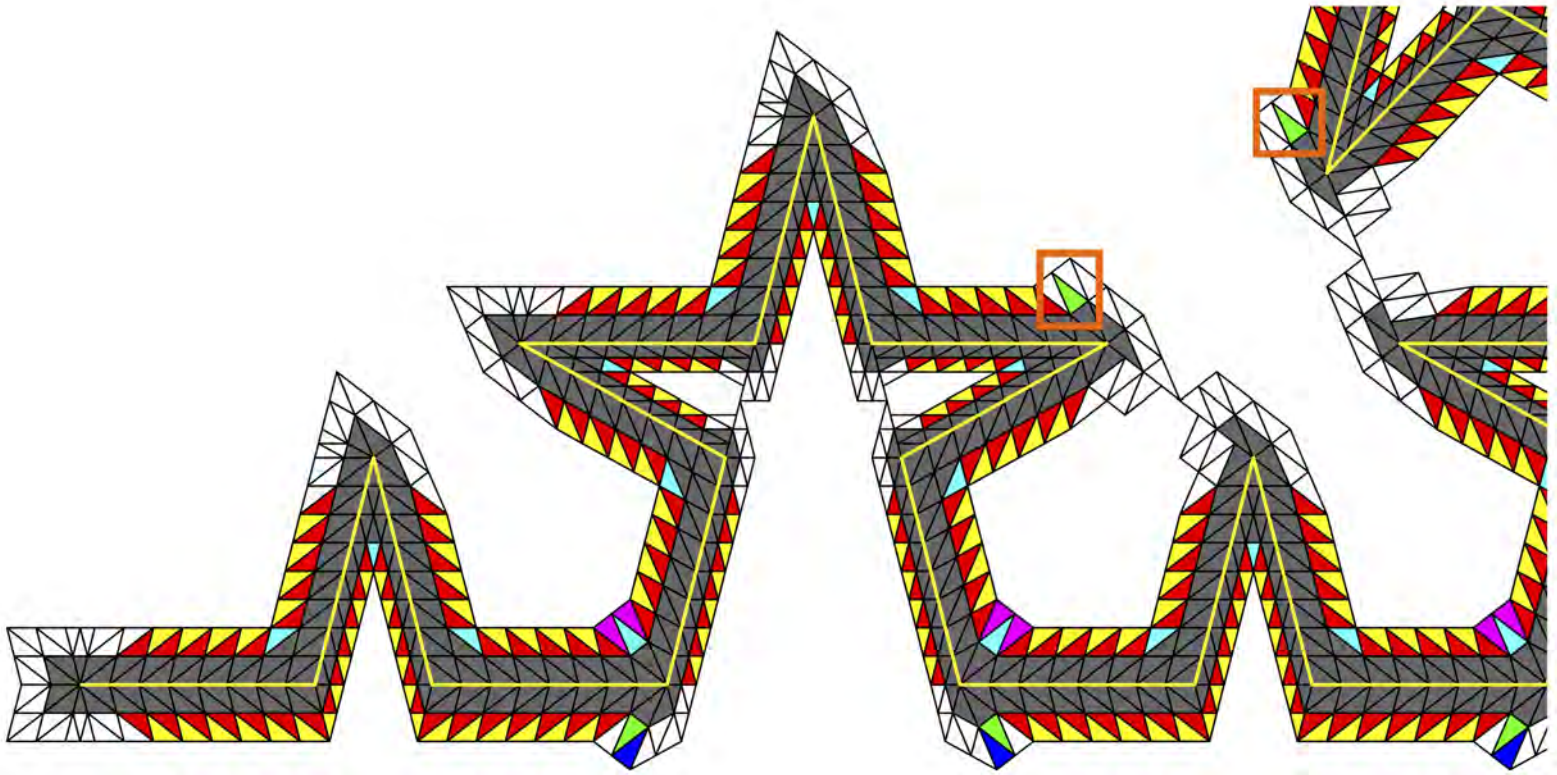

Figure 4.29: A categorization of seven types of triangles of Figure 4.2(b). The dark grey triangles represent the previously bounded primary sidecar triangles (see Lemmas 1 – 24 or Table 4.1); the white triangles are triangles to be bounded in Figures 4.30 – 4.41; and the remaining six colors (i.e., the yellow, red, cyan, green, blue, and magenta) triangles are bounded in this diagram. Triangles in the orange boxes represent triangles in $\omega_{TR_{TR}}$. See Table 4.2 for a complete list of upper bounds.

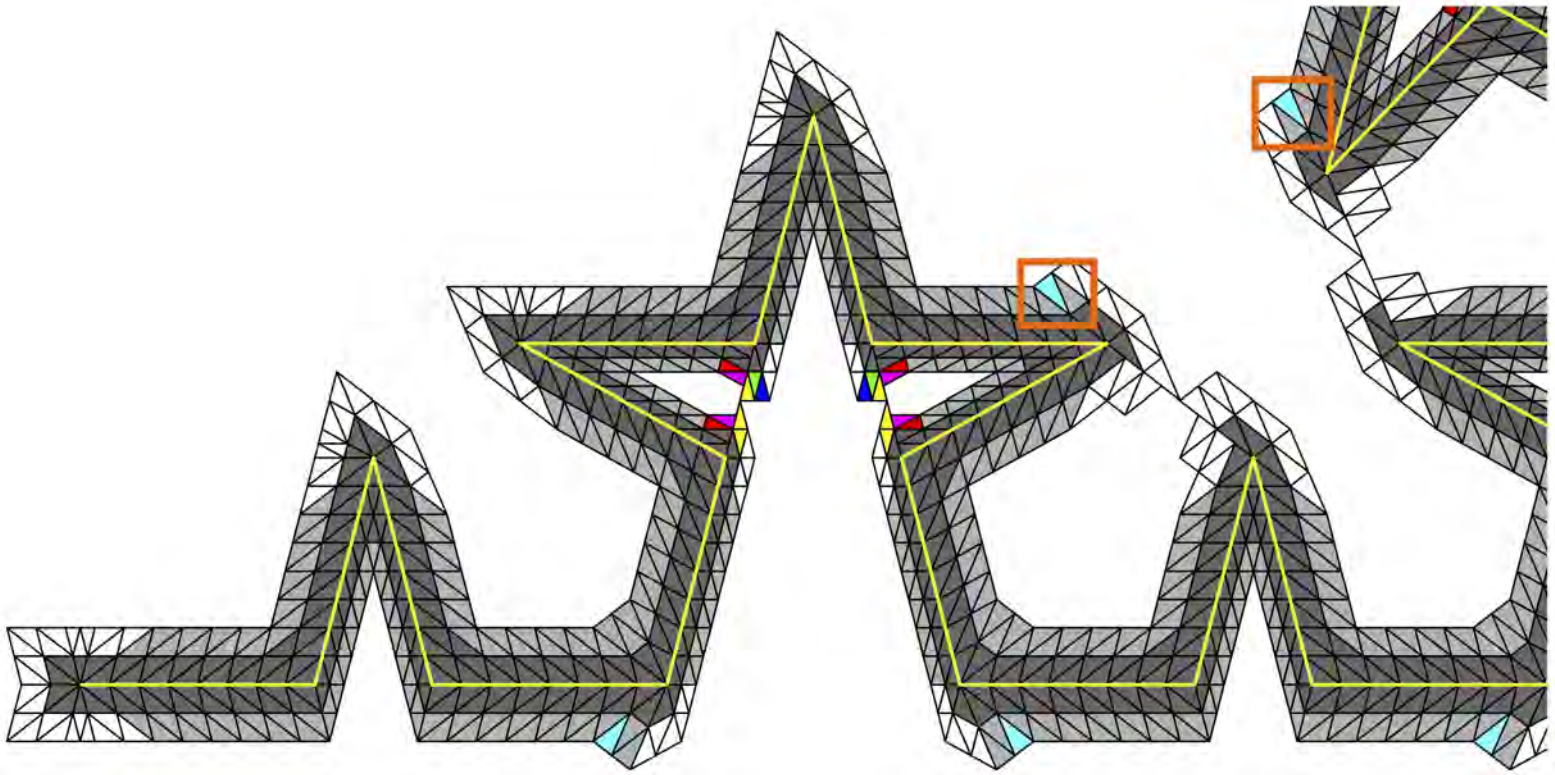

Figure 4.30: A categorization of seven types of triangles of Figure 4.2(b). The dark grey triangles represent the previously bounded primary sidecar triangles (see Lemmas 1 – 24 or Table 4.1); the white triangles are triangles to be bounded in Figures 4.31 – 4.41; the light grey triangles were bounded in Figures 4.29; and the remaining six colors (i.e., the yellow, red, cyan, green, blue, and magenta) triangles are bounded in this diagram. Triangles in the orange boxes represent triangles in $\omega_{TR_{TR}}$. See Table 4.2 for a complete list of upper bounds.

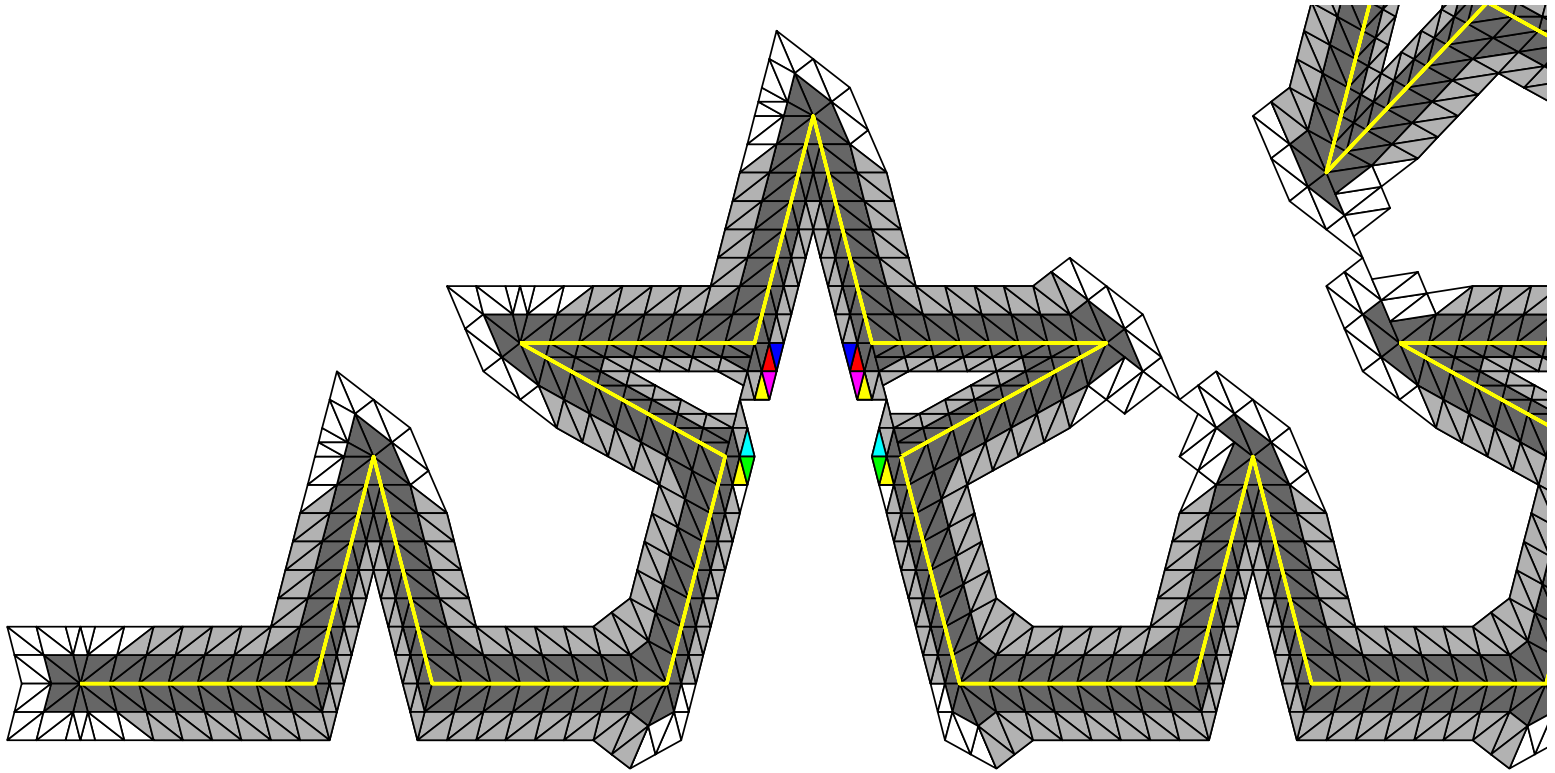

Figure 4.31: A categorization of six types of triangles of Figure 4.2(b). The dark grey triangles represent the previously bounded primary sidecar triangles (see Lemmas 1 – 24 or Table 4.1); the white triangles are triangles to be bounded in Figures 4.32 – 4.41; the light grey triangles were bounded in Figures 4.29 – 4.30; and the remaining six colors (i.e., the yellow, red, cyan, green, blue, and magenta) triangles are bounded in this diagram. See Table 4.2 for a complete list of upper bounds.

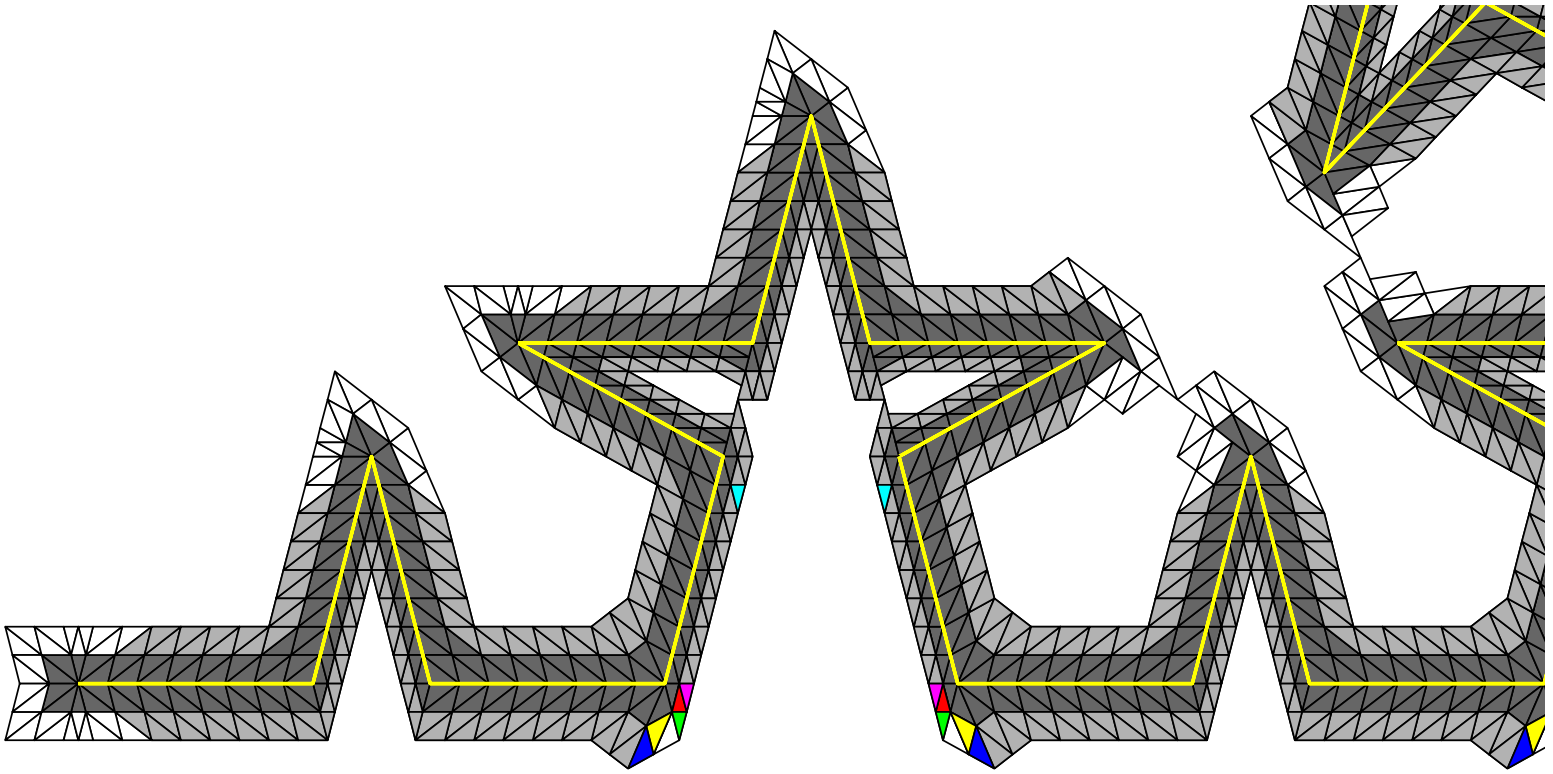

Figure 4.32: A categorization of six types of triangles of Figure 4.2(b). The dark grey triangles represent the previously bounded primary sidecar triangles (see Lemmas 1 – 24 or Table 4.1); the white triangles are triangles to be bounded in Figures 4.33 – 4.41; the light grey triangles were bounded in Figures 4.29 – 4.31; and the remaining six colors (i.e., the yellow, red, cyan, green, blue, and magenta) triangles are bounded in this diagram. See Table 4.2 for a complete list of upper bounds.

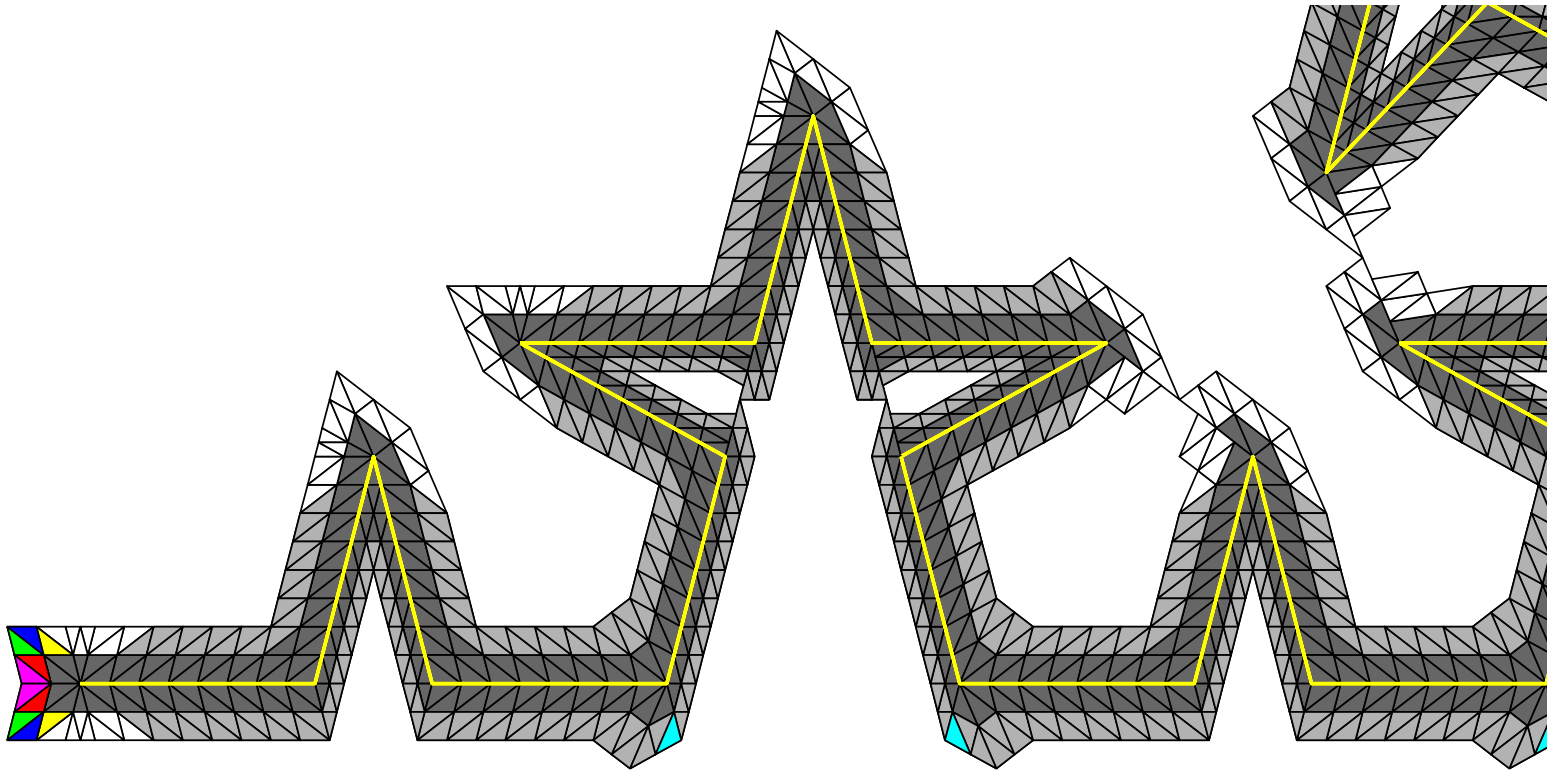

Figure 4.33: A categorization of six types of triangles of Figure 4.2(b). The dark grey triangles represent the previously bounded primary sidecar triangles (see Lemmas 1 – 24 or Table 4.1); the white triangles are triangles to be bounded in Figures 4.34 – 4.41; the light grey triangles were bounded in Figures 4.29 – 4.32; and the remaining six colors (i.e., the yellow, red, cyan, green, blue, and magenta) triangles are bounded in this diagram. See Table 4.2 for a complete list of upper bounds.

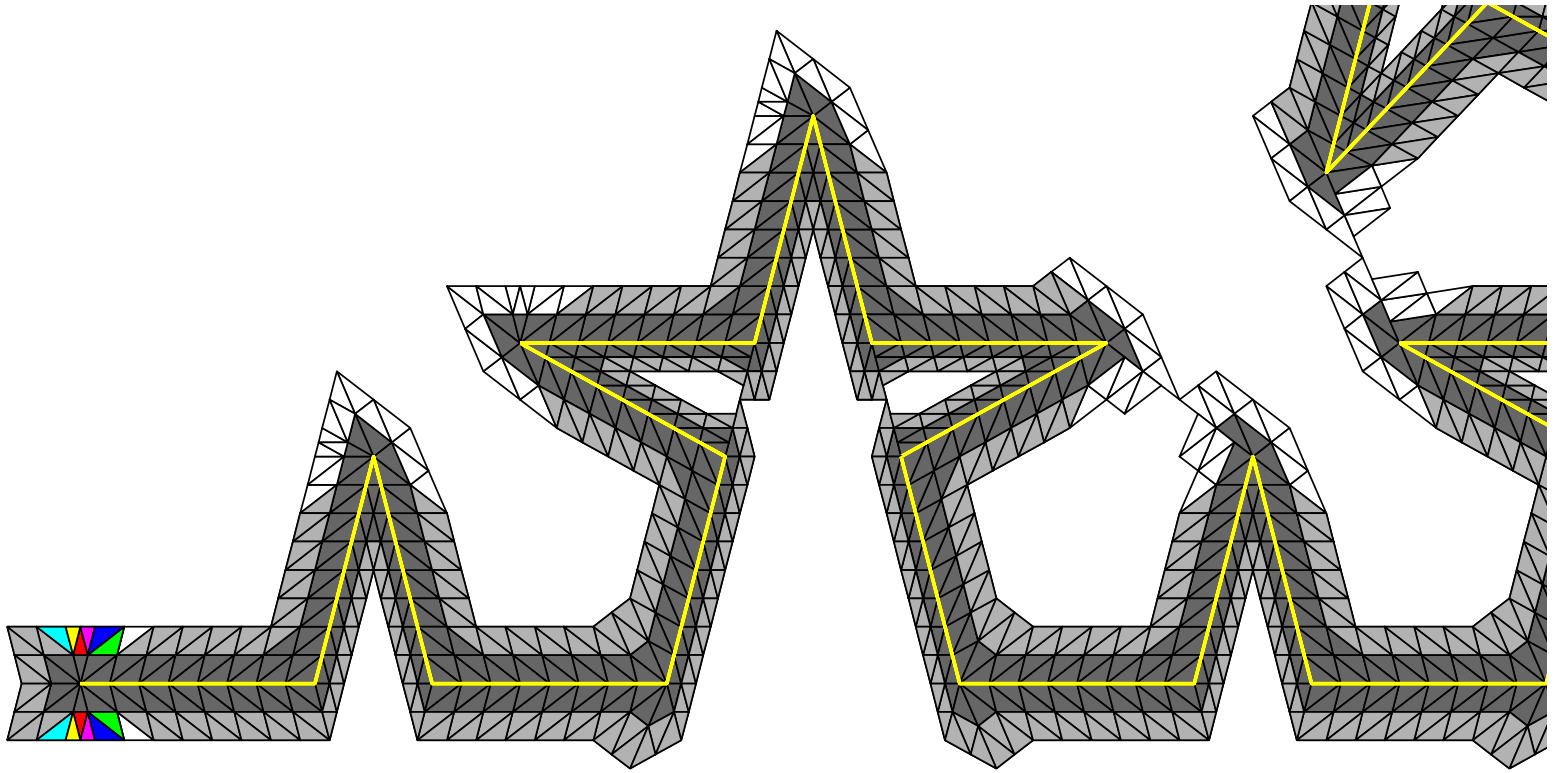

Figure 4.34: A categorization of six types of triangles of Figure 4.2(b). The dark grey triangles represent the previously bounded primary sidecar triangles (see Lemmas 1 – 24 or Table 4.1); the white triangles are triangles to be bounded in Figures 4.35 – 4.41; the light grey triangles were bounded in Figures 4.29 – 4.33; and the remaining six colors (i.e., the yellow, red, cyan, green, blue, and magenta) triangles are bounded in this diagram. See Table 4.2 for a complete list of upper bounds.

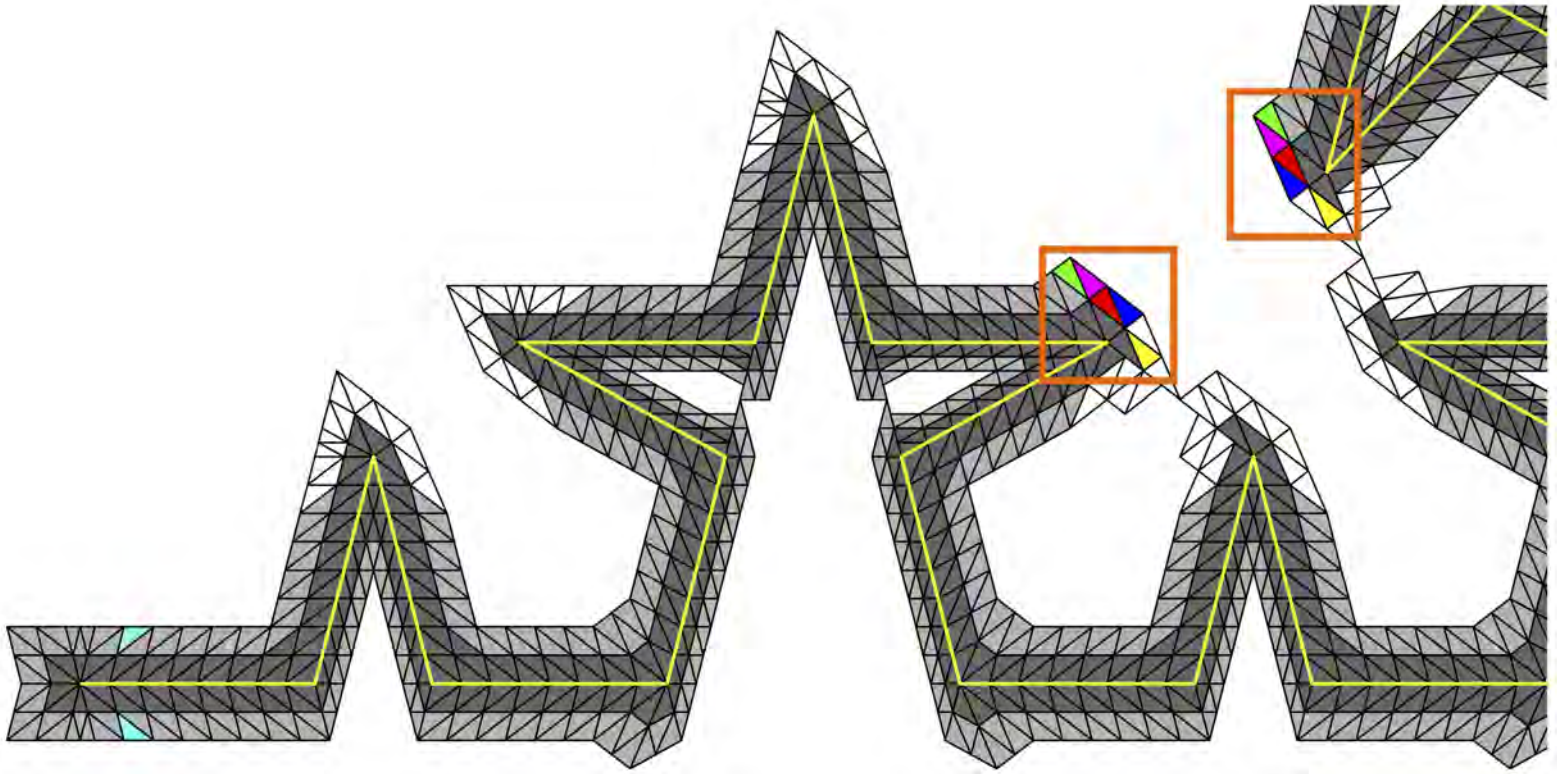

Figure 4.35: A categorization of six types of triangles of Figure 4.2(b). The dark grey triangles represent the previously bounded primary sidecar triangles (see Lemmas 1 – 24 or Table 4.1); the white triangles are triangles to be bounded in Figures 4.36 – 4.41; the light grey triangles were bounded in Figures 4.29 – 4.34; and the remaining six colors (i.e., the yellow, red, cyan, green, blue, and magenta) triangles are bounded in this diagram. Triangles in the orange boxes represent triangles in $\omega_{TR_{TR}}$. See Table 4.2 for a complete list of upper bounds.

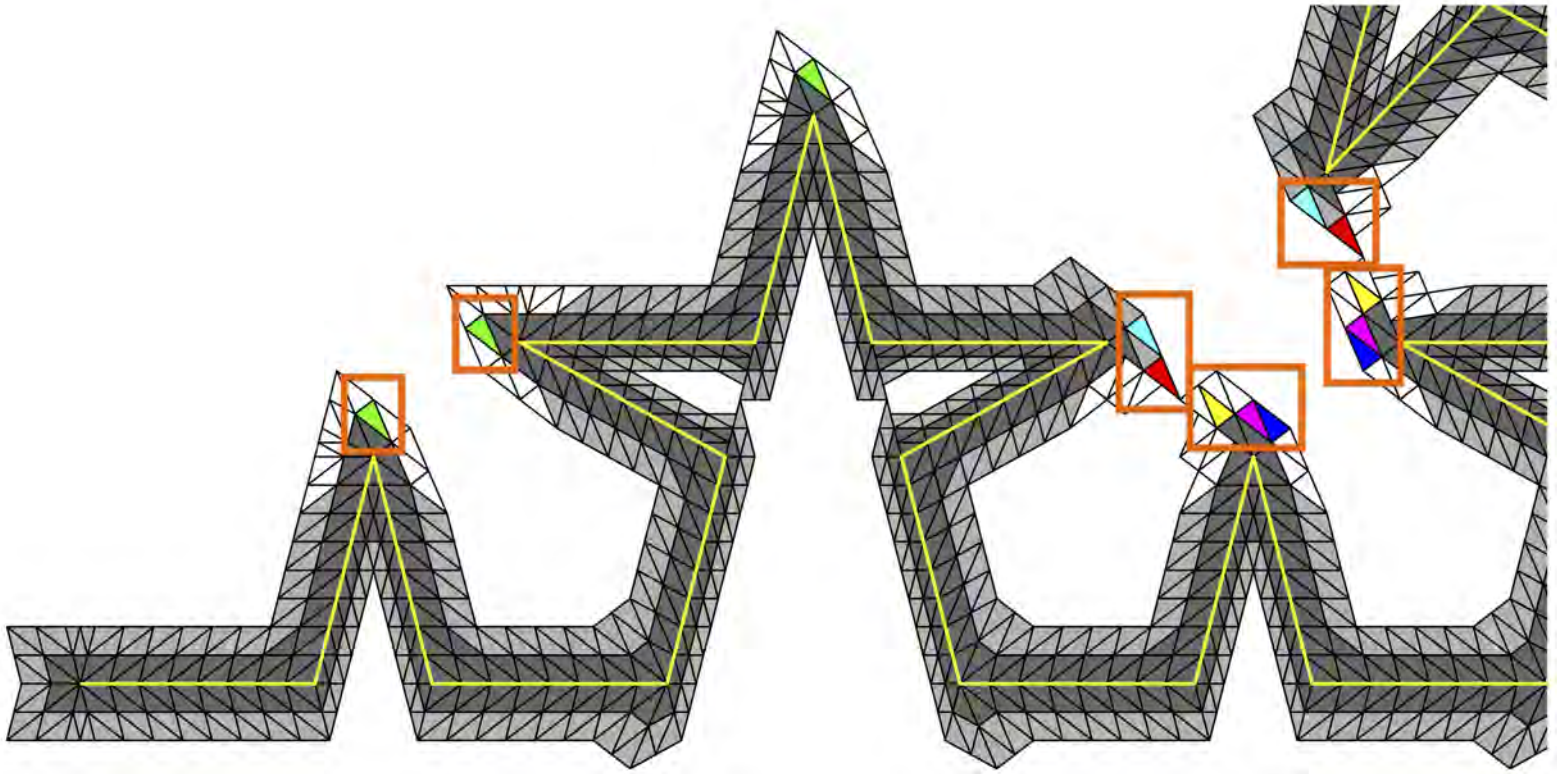

Figure 4.36: A categorization of seven types of triangles of Figure 4.2(b). The dark grey triangles represent the previously bounded primary sidecar triangles (see Lemmas 1 – 24 or Table 4.1); the white triangles are triangles to be bounded in Figures 4.37 – 4.41; the light grey triangles were bounded in Figures 4.29 – 4.35; and the remaining six colors (i.e., the yellow, red, cyan, green, blue, and magenta) triangles are bounded in this diagram. Triangles in the orange boxes represent triangles in $\omega_{TR_{TR}}$. See Table 4.2 for a complete list of upper bounds.

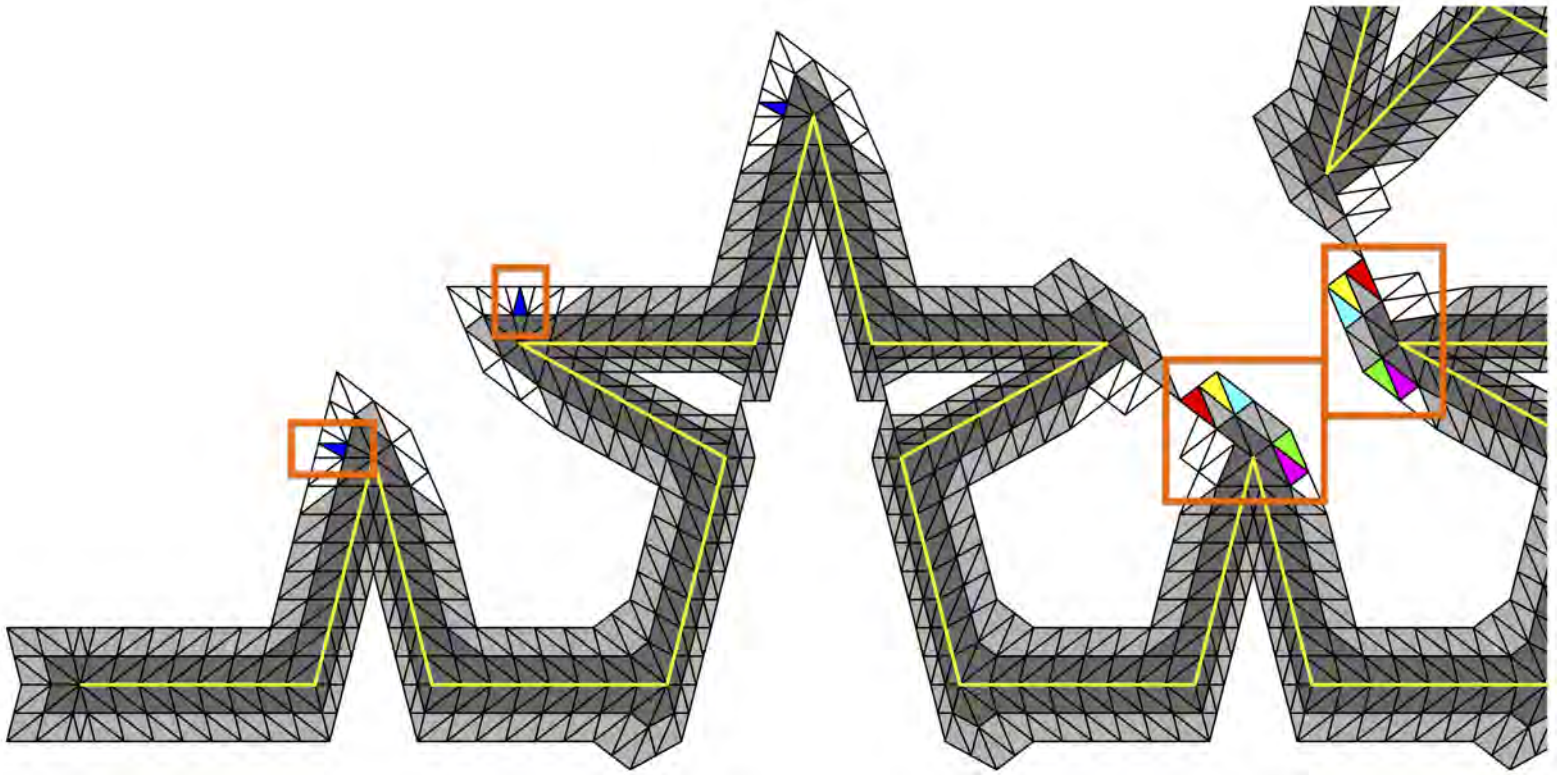

Figure 4.37: A categorization of seven types of triangles of Figure 4.2(b). The dark grey triangles represent the previously bounded primary sidecar triangles (see Lemmas 1 – 24 or Table 4.1); the white triangles are triangles to be bounded in Figures 4.38 – 4.41; the light grey triangles were bounded in Figures 4.29 – 4.36; and the remaining six colors (i.e., the yellow, red, cyan, green, blue, and magenta) triangles are bounded in this diagram. Triangles in the orange boxes represent triangles in $\omega_{TR_{TR}}$. See Table 4.2 for a complete list of upper bounds.

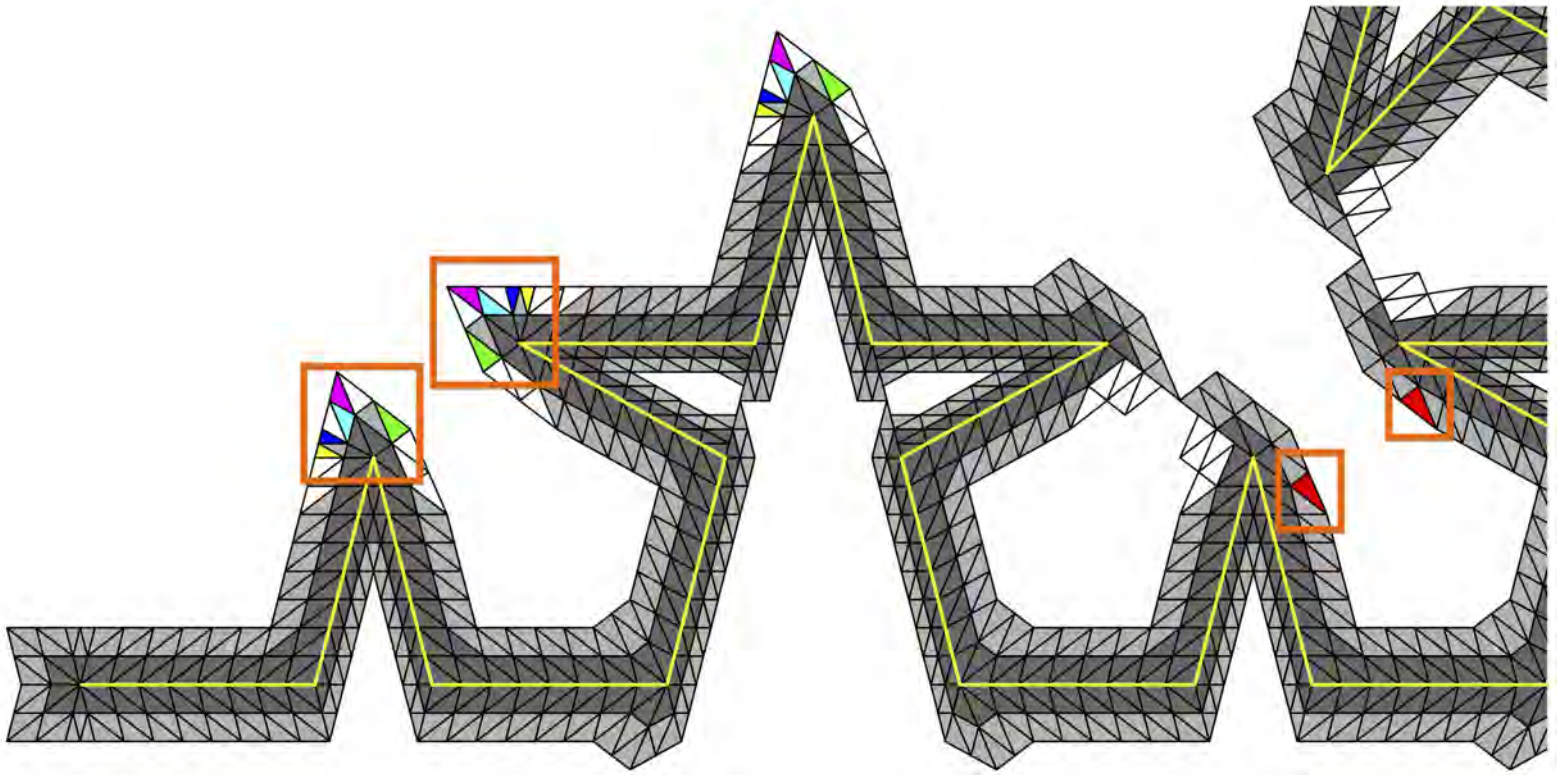

Figure 4.38: A categorization of eleven types of triangles of Figure 4.2(b). The dark grey triangles represent the previously bounded primary sidecar triangles (see Lemmas 1 – 24 or Table 4.1); the white triangles are triangles to be bounded in Figures 4.39 – 4.41; the light grey triangles were bounded in Figures 4.29 – 4.37; and the remaining six colors (i.e., the yellow, red, cyan, green, blue, and magenta) triangles are bounded in this diagram. Triangles in the orange boxes represent triangles in $\omega_{TR_{TR}}$. See Table 4.2 for a complete list of upper bounds.

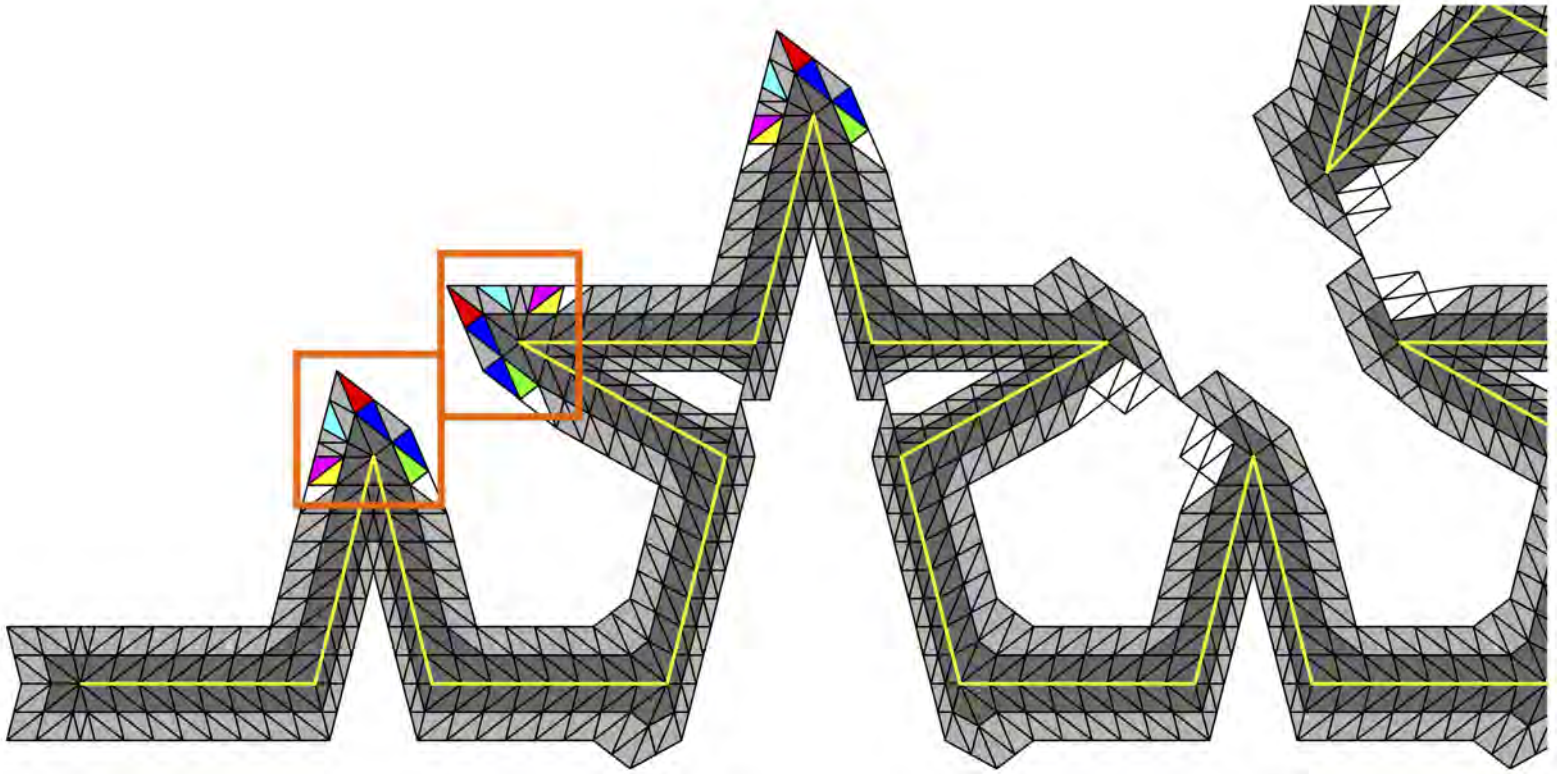

Figure 4.39: A categorization of twelve types of triangles of Figure 4.2(b). The dark grey triangles represent the previously bounded primary sidecar triangles (see Lemmas 1 – 24 or Table 4.1); the white triangles are triangles to be bounded in Figures 4.40 – 4.41; the light grey triangles were bounded in Figures 4.29 – 4.38; and the remaining six colors (i.e., the yellow, red, cyan, green, blue, and magenta) triangles are bounded in this diagram. Triangles in the orange boxes represent triangles in $\omega_{TR_{TR}}$. See Table 4.2 for a complete list of upper bounds.

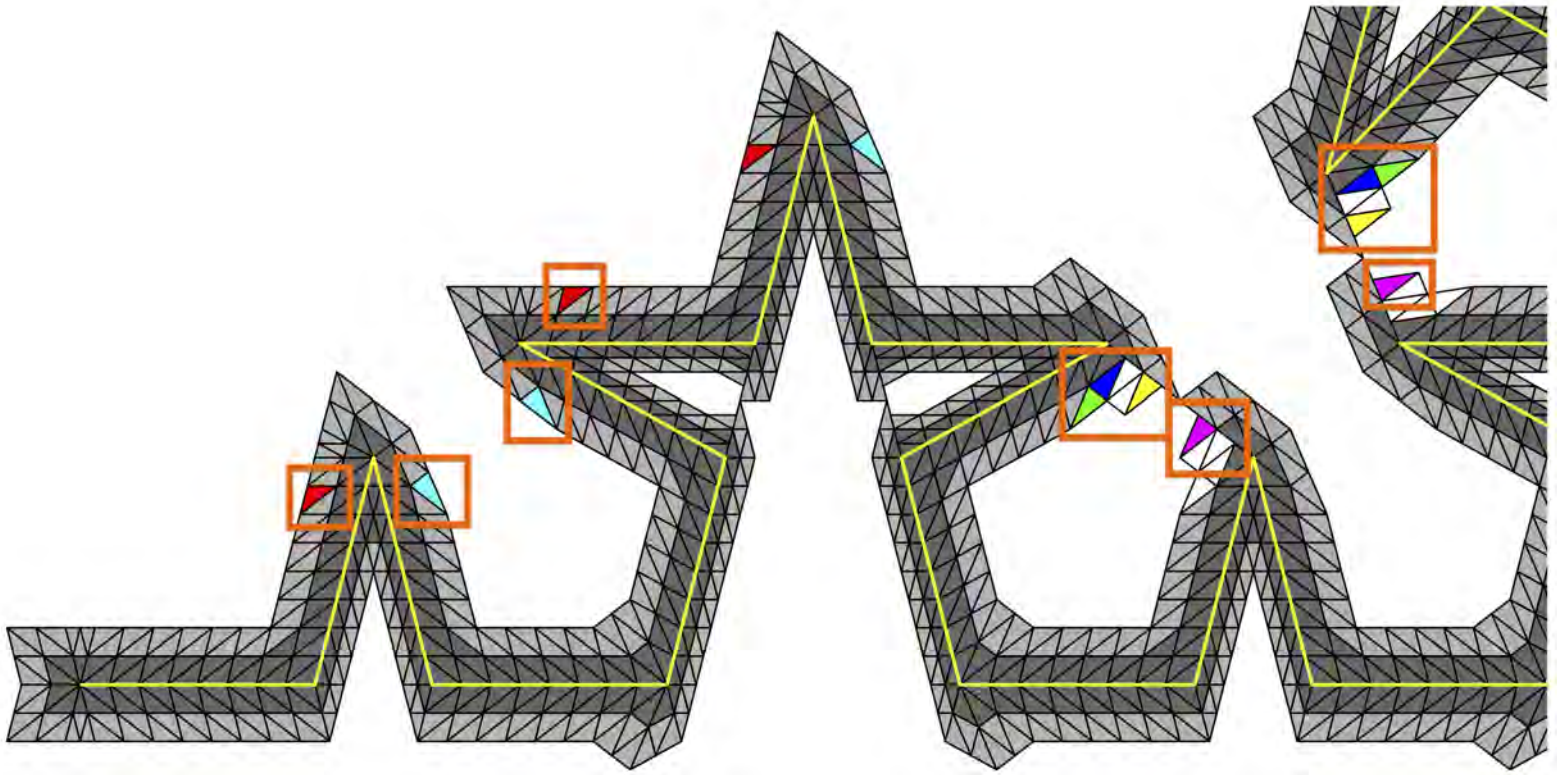

Figure 4.40: A categorization of eight types of triangles of Figure 4.2(b). The dark grey triangles represent the previously bounded primary sidecar triangles (see Lemmas 1 – 24 or Table 4.1); the white triangles are triangles to be bounded in Figure 4.41; the light grey triangles were bounded in Figures 4.29 – 4.39; and the remaining six colors (i.e., the yellow, red, cyan, green, blue, and magenta) triangles are bounded in this diagram. Triangles in the orange boxes represent triangles in $\omega_{TR_{TR}}$. See Table 4.2 for a complete list of upper bounds.

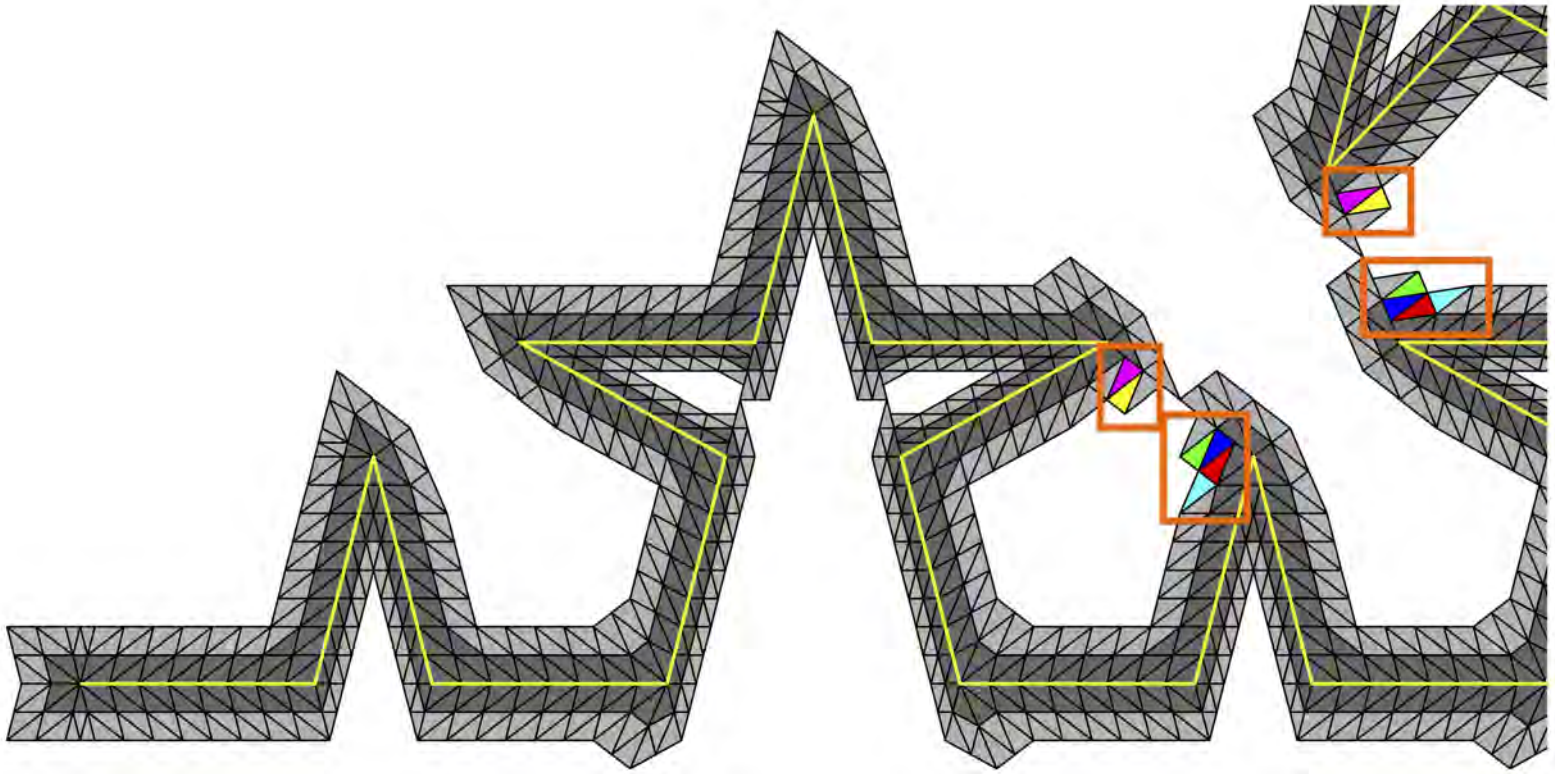

Figure 4.41: A categorization of six types of triangles of Figure 4.2(b). The dark grey triangles represent the previously bounded primary sidecar triangles (see Lemmas 1 – 24 or Table 4.1); the light grey triangles were bounded in Figures 4.29 – 4.40; and the remaining six colors (i.e., the yellow, red, cyan, green, blue, and magenta) triangles are bounded in this diagram. Triangles in the orange boxes represent triangles in $\omega_{TR_{TR}}$. See Table 4.2 for a complete list of upper bounds.

Lemma 28. *Let T_V and T_W be two triangles such that $T_V \cap T_W \neq \emptyset$. Let v be an affine function defined on T_V and w an affine function defined on T_W so that $v|_{T_V \cap T_W} = w|_{T_V \cap T_W}$. Assume further that, for some $\beta \in (0, 1]$, there are constants C_V and C_W so that*

$$\sup_{X,Y \in T_V} \frac{|v(X) - v(Y)|}{|X - Y|^\beta} \leq C_V$$

and

$$\sup_{X,Y \in T_V} \frac{|w(X) - w(Y)|}{|X - Y|^\beta} \leq C_W$$

hold. Define

$$z(X) = \begin{cases} v(X) & \text{if } X \in T_V \\ w(X) & \text{if } X \in T_W \setminus T_V \end{cases}$$

and $C_M = \max\{C_V, C_W\}$. Then

$$\sup_{X,Y \in T_V \cup T_W} \frac{|z(X) - z(Y)|}{|X - Y|^\beta} \leq 2C_M.$$

Proof. Let X and Y be arbitrary points in $T_V \cup T_W$. If X and Y are in the same triangle, then the inequality holds trivially. If not, we may assume without loss of generality that $X \in T_V$ and $Y \in T_W$. Since $T_W \cap T_V \neq \emptyset$, we get three cases, namely (i) T_V and T_W share an entire side, (ii) T_V and T_W share a single point, or (iii) (without loss of generality) an entire edge of T_V is only a partial edge of T_W. If (i), then $\overline{XY}$ is entirely contained with $T_V \cup T_W$ and we define $P = \overline{XY} \cap (T_V \cap T_W)$. If (ii), then define $P = T_V \cap T_W$. If (iii), we define P situationally; see Figure 4.42. Case (iii) is the portion of Figure 4.42 in the lower right corner. If $\overline{XY}$ is contained entirely within $T_V \cup T_W$, we define $P = \overline{XY} \cap (T_V \cap T_W)$ (see the blue P in Figure 4.42). If $\overline{XY}$ is not entirely contained within $T_V \cup T_W$, then we define P as the point $T_V \cup T_W$ closest to Y (see the yellow P in Figure 4.42). Since v and w

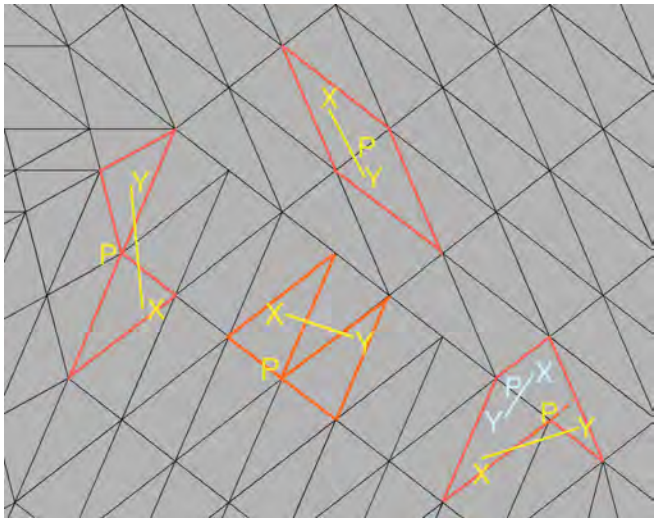

Figure 4.42: Cases for Lemma 28

are affine function on T_V and T_W, respectively, we have

$$\begin{aligned}
\frac{|z(X)-z(Y)|}{|X-Y|^\beta} &\leq \frac{|z(X)-z(P)|}{|X-Y|^\beta} + \frac{|z(P)-z(Y)|}{|X-Y|^\beta} \\
&\leq \frac{|v(X)-v(P)|}{|X-Y|^\beta} + \frac{|w(P)-w(Y)|}{|X-Y|^\beta} \\
&\leq \frac{C_V|X-P|^\beta}{|X-Y|^\beta} + \frac{C_W|P-Y|^\beta}{|X-Y|^\beta} \\
&\leq C_M \left[\left(\frac{|X-P|}{|X-Y|} \right)^\beta + \left(\frac{|P-Y|}{|X-Y|} \right)^\beta \right] \\
&\leq 2(\alpha-2)^{-1} C_M.
\end{aligned}$$

Since X and Y were arbitrary, the conclusion follows. □

Lemma 29. *Let n be fixed, V^n be a prefractal set and given a function u defined on V^n such that*

$$\frac{|u(P)-u(Q)|}{|P-Q|^\beta} \leq |u|_{K,\beta}$$

for all $P, Q \in V^n$ and for some $\beta \in (0,1]$. Let $u_n^\star$ be an extension to the domain ω as

previously defined. Then

$$\sup_{\substack{X,Y\in\omega_{SC}\\X\neq Y}} \frac{|u_n^\star(X)-u_n^\star(Y)|}{|X-Y|^\beta} \leq 136(\alpha-2)^{-(n+1)}|u|_{K,\beta}.$$

Proof. Define C_{MSC} as the maximum Hölder constant from Lemmas 1 – 24; then

$$C_{MSC} \leq 8(\alpha-2)^{-1}|u|_{K,\beta}.$$

We also observe that if X and Y belong to the same triangle T, the conclusion holds due to Lemmas 1 – 24. Moreover, if X and Y are elements of two triangles that share an entire edge, a partial edge, or a single point, Lemma 28 implies the conclusion holds. Thus, we are left to consider the case where X and Y are elements of T_X and T_Y, respectively, and that $T_X \cap T_Y$ is empty.

Since V^n is finite, there are points $P_X, P_Y \in V^n$ which are closest to X and Y, respectively. That is, $|P_X - X| \leq |P - X|$ for all other $P \in V^n$ and $|P_Y - Y| \leq |P - Y|$ for all other $P \in V^n$. Set $L = \alpha^{-n}$. Then $|P_X - X| \leq L$, $|P_Y - Y| \leq L$,

$$|P_X - P_Y| \leq |P_X - X| + |X - Y| + |Y - P_Y|,$$

and $|X - Y| \geq (\alpha-2)^n L/4$. Taking all of this into consideration, we have

$$\begin{aligned}
|u_n^\star(X)-u_n^\star(Y)| &\leq |u_n^\star(X)-u_n^\star(P_X)| + |u_n^\star(P_X)-u_n^\star(P_Y)| + |u_n^\star(P_Y)-u_n^\star(Y)| \\
&\leq C_{T_X}|X-P_X|^\beta + |u|_{K,\beta}|P_X-P_Y|^\beta + C_{T_Y}|P_Y-Y|^\beta \\
&\leq C_{MSC}(|X-P_X|^\beta + |P_X-P_Y|^\beta + |P_Y-Y|^\beta) \\
&\leq 17C_{MSC}(\alpha-2)^{-n}|X-Y|^\beta \\
&\leq 136(\alpha-2)^{-(n+1)}|u|_{K,\beta}|X-Y|^\beta.
\end{aligned}$$

Thus,

$$\frac{|u_n^\star(X) - u_n^\star(Y)|}{|X-Y|^\beta} \leq 136(\alpha-2)^{-(n+1)}|u|_{K,\beta}$$

for all $X, Y \in \omega_{SC}$. □

Lemma 30. *Let n be fixed and V^n be the prefractal set of K^n. Let u be a function defined on the vertices of V^n so that*

$$\frac{|u(P) - u(Q)|}{|P-Q|^\beta} \leq |u|_{K,\beta}$$

for all $P, Q \in V^n$ and some $\beta \in (0,1]$. Let $u_n^\star$ be an extension to the domain ω. Then

$$\frac{|u_n^\star(X) - u_n^\star(Y)|}{|X-Y|^\beta} \leq 17\max\{C_{MTR}, 136(\alpha-2)^{-(n+1)}|u|_{K,\beta}\}(\alpha-2)^{-n}|X-Y|^\beta$$

for any $X, Y \in \omega_{SC} \cup \omega_{TR}$ of the triangulation $\mathcal{T}^n$.

Proof. Define C_{MTR} as the maximum Hölder constant for triangles in the transition region; then $C_{MTR} \leq$. Let T_X and T_Y be the triangles containing the points X and Y, respectively. If $T_X = T_Y$ (i.e., X and Y are in the same triangle), then the bounds in Tables 4.1 and 4.2 imply the result. If $T_X \cap T_Y \neq \emptyset$, then the inequality holds because of the bounds in Tables 4.1 and 4.2 and Lemma 28. Thus we are left to consider the case where $T_X \cap T_Y$ is empty. There are three sub cases to consider.

Case 1. If T_X and T_Y are sidecar elements, Lemma 29 implies the result.

Case 2. Now assume $T_X, T_Y \in \omega_{TR}$. Define P_X as the point of $\omega_{SC} \cap T_X$ closest to X (we know at least one such point exists); we define P_Y in a similar manner. Set $L = \alpha^{-n}$ and observe that $|P_X - X| \leq L$, $|P_Y - Y| \leq L$,

$$|P_X - P_Y| \leq |P_X - X| + |X - Y| + |Y - P_Y|,$$

and $|X-Y| \geq (\alpha-2)^n L/4$. Then

$$\begin{aligned}
|u_n^\star(X) - u_n^\star(Y)| &\leq |u_n^\star(X) - u_n^\star(P_X)| + |u_n^\star(P_X) - u_n^\star(P_Y)| + |u_n^\star(P_Y) - u_n^\star(Y)| \\
&\leq C_{T_X}|X - P_X|^\beta + 136(\alpha-2)^{-(n+1)}|u|_{K,\beta}|P_X - P_Y|^\beta + C_{T_Y}|P_Y - Y|^\beta \\
&\leq \max\{C_{MTR}, 136(\alpha-2)^{-(n+1)}|u|_{K,\beta}\}\left[|X - P_X|^\beta + |P_Y - P_X|^\beta + |Y - P_Y|^\beta\right] \\
&\leq \max\{C_{MTR}, 136(\alpha-2)^{-(n+1)}|u|_{K,\beta}\}\left[4L + |X - Y|^\beta\right] \\
&\leq 17\max\{C_{MTR}, 136(\alpha-2)^{-(n+1)}|u|_{K,\beta}\}(\alpha-2)^{-n}|X - Y|^\beta.
\end{aligned}$$

Case 3. Finally, we consider the case with $T_X \in \omega_{SC}$ and $T_Y \in \omega_{TR}$. Since $X \in \omega_{SC}$, we only define P_Y. Let P_Y be the point of $\omega_{SC} \cap T_Y$ closest to Y. Set $L = \alpha^{-n}$ and observe that $|Y - P_Y| \leq L$,

$$|X - Y| \leq |X - Y| + |Y - P_Y|,$$

and $|X-Y| \geq (\alpha-2)^n L/4$.. Thus

$$\begin{aligned}
|u_n^\star(X) - u_n^\star(Y)| &\leq |u_n^\star(X) - u_n^\star(P_Y)| + |u_n^\star(P_Y) - u_n^\star(Y)| \\
&\leq 136(\alpha-2)^{-(n+1)}|u|_{K,\beta}|X - P_Y|^\beta + C_{T_Y}|P_Y - Y|^\beta \\
&\leq \max\{C_{MTR}, 136(\alpha-2)^{-(n+1)}|u|_{K,\beta}\}\left[|P_Y - X|^\beta + |Y - P_Y|^\beta\right] \\
&\leq \max\{C_{MTR}, 136(\alpha-2)^{-(n+1)}|u|_{K,\beta}\}\left[2L + |X - Y|^\beta\right] \\
&\leq 9\max\{C_{MTR}, 136(\alpha-2)^{-(n+1)}|u|_{K,\beta}\}(\alpha-2)^{-n}|X - Y|^\beta.
\end{aligned}$$

□

Lemma 31. *Let $\mathcal{T}^n$ be the triangulation of ω for the extension function $u_n^\star$, C_{MSC} be the maximum Hölder sidecar triangle constant, and C_{MTR} be the maximum Hölder transition triangle constant. Then*

$$\frac{|u_n^\star(X) - u_n^\star(Y)|}{|X - Y|^\beta} \leq \max\{C_{MSC}, C_{MTR}\}$$

for any X and Y is a single triangle T of $\mathcal{T}^n$.

Proof. Let T be the triangle containing X and Y. If $T \in \omega_{SC} \cup \omega_{TR}$, then the result holds by the seminorm bounds provided in Tables 4.1 and 4.2.

For $T \in \omega_{EX}$, let m be the iteration where the value of $u_n^\star(T)$ was last set; that is, $u_m^\star(X) \neq u_{m-1}^\star(X)$ for some $X \in T$ but $u_m^\star(X) = u_{m+i}^\star(X)$ for all $X \in T$ and $i \in \{1, \ldots, n-m\}$. Let T_m be the triangle from the triangulation $\mathcal{T}^m$ containing T. It follows from the construction of the extension function over ω that $T_m \in \omega_{SC} \cup \omega_{TR}$ for the triangulation $\mathcal{T}^m$. Thus

$$\frac{|u_m^\star(A) - u_m^\star(B)|}{|A-B|^\beta} \leq 17 \max\{C_{MTR}, 136(\alpha-2)^{-(n+1)}|u|_{K,\beta}\}(\alpha-2)^{-n}|X-Y|^\beta$$

for all $A, B \in T_m$. Since $T \subset T_m$, the previous observation then implies

$$\frac{|u_m^\star(X) - u_m^\star(Y)|}{|X-Y|^\beta} \leq \max\{C_{MSC}, C_{MTR}\}$$

for all $X, Y \in T_m$. Thus

$$\frac{|u_n^\star(X) - u_n^\star(Y)|}{|X-Y|^\beta} = \frac{|u_m^\star(X) - u_m^\star(Y)|}{|X-Y|^\beta} \leq \max\{C_{MSC}, C_{MTR}\}$$

for all $X, Y \in T_m$. □

Lemma 32. *Let $n = 1$ and K^1 be the first iteration of the prefractal Koch curve. Let u be defined on the vertices V^1 of K^1 so that*

$$\frac{|u(P) - u(Q)|}{|P-Q|^\beta} \leq |u|_{K,\beta}$$

for all $P, Q \in V^1$ and some $\beta \in (0, 1]$. Let $u_1^\star$ be the first extension to the ω. Then

$$\frac{|u_1^\star(X) - u_1^\star(Y)|}{|X-Y|^\beta} \leq 16\sqrt{2} \max\{C_{MTR}, C_{MSC}, |u|_{K,\beta}\}|X-Y|^\beta$$

for any $X, Y \in \omega$.

Proof. Let C_{MSC} be the maximum sidecar triangle constant from Table 4.1 and C_{MTR} be the maximum transition triangle constant from Table 4.2.

If X and Y are elements of the same triangle or if X and Y are elements of two separate triangles sharing at least one point, then the result holds by our previous arguments. If $X, Y \in \omega_{SC} \cup \omega_{TR}$, then the estimate holds by Lemma 31. Thus, without loss of generality, we are left to consider the case when $X \in \omega_{SC} \cup \omega_{TR}$ and $Y \in \omega \setminus (\omega_{SC} \cup \omega_{TR})$.

Let T_X and T_Y be the triangles containing X and Y, respectively. Let P_X be the point in $\omega_{SC} \cap T_X$ so that $|P_X - X|$ is minimized (this means $P_X = X$ if $X \in \omega_{SC}$). Let Q_X be the element of V^1 closest to the point P_X and Q_Y be the element of V^0 closest to Y. Set $L = \alpha^{-1}$ and observe that $|X - P_X| \leq 3L$, $|P_X - Q_X| \leq 3L$, and $|X - Y| \geq L/\sqrt{2}$ because $X \in \omega_{SC}$ (we have already dealt with the case of $X \in \omega_{TR}$ and $Y \in \omega_{TR}$). Thus

$$
\begin{aligned}
|u_n^\star(X) - u_n^\star(Y)| &\leq |u_1^\star(X) - u_0^\star(Y)| \\
&\leq C_{MTR}|X - P_X|^\beta + C_{MSC}|P_X - Q_X|^\beta + |u|_{K,\beta}|Q_X - Q_Y|^\beta + C_{MSC}|Y - Q_Y|^\beta \\
&\leq \max\{C_{MTR}, C_{MSC}, |u|_{K,\beta}\}(|X - P_X|^\beta + |P_X - Q_X|^\beta + |Q_X - Q_Y|^\beta \\
&\qquad + |Y - Q_Y|^\beta) \\
&\leq \max\{C_{MTR}, C_{MSC}, |u|_{K,\beta}\}((3L)^\beta + (3L)^\beta + (4L)^\beta + (4L)^\beta) \\
&\leq 16 \max\{C_{MTR}, C_{MSC}, |u|_{K,\beta}\} L^\beta \\
&\leq 16\sqrt{2} \max\{C_{MTR}, C_{MSC}, |u|_{K,\beta}\} |X - Y|^\beta.
\end{aligned}
$$

□

Chapter 5. Main Result

Proposition 1. *The extension operator Π_n is linear.*

Proof. Let K be a Koch curve with contraction factor α. Assume u and v are two $\beta-$Hölder continuous functions, $\beta < 1$, defined at the vertices of K so that

$$\frac{|u(A) - u(B)|}{|A - B|^\beta} \leq |u|_{K,\beta}$$

and

$$\frac{|v(A) - v(B)|}{|A - B|^\beta} \leq |v|_{K,\beta}$$

for all $A, B \in V^n$. Let $c \in \mathbb{R}$ and X be any element of ω. By construction, $\Pi_n u_n(X)$ can be written as

$$\Pi_n u_n(X) = \sum_{i=1}^{4^n+1} a_i u(P_i)$$

where $P_i \in V^n$, $0 \leq a_i \leq 1$, $\sum a_i = 1$, and the values of a_i are independent of u; $\Pi_n v_n(X)$ can be written in a similar manner. Thus

$$\begin{aligned}
c\Pi_n u_n(X) + c\Pi_n v_n(X) &= c\sum_{i=1}^{4^n+1} a_i u(P_i) + c\sum_{i=1}^{4^n+1} a_i v(P_i) \\
&= \sum_{i=1}^{4^n+1} ca_i u(P_i) + \sum_{i=1}^{4^n+1} ca_i v(P_i) \\
&= \sum_{i=1}^{4^n+1} \Big[ca_i u(P_i) + ca_i v(P_i) \Big] \\
&= \Pi_n \Big[cu_n + cv_n \Big] \\
&= \Pi_n \Big[c(u_n + v_n) \Big].
\end{aligned}$$

For $X \in \Omega \setminus \omega$, $\Pi_n u_n(X) = \Pi_n v_n(X) = 0$, which is clearly linear. Thus Π_n is linear. □

Proposition 2. *Let $n \geq 1$ be the iteration number, let K^n be the prefractal Koch curve with*

vertex set V^n, and u be defined at the vertices of the K^n so that

$$\frac{|u(A) - u(B)|}{|A - B|^\beta} \leq |u|_{K,\beta}$$

for all $A, B \in V^n$ and some $\beta \leq 1$. Let $\Pi_n u_n = u_n^\star$ be the n^{th} extension function to the domain ω. Then

$$\frac{|u_n^\star(X) - u_n^\star(Y)|}{|X - Y|^\beta} \leq 4624 \max\{C_{MTR}, C_{MSC}\}$$

for any $X, Y \in \omega$.

Proof. This is proved by collecting each upper bound thus far and observing that $\Pi_n u_n = u_n^\star$ is identically zero outside ω. □

Proposition 3. *For every n and every $u_n \in C^\beta(V^n)$, we construct a linear extension operator Π_n that brings functions defined on V^n and to functions defined on Ω for all $\beta \in (0, 1]$ so that $u_n \in C^\beta(V^n) \mapsto u_n^\star \in C^\beta(\Omega)$ and*

$$\|\Pi_n u_n\|_{\Omega,\beta} \leq 4732 \max\left\{\frac{C_{MTR}}{|u|_{K,\beta}}, \frac{C_{MSC}}{|u|_{K,\beta}}\right\} \|u\|_{K,\beta}.$$

Proof. The first of these assertions is clearly true by the construction and arguments we have provided thus far. For the second assertion, Proposition 2 implies

$$\frac{|u_n^\star(X) - u_n^\star(Y)|}{|X - Y|^\beta} \leq 4624 \max\{C_{MTR}, C_{MSC}\}$$

for all $X, Y \in \omega$ and any n. We first recall that $u_n^\star$ is identically zero outside ω.

Now we define another larger domain containing ω. Set the corner point of ω to be $A(-1, 0)$, $B(2, 0)$, $C(1/2, 3\sqrt{4 - (\alpha - 2)^2}/\alpha)$, and $D(1/2, -3\sqrt{4 - (\alpha - 2)^2}/\alpha)$. Define γ as the six new points $E(-4, 0)$, $F(-1, 6\sqrt{4 - (\alpha - 2)^2}/\alpha)$, $G(2, 6\sqrt{4 - (\alpha - 2)^2}/\alpha)$, $H(5, 0)$, $I(2, -6\sqrt{4 - (\alpha - 2)^2}/\alpha)$, and $J(-1, -6\sqrt{4 - (\alpha - 2)^2}/\alpha)$; this set of points creates a hexagon

around ω so that the right sides of ω are parallel to the right sides of γ, and similarly on the left, with the top and bottom sides parallel to the $x-$axis. See Figure 5.1.

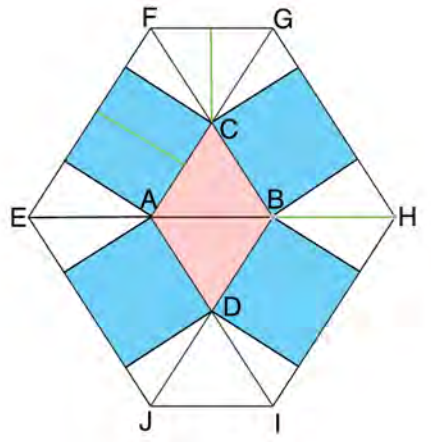

Figure 5.1: The pink region is ω, the blue region is γ_{SC}, and the white region is γ_{EX}. We have $\gamma = \gamma_{SC} \cup \gamma_{EX} \cup \omega$.

Now decompose γ. Let $\gamma = \gamma_{SC} \cup \gamma_{EX} \cup \omega$, where ω is defined as before, $\gamma_{EX} = \gamma \backslash (\omega \cup \gamma_{SC})$, and γ_{SC} the the set of four rectangles attached to the sides of ω. More precisely, we construct γ_{SC} in the following manner.

(i) Draw a line ℓ perpendicular to $\overline{BC}$ through B and set $K = \ell \cap \overline{GH}$.

(ii) Draw a line ℓ perpendicular to $\overline{BC}$ through C and set $L = \ell \cap \overline{GH}$.

(iii) Define R_1 to be the rectangle passing through B, C, K, and L.

(iv) Define R_2, R_3, and R_4 is a similar manner using the other edges of ω.

(v) Set $\gamma_{SC} = R_1 \cup R_2 \cup R_3 \cup R_4$.

Finally, we define two more points, namely P and Q. If $X \in \gamma_{SC}$, set P as the orthogonal projection of X onto $\partial\omega$ and Q as the orthogonal projection of X onto $\partial\gamma$. If $X \in \gamma_{EX}$, set P as the element of $\{A, B, C, D\}$ that minimizes $|X - P|$ and construct the line determined by P and X; define Q as the point of intersection on $\overline{XP}$ and $\partial\gamma$ closest to X.

Now we move on to the core argument. Let X_1 and X_2 be arbitrary points in γ and set L as the minimal distance between the bounders of γ and ω. If $X_1 \in \omega$, set $P_1 = X_1$ and

$C_1 = 1$. If $X_1 \in \gamma_{SC}$, set $P_1 = P$, $Q_1 = Q$, and $C_1 = |Q_1 - X_1|/L$. If $X_1 \in \gamma_{EX}$, set $P_1 = P$, $Q_1 = Q$, and $C_1 = |Q_1 - X_1|/|P_1 - Q_1|$. Define P_2, Q_2, and C_2 in the same way, except interchange the subscripts.

It is clear that $C_1, C_2 \in [0, 1]$ and that

$$0 \leq |C_1 - C_2| \leq \frac{|X_1 - X_2| + |Q_1 - Q_2|}{L},$$

so

$$\begin{aligned}
\frac{|u_n^\star(X_1) - u_n^\star(X_2)|}{|X_1 - X_2|^\beta} &= \frac{|C_1 u_n^\star(P_1) - C_2 u_n^\star(P_2)|}{|X_1 - X_2|^\beta} \\
&\leq \frac{C_1 |u_n^\star(P_1) - u_n^\star(P_2)|}{|X_1 - X_2|^\beta} + \frac{|C_1 - C_2| u_n^\star(P_2)|}{|X_1 - X_2|^\beta} \\
&\leq \frac{|u_n^\star(P_1) - u_n^\star(P_2)|}{|X_1 - X_2|^\beta} + \frac{|C_1 - C_2|}{|X_1 - X_2|^\beta} \sup_{X \in K} |u(X)| \\
&\leq 4624 \max\{C_{MTR}, C_{MSC}\} + \left[\frac{|X_1 - X_2|}{L|X_1 - X_2|^\beta} + \frac{|Q_1 - Q_2|}{L|X_1 - X_2|^\beta} \right] \sup_{X \in K} |u(X)| \\
&\leq 4624 \max\left\{ \frac{C_{MTR}}{|u|_{K,\beta}}, \frac{C_{MSC}}{|u|_{K,\beta}} \right\} |u|_{K,\beta} + 2\|u\|_{K,\beta} \left[\frac{|X_1 - X_2|}{L} \right]^{1-\beta} L^{-\beta}.
\end{aligned}$$

By construction of γ and definition of L, constructing a lower bound on L is equivalent to solving

$$\min\left\{ 3, g(\alpha), \frac{3\sqrt{4 - (\alpha - 2)^2}}{\alpha} \right\} \leq L$$

for $\alpha \in [2, 3]$ where $g(\alpha)$ is defined as the minimum distance between P and Q for $X \in \gamma_{SC}$ and all $\alpha \in [2, 3]$. The function $f(\alpha) = 3$ is clearly minimized at any α because it is constant. The function

$$f(\alpha) = \frac{3\sqrt{4 - (\alpha - 2)^2}}{\alpha}$$

is a strictly decreasing function on $[2, 3]$, so the minimum occurs at $(3, \sqrt{3})$. Finally, minimizing $g(\alpha)$ is the same and minimizing $h(\alpha) = g^2(\alpha)$. A nontrivial—but straightforward—

calculation implies

$$h(\alpha) = \frac{64\left[(\alpha-2)^2-6\right]^2}{\left[\alpha^2-4(\alpha-2)^2+16\right]\left[16-4(\alpha-2)^2\right]}.$$

This function is also strictly decreasing on $[2,3]$, so the minimum occurs at $(3, 400/63)$. Thus $g(\alpha)$ is minimized at $\alpha = 3$ and is $g(3) = 20/3\sqrt{7}$. So $\sqrt{3} \leq L$. Returning to our estimate gives

$$\begin{aligned}
\frac{|u_n^\star(X_1) - u_n^\star(X_2)|}{|X_1 - X_2|^\beta} &\leq 4624 \max\left\{\frac{C_{MTR}}{|u|_{K,\beta}}, \frac{C_{MSC}}{|u|_{K,\beta}}\right\}|u|_{K,\beta} + 2\|u\|_{K,\beta}\left[\frac{|X_1 - X_2|}{L}\right]^{1-\beta} L^{-\beta} \\
&\leq 4624 \max\left\{\frac{C_{MTR}}{|u|_{K,\beta}}, \frac{C_{MSC}}{|u|_{K,\beta}}\right\}\|u\|_{K,\beta} \\
&\qquad + 2\sqrt{3}\left(\frac{18\sqrt{4-(\alpha-2)^2}}{\alpha}\right)^{1-\beta}\|u\|_{K,\beta} \\
&\leq 4624 \max\left\{\frac{C_{MTR}}{|u|_{K,\beta}}, \frac{C_{MSC}}{|u|_{K,\beta}}\right\}\|u\|_{K,\beta} + 108\|u\|_{K,\beta} \\
&\leq 4732 \max\left\{\frac{C_{MTR}}{|u|_{K,\beta}}, \frac{C_{MSC}}{|u|_{K,\beta}}\right\}\|u\|_{K,\beta}. \qquad \square
\end{aligned}$$

Now we move on to the main result.

Theorem 4 (Main Theorem)**.** *Let $m \in \mathbb{N}$ define a contraction factor $\alpha = 2 + 1/m$, and assume that K is the Koch curve corresponding to α with vertex set V. Assume further that Ω is a domain containing K and u is any Hölder continuous function on K. We define a continuous linear operator Π_n such that*

(i) $\Pi_n : C^\beta(K) \mapsto C^\beta(\Omega)$,

(ii) $\|\Pi_n u\|_{\Omega,\beta} \leq C_1\|u\|_{K,\beta}$,

(iii) and $\sup_{X\in\Omega} |\Pi_n u(X) - \Pi_{n+p}u(X)| \leq C_2\|u\|_{S,\beta}$

where C_1 and C_2 are numerical constants independent of u but dependent on α and n.

Proof. We note that (i) and (ii) are merely restatements of our previous work, so we proceed to show (iii).

Fix $p \in \mathbb{N}$ and observe that our construction implies consecutive extension functions (i.e., $u_n^\star$ and $u_{n+p}^\star$) are identical everywhere, except possibly on the $\omega_{SC} \cup \omega_{TR}$ region of the $u_{n+p}^\star$ extension. So assume $X \in \omega_{SC} \cup \omega_{TR}$ of the $(n+p)$ extension and let Y denote the element of V^n closest to X. Then

$$\begin{aligned} |u_n^\star(X) - u_{n+p}^\star(X)| &\leq |u_n^\star(X) - u(Y)| + |u(Y) - u_{n+p}^\star(X)| \\ &\leq 2\|u\|_{K,\beta}|X - Y|^\beta \\ &\leq 9464 \max\left\{\frac{C_{MTR}}{|u|_{K,\beta}}, \frac{C_{MSC}}{|u|_{K,\beta}}\right\}\|u\|_{K,\beta}. \end{aligned}$$

□

Chapter 6. Future Work

Due to a few complications in Table 4.2, we were unable to prove a general theorem for this class of fractals. In particular, we were unable to prove

Theorem 5. *Assume we have an $m \in \mathbb{N}$, a contraction factor $\alpha = 2 + 1/m$, and a Koch curve K corresponding to α with vertex set V. Let Ω be a domain containing K and u be a Hölder continuous function on K. We define a continuous linear operator Π such that*

(i) $\Pi : C^\beta(K) \mapsto C^\beta(\Omega)$,

(ii) $\|\Pi u\|_{\Omega,\beta} \leq C_1 \|u\|_{K,\beta}$,

(iii) $\sup_{X \in \Omega} |\Pi_n u(X) - \Pi_{n+p} u(X)| \leq C_2 \|u\|_{K,\beta} \alpha^{-n}$,

(iv) and $\Pi_n u$ converges uniformly to Πu on Ω

where C_1 and C_2 are numerical constants independent of u and n.

This theorem is substantially stronger than the result we proved in a few respects. First and foremost, our result only demonstrated Hölder continuity for any finite sequence of extension, but lacks proof in the limit due to the first couple entries of Table 4.1. The second respect in which this differs is that our sequence of functions $\Pi_n u_n$ does not converge uniformly to any known quantity. We suspect an adjustment of our method will handle each of the claims with no trouble, but the adjustment would need to be a fundamentally different approach than we have taken.

We say a fundamentally different approach may be needed because the current argument attempts to bound the seminorm by calculating the number of subdivisions along any segment $\overline{A_i A_{i+1}}$ of the fractal (A_i and A_{i+1} are consecutive points in V^n). This method worked when we were bounding the primary sidecar triangles (Lemmas 1 – 24), but, in reflection, this method was only robust enough because of well-placed cancelations. The same cancelations properties do not hold for each triangle of Table 4.2, so the upper bound is likely

growing over the transition triangle regions in the limit (at least that is what our technique implies).

Assuming we can work out the kink discussed in the preceding paragraph, we would like to extend this result to all α of the form $\alpha = 2 + p/q \in (2, 4]$. If this argument works, we can likely apply an identical technique to gain Theorem 5. Once we have Theorem 5, it should be natural to extend to all $\alpha \in (2, 4]$ via a density argument.

Finally, I plan to consider this problem for other fractals. In particular, I would like to consider this extension problem after solving the problem of generating a regular triangulation for (extremely) non-standard Koch curves, (i.e., mixed α values). That is, we would develop a method to triangulate things like Figure 6.1 – 6.3, and then we would consider our current problem.

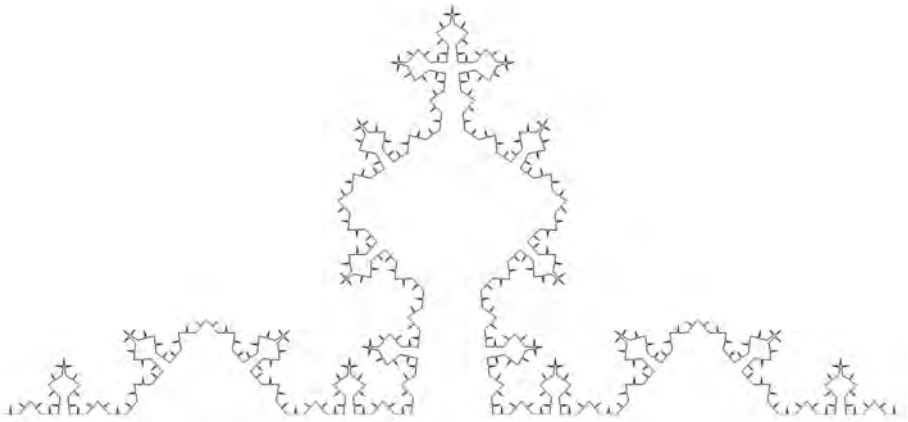

Figure 6.1: An example of two mixed alpha values. In this diagram, $\alpha_1 = 2.2$ and $\alpha_2 = 3.3$ with five iterations.

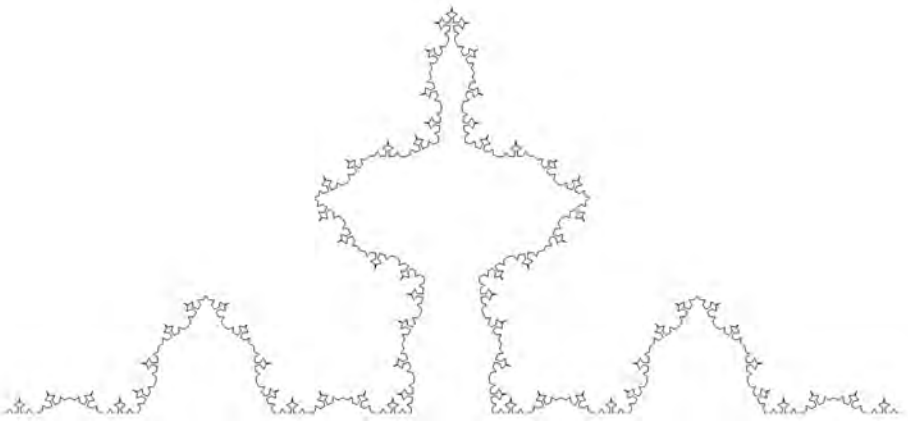

Figure 6.2: An example of three mixed alpha values. In this diagram, $\alpha_1 = 3$, $\alpha_2 = 2.2$, and $\alpha_2 = 3.8$ with five iterations.

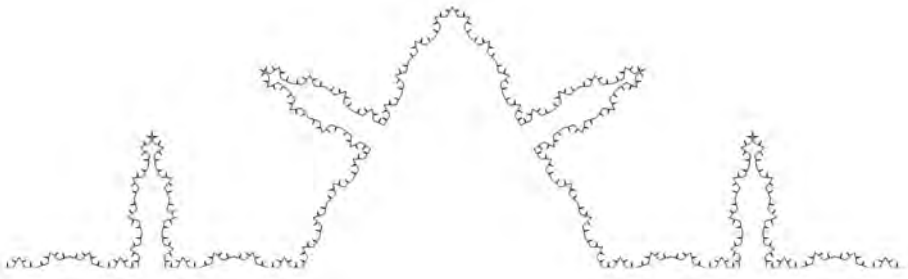

Figure 6.3: An example of three mixed alpha values. In this diagram, $\alpha_1 = 2.2$, $\alpha_2 = 3$, and $\alpha_3 = 3.9$ with five iterations.

Bibliography

[1] Hassler Whitney. Analytic extensions of differentiable functions defined in closed sets. *Trans. Amer. Math. Soc.*, 36(1):63–89, 1934.

[2] Hassler Whitney. Differentiable functions defined in closed sets. I. *Trans. Amer. Math. Soc.*, 36(2):369–387, 1934.

[3] Hassler Whitney. Functions differentiable on the boundaries of regions. *Ann. of Math. (2)*, 35(3):482–485, 1934.

[4] Georges Glaeser. Étude de quelques algèbres tayloriennes. *J. Analyse Math.*, 6:1–124; erratum, insert to 6 (1958), no. 2, 1958.

[5] Edward Bierstone, Pierre D. Milman, and Wiesław Pawłucki. Differentiable functions defined in closed sets. A problem of Whitney. *Invent. Math.*, 151(2):329–352, 2003.

[6] Yuri Brudnyi and Pavel Shvartsman. Generalizations of Whitney's extension theorem. *Internat. Math. Res. Notices*, (3):129 ff., approx. 11 pp. (electronic), 1994.

[7] Yuri Brudnyi and Pavel Shvartsman. The Whitney problem of existence of a linear extension operator. *J. Geom. Anal.*, 7(4):515–574, 1997.

[8] Charles Fefferman. Extension of $c^{m,\omega}$-smooth functions by linear operators. *Rev. Mat. Iberoam.*, 25(1):1–48, 2009.

[9] Charles Fefferman. Whitney's extension problems and interpolation of data. *Bull. Amer. Math. Soc. (N.S.)*, 46(2):207–220, 2009.

[10] M. R. Lancia and M. A. Vivaldi. Asymptotic convergence of transmission energy forms. *Adv. Math. Sci. Appl.*, 13(1):315–341, 2003.

[11] Alf Jonsson and Hans Wallin. Function spaces on subsets of $\mathbf{R}^n$. *Math. Rep.*, 2(1):xiv+221, 1984.

[12] Alf Jonsson and Hans Wallin. The dual of Besov spaces on fractals. *Studia Math.*, 112(3):285–300, 1995.

[13] Emily J. Evans. A finite element approach to Hölder extension using prefractals. *Methods Appl. Anal.*, 19(2):161–186, 2012.

[14] Emily Evans. A novel finite element meshing technique driven by fractal Koch curves. Technical Report 8-19-41, WPI Mathematical Sciences Department, 2008.

Nomenclature

α	The contraction factor for the fractal Koch curve K. This parameter satisfies $\alpha \in (2, 4]$. See page 12.
$[\alpha]$	The integer part of α. See [10].
β	The exponent of continuity in the definition of Hölder continuity. See page 1.
$B_\alpha^{p,q}(F)$	The Besov space for the closed d-set F. In this context, $1 \leq p \leq q\infty$, $1 \leq q \leq \infty$, and $\alpha > 0$. See page 4.
$C(\mathbb{R}^n)$	The set of continuous functions on $\mathbb{R}^n$ mapping to $\mathbb{R}$.
$C^\beta(\Omega)$	The space of β-Hölder continuous functions on Ω. See page 1.
C_{MEX}	The maximum exterior triangle constant. This constant is dependent on n. See Lemma 25 on page 78.
C_{MSC}	The maximum primary sidecar constant. This constant is independent on n. See Table 4.1.
C_{MTR}	The maximum transition triangle constant. This constant accounts for triangles in $\omega_{TR_{SC}}$ and $\omega_{TR_{TR}}$. This constant is dependent on n. See Table 4.2.
$\partial\omega$	The boundary of ω. See page 14.
$\partial\gamma$	The boundary of γ. See Figure 5.1 on page 113 and surrounding material for a precise definition and construction.
E	A set in $\mathbb{R}^n$ unless otherwise stated.
f	A function from $\mathbb{R}^n$ to $\mathbb{R}$ unless otherwise stated.
F	A fixed d-set or a particular extension function of f. The exact choice of F is situationally dependent.

γ The hexagonal domain containing ω. See Figure 5.1 on page 113 and surrounding material for a precise definition and construction.

γ_{EX} The region of γ not considered by ω or γ_{SC}, i.e., $\gamma_{EX} = \gamma \setminus (\omega \cup \gamma_{SC})$. See Figure 5.1 on page 113 and surrounding material for a precise definition and construction.

γ_{SC} The rectangular regions contained in γ attached to the sides of ω. See Figure 5.1 on page 113 and surrounding material for a precise definition and construction.

$i|n$ The n-tuple of indices $(i_1, i_2, \ldots, i_n)$. Each $i_j \in \{1, 2, 3, 4\}$. See page 8.

k The number of subdivisions of any segment in S^n. This value is iteration dependent. See page 7.

K The fractal Koch curve with contraction factor α. See page 9.

K^n The prefractal Koch curve. The prefractal is thought of as having a segment set S^n and vertex set V^n. See page 7.

$\mathcal{N}$ A net with mesh r. See page 4.

μ A fixed d-measure. See page 3.

n The number of iterations. This parameter must be a nonnegative integer.

ω The domain containing an embedding of K. See page 14.

ω_{EX} The set of exterior triangles. This set is defined as the triangles of $\mathcal{T}$ not in ω_{SC} or ω_{TR}. This set is iteration dependent. See page 17.

ω_{SC} The set of primary sidecar triangles. These triangles have at least one vertex along K^n; this vertex may be a point along any segment of S^n or in the vertex V^n. This set is iteration dependent. See page 17.

ω_{TR} The set of transition triangles. These triangles have at least one vertex in common with the set of vertices defining ω_{SC}. This set is iteration dependent and includes no triangle in ω_{SC}. See page 17.

Ω The set we extend into. This set contains ω.

Π The extension operator in the limit. See page 117.

Π_n The extension operator at iteration n. See page 5.

$\Pi_n u$ The extension function. See page 20.

$\Pi_n u_n$ The restriction of the n^{th} extension function to the set V^n. See page 117.

$\mathcal{P}_k(\mathcal{N})$ The set of functions which on each cube Q in the net $\mathcal{N}$ coincide with a polynomial of degree at most k. See [12].

ψ_i One of four contractive similitudes used in defining the fractal Koch curve. These functions have three parameters, namely α, θ, and z. See page 7.

$\psi_{i|n}$ The composition of ψ_1, ψ_2, ψ_3, and ψ_4 in the order prescribed by $i|n$. This means $\psi_{i|n} = \psi_{i_1} \circ \psi_{i_2} \circ \cdots \circ \psi_{i_n}$. See page 8.

σ_k All combinations of k^{th} order multi-indexes. See [3, 2, 1].

S^n The segment set of K^n. See page 7.

T A particular triangle of the triangulation thought of in standard position (i.e., the lower left vertex is at the origin, the lower right vertex is along the positive x-axis, and the third vertex is in the first quadrant). See page 23.

$\mathcal{T}^n$ The triangulation at iteration n. See page 9 – 14.

θ The base angle used in construction of the prefractal. This parameter is determined as a function of α, and is given by $\theta = \cos^{-1}(\alpha/2 - 1)$. See page 7.

u The Hölder continuous function defined on the vertex set V of K.

$u_n^\star$ A short-hand for the extension function $\Pi_n u$. See $\Pi_n u$.

$|u|_{K,\beta}$ The Hölder seminorm of u on K is defined as $|u|_{K,\beta} = \sup_{\substack{X_1,X_2\in K \\ X_1\neq X_2}} \dfrac{|u(X_1)-u(X_2)|}{|X_1-X_2|^\beta}$. See page 16.

$\|u\|_{K,\beta}$ The Hölder norm of u on K is defined as $\|u\|_{K,\beta} = |u|_{K,\beta} + \sup_{X\in K} |u(X)|$. See page 112.

V The vertex set of the fractal Koch curve K. See page 9.

V^n The vertex set of the prefractal Koch curve K^n. See page 7.

z A point of $\mathbb{C}$. We identify $z = x + iy$ with the corresponding point (x, y) in $\mathbb{R}^2$. See page 7.

Index